Interfaces in fluids of charged platelike colloids

Von der Fakultät für Mathematik und Physik der Universität Stuttgart zur Erlangung der Würde eines Doktors der Naturwissenschaften (Dr. rer. nat.) genehmigte Abhandlung

Vorgelegt von
Markus Bier
aus Lauda

Hauptberichter: Prof. Dr. S. Dietrich
Mitberichter: Prof. Dr. U. Seifert

Tag der Einreichung: 6. Oktober 2006
Tag der mündlichen Prüfung: 15. Dezember 2006

Max-Planck-Institut für Metallforschung,
Stuttgart

und

Institut für Theoretische und Angewandte Physik,
Universität Stuttgart

2007

This thesis is related to the following publications:

Ref. [Bier2005]:
M. Bier, L. Harnau, and S. Dietrich, *Free isotropic-nematic interfaces in fluids of charged platelike colloids*, J. Chem. Phys. **123**, 114906 (2005).

Ref. [Bier2006]:
M. Bier, L. Harnau, and S. Dietrich, *Surface properties of fluids of charged platelike colloids*, J. Chem. Phys. **125**, 184704 (2006).

Contents

List of Figures

Acknowledgements

I am deeply indebted to *Prof. Dr. S. Dietrich* for giving me the opportunity to perform my doctoral studies at his department at the Max-Planck-Institut für Metallforschung in Stuttgart. His critical comments and constructive suggestions on various aspects of the present work were invaluable to this project. Moreover, I am grateful for the chances to participate in numerous conferences and workshops.

I like to thank *Prof. Dr. U. Seifert* for co-refereeing this thesis.

I want to express my deepest gratitude to *Dr. L. Harnau* for supervising my work at Prof. Dietrich's department. I am grateful for many interesting discussions and a lot of helpful advice ranging from technical details to conceptual aspects.

Many thanks to *Ms. A. Geigle* for lots of valuable assistence on administrative issues as well as for running a local travel agency.

I am grateful to the *computer department of the Max-Planck-Institut für Metallforschung* for constantly rapid and competent help with technical issues.

Finally, I wish to thank my present and former *colleagues* at Prof. Dietrich's department for the nice and cooperative atmosphere.

Markus Bier
Stuttgart, October 2006

Zusammenfassung

Die technologische Bedeutung von Fluiden geladener plättchenförmiger Kolloide wie Ton basiert auf einem facettenreichen Phasenverhalten mit Sol-Gel-Übergängen, Ausflockung und sogar flüssigkristallinen Phasen getragen von Translations-, Orientierungs- und Ladungsfreiheitsgraden. Die gezielte Steuerung von Fluiden geladener plättchenförmiger Kolloide unter technologisch relevanten Gegebenheiten setzt ein tiefgehendes Verständnis dieser Systeme voraus, das nicht nur homogene Fluide, sondern auch die Gegenwart von räumlichen Inhomogenitäten wie Grenzflächen umfasst. Letztere sind als geladene Grenzflächen von besonderer Bedeutung, da Fluide geladener Teilchen leicht durch Elektroden beeinflusst werden können. Während die Volumeneigenschaften von Fluiden geladener plättchenförmiger Kolloide schon Gegenstand einiger theoretischer Studien waren, fehlten bisher theoretische Untersuchungen zu Inhomogenitäten in solchen Systemen.

Im Rahmen dieser Arbeit wird ein Modellfluid bestehend aus einer ternären Mischung von monodispersen plättchenförmigen Makroionen und von Salzionen betrachtet. Die Teilchen werden als harte Quader modelliert, deren Kanten ausschließlich parallel zu den kartesische Achsen ausgerichtet sind (Zwanzig-Modell) und in deren Zentren die Ladungen der Teilchen konzentriert sind. Die Ladungen werden als vorgegebene Modellparameter aufgefasst. Es wird eine Dichtefunktionaltheorie entwickelt, mit deren Hilfe das Modellfluid aus Makroionen und Salz sowohl im Volumen als auch mit freien Grenzflächen oder in Gegenwart geladener Grenzflächen beschrieben werden kann. Sie ist qualitativer Natur, da der Zusammenhang zwischen tatsächlichen Ladungen und den effektiven Modellladungen nicht bestimmt wird. Von technisch begründeten Näherungen wie etwa der Verwendung des Zwanzig-Modells wird hingegen kein qualitativer Einfluss auf die Resultate erwartet.

Dichte-Dichte-Phasendiagramme für die Volumenphasen (Fig. 3.1) zei-

gen eine isotrope und eine nematische Phase getrennt durch einen Phasenübergang erster Ordnung. Das Zweiphasenkoexistenzgebiet verschiebt sich bei zunehmender Makroionenladung und festgehaltender Salzdichte zu größeren Makroionenpackungsdichten hin. Für festgehaltene Makroionenladung und zunehmende Salzdichte wird der Grenzfall quasiharter Plättchen erreicht. Das Donnan-Potential (Fig. 3.2) zwischen koexistierenden Phasen lässt sich aus den chemischen Potentialen im Rahmen einer Volumenstrukturrechnung gewinnen.

Volumen- und Oberflächenphasendiagramme (Fig. 3.3) als Funktionen von Makroionenladung, Übersättigung und Oberflächenladung werden mittels asymptotischer Analyse des effektiven Grenzflächenpotentials und numerischer Lösung der Euler-Lagrange-Gleichungen berechnet. Das effektive Grenzflächenpotential zeigt das gleiche asymptotische Verhalten wie in Systemen mit nichtretardierten isotropen Dispersionskräften obwohl das Modell *keine* Dispersionskräfte enthält. Dieses Phänomen lässt sich zurückführen auf die im Rahmen der Dichtefunktionaltheorie verwendete Teilchen-Teilchen Paarverteilungsfunktion mit Debye-Hückel-artigem asymptotischem Abfall.

Die vorgestellte Dichtefunktionaltheorie ist in der Lage, die Struktur freier fluid-fluid-Grenzflächen zu beschreiben. Diese Eigenschaft ist im Falle von Fluiden geladener Teilchen nicht trivial. Die Dichteprofile und die Profile des nematischen Ordnungsparameters an freien Grenzflächen zwischen koexistierenden isotropen und nematischen Phasen (Figs. 4.1 und 4.2) zeigen nichtmonotones Verhalten. Der Wert des nematischen Ordnungsparameters im Innern der nematischen Phase nimmt mit zunehmender Makroionenladung ab. Die Breite der Grenzfläche ist durch die Debye-Länge gegeben. Die Grenzflächenspannung nimmt mit zunehmender Makroionenladung ab. An der freien Grenzfläche bildet sich eine elektrische Doppelschicht (Fig. 4.3). Die zugehörigen Profile des elektrostatischen Potentials (Fig. 4.4) zeigen ein monotones Verhalten.

Vollständige Benetzung einer geladenen Oberfläche in Kontakt mit einer isotropen Phase durch eine nematische Phase tritt zwischen zwei Benetzungsübergangspunkten erster Ordnung auf der Isotrop-Nematisch-Koexistenzlinie auf (Fig. 4.5). Entlang der übrigen Teile der Isotrop-Nematisch-Koexistenzlinie ist die Benetzung nur unvollständig (Fig. 4.6). Das Verhalten von Adsorption (Fig. 4.7) und Benetzungsfilmdicke (Fig. 4.8) bei Annäherung an die Benetzungsübergangspunkte wird zur Bestimmung der Benetzungsübergangspunkte im Phasendiagramm benutzt. Während sich die Ordnung der Benetzungsübergange und das asymptotische Potenzgesetz der Adsorption bei vollständiger Benetzung aus analytischen Überlegungen ergibt, müssen die Positionen der Benetzungsübergangspunkte im Phasendiagramm numerisch bestimmt werden. Die zugehörigen Vorbenetzungslinien werden numerisch nicht aufgelöst.

Benetzungübergänge erster Ordnung einer geladenen Oberfläche in Kontakt mit einer nematischen Phase durch eine isotrope Phase werden auf der Isotrop-Nematisch-Koexistenzlinie durch eine unstetige Divergenz der Adsorption beim Überqueren des Benetzungsübergangspunkts bestimmt (Fig. 4.9). Die Vorbenetzungslinien, wo die Adsorption endliche Unstetigkeiten zeigt (Fig. 4.11), enden in kritischen Punkten (Fig. 4.10). Salz- und Gegenionendichte in Wandnähe werden erwartungsgemäß stark von Oberflächenladungen beeinflusst (Fig. 4.12).

Bilden sich quasi-freie Isotrop-Nematisch-Grenzflächen zwischen dem Volumeninnern und Benetzungsfilmen endlicher Dicke aus, so kommt es bei Veränderung der Oberflächenladung zu einem Übergang von monotonen zu nichtmonotonen Profilen des elektrostatischen Potentials (Fig. 4.13). Nichtmonotone Profile des elektrostatischen Potentials sind äquivalent zum Auftreten einer Ladungsinversion. Oberflächenpotential und -ladung verschwinden *nicht* gleichzeitig (Fig. 4.14), d.h. Ladungsnullpunkt und isoelektrischer Punkt fallen nicht zusammen, da neben der Coulomb-Kraft noch Hartkörperkräfte wirken.

Summary

The technological importance of fluids of charged platelike colloids, such as clay, is based on a rich phase behaviour including sol-gel transitions, flocculation, and even liquid crystalline phases promoted by translational, orientational, as well as charge degrees of freedom of the constituting particles. In order to control fluids of charged platelike colloids in technologically relevant set-ups, these systems have to be understood not only with respect to their bulk properties but also in the presence of spatial inhomogeneities such as fluid-fluid or fluid-substrate interfaces. The latter case for charged substrates is of particular importance because electrodes are a common means to manipulate fluids of charged particles. Whereas some theoretical studies of bulk fluids of charged platelike colloids have been performed in the past, no theoretical investigations of inhomogeneities of such systems have been undertaken prior to this work.

Within the present work, a model fluid composed of a ternary mixture of monodisperse platelike macroions and salt ions is considered. The particles are modelled by hard cuboids with their edges constrained to be parallel to the Cartesian axes corresponding to the Zwanzig model and the charges of the particles are kept fixed and concentrated in their centres (Fig. 2.1). A density functional theory is developed which is able to describe the model fluid of macroions and salt in bulk configurations, with a free interface between coexisting bulk phases, as well as in the presence of a charged substrate. It provides a qualitative approach because it does not determine the relation between the actual and the effective charges entering into the model. Technically motivated approximations, such as using the Zwanzig model, are expected not to influence the results qualitatively.

The bulk phase diagrams in terms of densities (Fig. 3.1) exhibit one isotropic phase and one nematic phase separated by a first-order phase transition. For increasing macroion charge and fixed salt densities, the two-phase coexistence region is shifted to larger macroion packing frac-

tions. For fixed macroion charge and increasing salt density, the limit of quasi-hard platelets is approached. The Donnan potential between coexisting phases (Fig. 3.2) can be expressed in terms of the particle chemical potentials obtained from bulk structure calculations.

Bulk and surface phase diagrams (Fig. 3.3) in terms of macroion charge, supersaturation, and surface charge density are calculated by means of an asymptotical analysis of effective interface potentials and by numerical solutions of the Euler-Lagrange equations. The effective interface potentials exhibit the same asymptotic behaviour as systems governed by non-retarded isotropic dispersion forces although the model does *not* include dispersion forces. The origin of this phenomenon can be traced back to using within the density functional a particle-particle pair distribution function which decays asymptotically with a Debye-Hückel form.

The proposed density functional theory is able to describe the structure of free fluid-fluid interfaces. This property is not trivial in the case of fluids of charged particles. Density and nematic order parameter profiles at free interfaces between isotropic and nematic phases at coexistence (Figs. 4.1 and 4.2) show non-monotonic behaviours. The value of the nematic order parameter in the nematic bulk phase decreases upon increasing the macroion charge. The width of the interface is approximately given by the Debye length. The interfacial tension decreases upon increasing the macroion charges. An electrical double layer forms at the free interface (Fig. 4.3). The corresponding electrostatic potential profiles (Fig. 4.4) exhibit a monotonic behaviour.

Complete wetting of a charged substrate in contact with an isotropic bulk phase by a nematic phase occurs in between two first-order wetting transition points on the isotropic-nematic bulk coexistence curve (Fig. 4.5) whereas only partial wetting occurs at the remaining parts of the isotropic-nematic coexistence line (Fig. 4.6). The continuous but limited increase of the excess adsorption (Fig. 4.7) and of the wetting film thickness (Fig. 4.8) upon approaching the wetting transition points is used to locate the wetting transition points within the phase diagrams. Whereas the first-order character of the wetting transitions and the asymptotic power law of the excess adsorption upon complete wetting have been inferred from analytical considerations, the location of the wetting transition points must be obtained numerically. The corresponding prewetting lines are not resolved numerically.

First-order drying of a charged substrate in contact with a nematic bulk phase by the isotropic phase, characterised by a discontinuous divergence of the excess adsorption upon crossing the drying transition point, is found at isotropic-nematic coexistence (Fig. 4.9). The predrying line, where the excess adsorption shows a finite discontinuity (Fig. 4.11), terminates at a critical point (Fig. 4.10). As expected, salt ion densities and counter ion densities close to the wall are strongly influenced by the surface charges (Fig. 4.12).

If quasi-free isotropic-nematic interfaces between the bulk and wetting films of finite thickness form, a crossover is found from monotonic to non-monotonic electrostatic potential profiles upon varying the surface charge density (Fig. 4.13). Non-monotonic electrostatic potential profiles are equivalent to the occurrence of charge inversion. Surface potential and surface charge do *not* vanish simultaneously (Fig. 4.14), i.e., the point of zero charge and the isoelectric point of the surface do not coincide due to the presence of both Coulomb interactions and hard-core repulsion.

Chapter 1

Introduction

The scientific and technological importance of clays as colloidal suspensions composed of charged platelike particles is discussed and the goals of this work, revolving around the modelling of inhomogeneities in fluids composed of charged platelike colloids, are specified. From the scientific point of view, fluids of charged platelike colloids are located at the borderlines between electrochemistry, physics of complex fluids, and colloid science. Hence there is the opportunity to combine successful concepts of these fields and, moreover, to learn about their interrelation. In order to embed the present work into the current scientific context, selected issues are briefly reviewed.

1.1 Aim of the present work

Clay is one of the oldest and most versatile materials being used by mankind. If wet it is soft and able to take almost any shape whereas it becomes hard and fragile when dried. Loosely distributed clay is a necessary condition for fertile soil, the stability of concrete hinges upon the crosswise arrangement of clay particles, catalytic converters and filters often use porous clay matrices, clay is a widely used filling material in cosmetics and paper industries, etc. Moreover, the properties of clay are related to various environmental phenomena such as the occurrence of mud avalanches at treeless hillsides or the decay of soil productivity upon flooding with sea water.

Therefore, it is understandable that clay has been a subject of research for a long time. In 1938, Langmuir observed an isotropic-anisotropic transition by performing a thorough analysis of bentonite [Langmuir1938], which form upon the weathering of volcanic ashes. By means of birefringence and rheological measurements, which are nowadays standard methods [Mourchid1995], he characterised the anisotropic structure as a gel. Bentonite comprises mostly the clay mineral montmorillonite, which has been investigated intensively [Leach2005, Norrish1954, Rand1980]. For a comprehensive overview over clay minerals see the book of Giese and van Oss [Giese2002].

The distinct properties of clay are brought about by particles of platelike shape which are decorated with charged groups. The actual shape and size of clay particles is determined by their evolution or fabrication process. The clay surface charge, however, varies according to the electrolytic environment, particularly upon changing the pH. Moreover, due to the typical size of their constituting particles in the range between 10 nm and 1 μm, clays can be considered as colloids [Hunter2001, Russel1989, Shaw1980]. The colloidal particles interact with each other due to the charges as well as due to their intrinsic platelike volume, which gives rise to entropically induced liquid crystal transitions. Moreover, dispersion forces provide an attractive interaction which can lead to flocculation if the charges are too small or too strongly screened.

Whereas either the charge or the platelike character has been addressed in investigations of *inhomogeneous* colloids, no such studies of the combination of both properties have been performed prior to the present work. Possible inhomogeneities in colloids are *free interfaces* due to the spatial contact between thermodynamically coexisting bulk phases, *fluid-substrate interfaces* due to system boundaries, or density gradients due to *external fields* such as gravitation. Electrically charged surfaces, e.g., electrodes, are of particular technological importance for charged colloids as they offer the possibility to manipulate the fluid behaviour in a simple way. In order to control the fluid properties by means of an electrode, the surface phase behaviour of that fluid has to be known.

The purpose of the present work is twofold: First, a well-defined, physically sensible, and numerically tractable model of fluids of charged platelike colloids will be developed which allows one to describe homogeneous as well as inhomogeneous systems on the same footing. This non-trivial task is addressed in Ch. 2. Secondly, the model developed in Ch. 2 will be thoroughly investigated with respect to the bulk phase behaviour (Sec. 3.1), to the structure of free interfaces between coexisting isotropic and nematic bulk phases (Sec. 4.1), to the surface phase behaviour (Sec. 3.2) considering wetting (Sec. 4.2) and drying (Sec. 4.3) of a charged substrate, as well as to the electrostatic properties of the model fluid in contact with an electrode (Sec. 4.4).

In view of many experimentally undetermined parameters describing fluids of charged platelike colloids and the technically demanding anisotropic particle-particle interactions, the investigation within the present work is carried out only on a *qualitative* level. This has to be considered already as significant progress because present experimental and computer simulational techniques are not yet developed to such an extent in order to perform precise analogous studies of interfacial structures or wetting of charged substrates in fluids of charged platelike colloids. This work is intended to establish a model exhibiting a rich bulk and surface phase behaviour which is expected to provide guidance for future experimental and theoretical studies.

Modelling inhomogeneities in fluids of charged platelike colloids implies the consideration of bulk as well as interfacial and surface properties. Hence the remaining sections of this chapter are devoted to a brief review of relevant aspects of bulk fluids (Sec. 1.2) and inhomogeneous fluids (Sec. 1.3).

1.2 Bulk fluids

1.2.1 General theoretical approaches

Throughout the 19th century equilibrium bulk fluids have been described in terms of the empirical ideal gas equation of state modified by activity coefficients or later by the van der Waals equation of state. These equations of state contain a priori undetermined parameters which have to be adapted in order to fit measurements. Since the advent of statistical mechanics it is in principle possible to construct theories of fluids by merely defining the interaction potentials [Hansen1986, McQuarrie2000]. Unfortunately, only very simplistic models such as the one-dimensional hard particle fluid [Herzfeld1934, Tonks1936] are analytically soluble. In order to handle more complicated systems such as fluid mixtures [Kirkwood1951, McMillan1945], graphical methods [Hansen1986, Mayer1958, McDonald1978, Uhlenbeck1962], variational formulations [deDominicis1962], and perturbation schemes [Barker1967/1, Barker1967/2, McQuarrie1966, Weeks1971, Zwanzig1954] have been developed.

One class of general descriptions of bulk fluids is furnished by integral equation theories. The main ingredient besides the Ornstein-Zernike equation [Ornstein1914], which relates the pair correlation function and the direct correlation function, is a closure relation, which provides an independent relation between the pair correlation function and the direct correlation function [Caccamo1996, Hansen1986]. The fact that closure relations are not exactly known renders integral equation theories approximative. Classical closure relations are due to Percus and Yevick (PY) [Percus1958, Percus1962] as well as the hypernetted chain (HNC) approximation due to Morita [Morita1958, Morita1959, Morita1960/1, Morita1960/2]. The PY theory has been solved analytically for one-component fluids [Thiele1963, Wertheim1963, Wertheim1964] as well as for mixtures [Lebowitz1964]. Due to the approximative character of closure relations, thermodynamic consistency between the virial route, the energy route, and the compressibility route are not obvious from the outset. For example, virial and compressibility route within PY theory lead to different equations of state [Hansen1986].

A generalisation of the PY closure for hard-sphere fluids to arbitrary interaction potentials is the so-called mean spherical approximation (MSA). The corresponding integral equation theory has been solved exactly for charged hard spheres [Waisman1970, Waisman1972/1, Waisman1972/2]. Due to the availability of an analytical solution, the thermodynamics of this MSA model in the bulk [Blum1977] and at charged walls [Henderson1978] has been elaborated extensively. Like PY theory, the MSA theory for charged hard spheres is thermodynamically inconsistent. In order to remedy this inconsistency, the generalised mean spherical approximation (GMSA) has been introduced [Hoye1974]. Although the GMSA of ionic fluids has not been solved analytically the asymptotic decay of the correlation functions has been obtained by means of a pole analysis [LeotedeCarvalho1994], which is also applicable to other integral equation theories [Evans1994]. An exactly soluble integral equation theory is obtained by choosing the so-called *Yukawa closure*, which is in principle the MSA of a linear combination of Yukawa potentials [Hoye1977]. The basic idea behind the introduction of the Yukawa closure is to approximate a given interaction potential, e.g., of Lennard-Jones type, by a sufficiently large sum of suitably chosen Yukawa potentials and thereby finding an approximately analytical MSA solution of the potential of interest. Moreover, the integral equation theory of the Yukawa closure has been solved for mixtures [Blum1980].

Besides their application as model systems, fluids of hard particles are widely used as reference systems within liquid state theory. Scaled particle theory [Helfand1960, Oversteegen2005] is a general approach to fluids of hard particles, which has first been applied to hard spheres [Helfand1961, Reiss1959, Reiss1977]. A generalisation to mixtures of hard particles is straightforward [Lebowitz1965]. Over the years, the important hard sphere fluid has attracted a lot of attention leading to some quite reliable equations of state. The probably most popular compromise between precision and simplicity is furnished by the equation of state proposed by Carnahan and Starling [Carnahan1969] which has been extended to mixtures by Mansoori and coworkers [Mansoori1971]. Generalisations of these equations of state are proposed until recently [HansenGoos2006]. Scaled particle theory is well applicable to hard particles of any shape. The reference system composed of hard platelets which will be used within the present work, is based on scaled particle theory. Another general method to describe the interaction between fluid particles of arbitrary shape is the reference interaction site model (RISM) [Chandler1972].

A general feature of mixtures of large and small particles with hard cores is the presence of an effective interaction on purely entropic grounds: Any large colloid particle produces an excluded volume for the small particles. If the excluded volumes of two large colloidal particles overlap the small particles gain translational entropy which leads to an effective attraction between the large colloidal particles. As the small particles are depleted from the space between the colloidal particles, this entropic attraction is called *depletion force*. A theoretical prediction has been given by Asakura and Oosawa [Asakura1954, Asakura1958] and experimental phase diagrams of colloid-polymer mixtures have been well established [Helden2004, Lekkerkerker1992]. Moreover, theoretical work aiming at quantitative description of depletion potentials by means of density functional theory is nowadays available [Roth2000, Roth2003, Roth2006]. The model presented in this work can also be considered as a mixture of large and small particles with hard cores. Depletion interactions, which particularly manifest themselves in a pronounced attraction of large particles to a hard substrate, are implicit in the density functional to be described in Ch. 2.

1.2.2 Fluids of charged particles

Fluids of charged particles such as electrolyte solutions exhibit a completely different behaviour as compared to hard particle fluids due to the Coulomb interaction between charges. The emergence of bulk theories of electrolytes is connected with the proposition of dissociation of salt into ions upon dissolution in water. This fact was not obvious from the outset and quite some progress has been made by determining the correct number of particles dispersed in the system which allowed one to calculate approximately the osmotic pressure by means of van't Hoff's law [Arrhenius1887]. Whereas the approximation of ions by noninteracting particles proved valid for weak electrolytes, which produce only a small amount of ions, there were large deviations between theory and experimental results in the case of strong electrolytes. Debye and Hückel [Debye1923] resolved this problem for the case of dilute solutions of strong electrolytes by introducing the concept of what is nowadays called *correlations*: Although the solution is locally charge neutral on average, close to a positively charged ion there will be preferably negatively charged ones and vice versa. By solving the linearised radial Poisson-Boltzmann equation within a comoving frame of a single ion, approximate analytical expressions for the free energy and the pair distribution functions can be obtained. The probably most important property revealed by Debye and Hückel is the exponential screening of the ion charge by the surrounding cloud of oppositely charged ions. These results are asymptotically correct in the limit of high dilution [Kirkwood1954, McQuarrie2000]. The opposite limit of concentrated electrolytes has been studied by Onsager [Onsager1933]. Debye-Hückel theory has been extended in many respects. One important extension, initiated by Bjerrum [Levin1996, Levin2002], is related to the formation of so-called *ion pairs* which consist of ions whose attractive electrostatic interaction energy is larger than the thermal energy [Fuoss1934, Levin1996, Lovett1968, Poirier1961, Reiss1956, Stillinger1968/1, Tamashiro1998].

The fundamental question about the existence of the thermodynamic limit of electrolyte solutions is non-trivial due to the long-ranged Coulomb interaction between the dissolved ions. For globally charge neutral systems composed of charged hard particles the existence as well as the independence of the boundaries in the thermodynamic limit have been proved by Lebowitz and Lieb [Lebowitz1969, Lieb1972]. Furthermore exact sum rules have been established. Two sum rules concerning bulk electrolyte solutions are due to Stillinger and Lovett [Stillinger1968/1, Stillinger1968/2]: The first asserts that the charge of an ion is completely screened by its surrounding screening cloud whereas the second furnishes a somewhat technical condition on the second moment of the distance with respect to the radial distribution function.

A simplifying model of ionic solutions is given by the *one-component plasma*, which is the classical analogue to the jellium model for the electron gas within solids. It comprises one ionic species dispersed in a structureless, uniformly charged background, which leads to a globally charge neutral system. This model offers the possibility to test theoretical approaches analytically in order to assess the physical nature of certain approximations [Baus1980, Nordholm1984, Tamashiro1999].

Models for charged spherical colloids are of great interest in colloid science. The celebrated DLVO theory [Hunter2001, Russel1989, Verwey1948] is based on the model of hard spherical colloids interacting via Coulomb and van der Waals interactions. It has been reviewed quite recently [Belloni2000, Hansen2000]. DLVO theory inspired many investigations of various aspects of interactions between charged spheres such as the effective interaction [Harnau2002/2, vanRoij2000], phase behaviour [Sogami1984, Tamashiro2003, vanRoij1999, vonGrunberg2001, Warren2000, Zoetekouw2006], or counterion condensation [Levin1998, Lowen1993].

Charged *platelike* particles provide an analytical challenge because of their reduced rotational symmetry as compared to spherical particles. Approaches with a maximum of remaining symmetry are Wigner-Seitz cell methods [Trizac1997]. Far-field approximations, similar to the multipole expansion of classical electrostatics, reveal an anisotropic effective plate-plate interaction [Agra2004, Trizac2002]. The structure factor of charged discs obtained by means of an interaction site model compares well with results from neutron scattering at laponite platelets [Harnau2001]. Moreover, theoretical bulk phase diagrams of charged discs have been elaborated in terms of an effective hard-platelet model [Rowan2002] or by field-theoretical methods [Lue2006]. An important observation related to the interaction potential of charged colloids is the applicability of asymptotic expressions, such as the screened Coulomb potential within Debye-Hückel theory, provided the bare charges are replaced by effective charges [Alexander1984, Bocquet2002]. The usage of effective limiting laws for large colloid-colloid separations are computationally advantageous because they are of particular simple form. In this work an effective pair distribution function of Debye-Hückel form will be applied.

Upon bringing two fluids into contact separated by a semipermeable membrane, particle currents occur in order to establish thermodynamic equilibrium. Necessary conditions are equal chemical potentials of the particles which can pass the membrane. For the case of electrolytic solutions this condition does not imply equal concentration because an electrostatic potential difference occurs at the membrane which is able to stabilise a concentration gradient [Donnan1911, Donnan1924]. This phenomenon is called *Donnan effect* and the electrostatic potential difference at the membrane is termed *Donnan potential* [Adamson1973]. Within the present work, this effect will also occur at fluid-fluid interfaces.

Field theories for ionic systems [Caillol2003, Caillol2005, Ciach2005] have been applied to a large extent during the last years because they provide formally exact representations of the model under consideration. Such exact representations offer the possibility to introduce approximations in a controlled way thereby clarifying their range of validity. Poisson-Boltzmann theory, e.g., is recovered as the mean-field, i.e., zero-loop, description in the weak coupling limit [Coalson1992, Netz1999, Netz2000/1, Netz2000/2]. The corresponding mean-field equation is the sine-Gordon equation, which resembles the Poisson-Boltzmann equation [Caillol2001, Caillol2004, Raimbault2001]. Systematic improvements are possible within field theory: In the strong coupling limit, for instance, a virial or high-temperature, expansion is applicable [Netz2000/2]. Expansions beyond mean-field theory serve to study the critical behaviour of ionic systems [Ciach2000, Ciach2001, Ciach2002, Ciach2003].

The pairwise *attraction* of oppositely charged particles within a mixture of charged hard spheres fulfils a necessary condition of ”liquid-vapour” phase separation. The existence of such a phase separation and the corresponding critical point in the case of the restricted primitive model (RPM), which comprises a binary mixture of oppositely charged hard spheres of equal size and valency, has been established by Stell and coworkers [Stell1976]. Later Stell [Stell1992] argued that the RPM critical point belongs to the Ising universality class which has recently been confirmed by computer simulations [Caillol2002, Luijten2002]. In view of the exponential screening of Coulomb potentials within electrolyte solutions this result might appear to be not too surprising. On the other hand, at that time there seem to exist two classes of ionic systems: those which exhibit Ising critical behaviour and those which exhibit mean-field (or classical) critical behaviour [Fisher1994, Stell1995]. This different behaviour has been suspected to arise from different mechanisms: If Coulomb interactions drive the phase separation, as for the RPM, so-called *Coulombic criticality* occurs, whereas phase separation due to solvent-solute repulsion results in so-called *solvophobic criticality* [Fisher1994, Stell1995]. Numerous analytical [Ciach2001, Ciach2002, Fisher1993, Levin1994, Levin1996] as well as computer simulational [Artymov2003, Kobelev2002/1, Kobelev2002/2, Panagiotopoulos2005] studies of ionic criticality have been performed in recent years. First experimental studies of criticality in ionic systems pointed towards both Ising [Johnson1964] as well as mean field [Pitzer1985] behaviour. However, after recent thorough cross-checks, no convincing experimental evidences for mean-field critical behaviour of ionic fluids remain and it is expected that actual ionic fluids generally exhibit Ising criticality [Schroer2006].

1.2.3 Liquid crystalline phases in platelike colloids

Liquid crystal phase transitions [deGennes1993, Singh2000] in suspensions of *rodlike* colloids have been studied for decades. Widely used model systems are suspensions of V_2O_5 needles or tobacco mosaic virus [Dogic2006] as well as more recently investigated mineral systems such as boehmite dispersions [Buining1993, Buining1994]. Compared to rodlike colloids, observing liquid crystal transitions in suspensions of *platelike* colloids is rather challenging because these transitions are usually preempted by gelation [Davidson2005, Langmuir1938]. In recent years, this gelation transition has been widely studied for the model clay laponite [Gabriel1996, Knaebel2000, Levitz2000, Mourchid1995, Mourchid1998, Nicolai2000, Nicolai2001, Porion2001]. True liquid crystal transitions of platelike colloids became possible only in recent years due to the development of methods to synthesise model systems which do not merely undergo gelation. The most intensively studied material is gibbsite ($Al(OH)_3$) [vanderBeek2003, vanderBeek2004, vanderKooij1998, vanderKooij2000/1, vanderKooij2000/2, vanderKooij2001, Wijnhoven2005]. Suspensions of gibbsite platelets can be either charge or sterically stabilised. Other systems under investigation are composed of layered double hydroxides [Liu2003, Wang2005] or nickel(II) hydroxide ($Ni(OH)_2$) [Brown1998, Brown1999].

The application of standard computer simulational techniques [Allen1987] for investigations of platelike particles is quite demanding because of low acceptance rates of Monte Carlo moves or short time scales within molecular dynamics due to the platelike geometry. Due to increasing computer power and by improving the simulational techniques, in particular due to the development of the transition path sampling method [Dellago1998], modern computer simulation studies of platelike particles not only lead to phase diagrams [Casey1995, John2005, Meyer2001/1, Meyer2001/2, Veerman1992] but can even serve to calculate interfacial properties [Vink2005/1, Vink2005/2]. Due to this progress, computer simulations become an alternative to actual experiments.

The increasingly large amount of experimental and computer simulational data on liquid crystalline systems calls for more and more sophisticated theoretical descriptions in terms of which these data can be interpreted. Theoretical studies of liquid crystal phase transitions have been performed intensively on the level of phenomenological theories within the framework of Franck elasticity theory [deGennes1993, Singh2000]. On the other hand, microscopic models of such phase transitions in fluids of rodlike or platelike particles are still under construction. The first approach to describe *rodlike* colloidal particles is the second-order virial approximation of infinitely long thin needles due to Onsager [Onsager1942, Onsager1949]. This theory is very popular and it gave rise to various extensions relaxing some or all geometrical restrictions on the particles [Lekkerkerker1984, Shundyak2001, Shundyak2002, Shundyak2003, Shundyak2004, Shundyak2006, vanRoij2005, Varga2005]. Although introduced for rodlike particles, an Onsager-like theory is also applicable to *platelike* particles [Forsyth1978, Wensink2001]. Only a few investigations of freely rotating platelike particles go beyond the Onsager theory [Harnau2002/1]. Zwanzig simplified the Onsager theory for rods even more by restricting the orientations of the rods to only three mutually orthogonal directions which allowed him to calculate virial coefficients up to 6th order [Zwanzig1963]. This Zwanzig approximation has been applied to rodlike as well as to platelike particles [Cuesta1999]. In contrast to infinitely long thin needles, where a second-order virial theory is sufficient [Zwanzig1963], one needs at least third-order density terms for infinitely wide thin plates [Harnau2002/4]. Within the present work, a fundamental measure functional for parallel hard parallelepipeds [Cuesta1997/1, Cuesta1997/2], which reproduces the exact second and third virial coefficients for bulk systems, will be applied. The *bulk* phase behaviour within this model has been investigated to some extent for cubes [MartinezRaton1999] as well as for rod- and platelike objects in three-dimensional [Bier2004, Harnau2002/4, MartinezRaton2003, MartinezRaton2004] and in two-dimensional [MartinezRaton2005] systems. In contrast, studies of *interfaces* in fluids of hard platelike particles within Zwanzig approximation have been rarely performed so far [Bier2004, Harnau2002/3, Moore1992].

1.3 Inhomogeneous fluids

1.3.1 Density functional theories of classical fluids

Density functional theories, which describe fluids in terms of one-particle density profiles, are the method of choice for studies of inhomogeneous classical [Evans1979, Evans1989, Evans1992, Wu2006] as well as quantum [Ebner1975, Padmore1974, Saam1975, Stringari1987] fluids. The density functional method has been first formulated in the 1960s within studies of the electron gas in solids [Hohenberg1964, Mermin1965]. However, it has been implicitely applied in much earlier theories of classical fluids [Onsager1942, Onsager1949, Rowlinson1979, vanderWaals1894]. Early classical density functional theories applied the random phase approximation (RPA) [Johnson1981, Harrowell1982, Hooper1980, Hooper1981/1, Hooper1981/2, Hooper1982, Nordholm1980/1, Nordholm1980/2, Nordholm1981, Nordholm1982/1, Nordholm1982/2]. However, these theories were not able to appropriately accounted for the freezing transition because the density configurations corresponding to solid phases are rapidly varying in space. Hence the freezing transition has been considered as a benchmark for reliable density functionals [Baus1985, Colot1985, Colot1986, Curtin1988, Haymet1986, Lutsko1990/1, Lutsko1990/2]. Progress has been made by the introduction of weighted density approximations (WDA) of various levels of sophistication [Curtin1985, Denton1989, Tarazona1984, Tarazona1985].

A special class of WDA is formed by so-called fundamental measure theories (FMT) which have been introduced by Rosenfeld [Rosenfeld1989] for a fluid of hard spheres. The key idea of FMT is the choice of the weight functions according to geometric quantities of single particles (*fundamental measures*) such as the particle number, the diameter, the surface area, or the volume, instead of two-particle quantities such as excluded volumes. An alternative but equivalent form of Rosenfeld's FMT has been derived by Kierlik and Rosinberg [Kierlik1990, Phan1993]. Rosenfeld's theory for spatially homogeneous densities reproduces the Percus-Yevick equation of state. In contrast, the so-called White Bear functional by Roth and coworkers [Roth2002] is constructed in order to lead to the generalised Carnahan-Starling equation of state [Mansoori1971]. The possibility of constructing fundamental measure theories of fluids of non-spherical particles has been studied [Rosenfeld1994, Rosenfeld1995, Wertheim1994]. It has been found that this problem is *not* generally soluble with a *finite* number of weight functions. With respect to freezing the original Rosenfeld FMT led to an unstable solid for *all* packing fractions. In order to avoid this unphysical property, density functionals with correct *dimensional crossovers* have been developed [Rosenfeld1996, Rosenfeld1997], i.e., the density functional evaluated for density profiles corresponding to confined geometries of effectively lower dimension reduce to the density functional corresponding to that lower dimension. For hard sphere fluids it is possible to construct fundamental measure functionals of arbitrary dimension by requiring correct dimensional crossovers to the known zero-dimensional density functional [Tarazona1997]. One could also set out from the one-dimensional system because the corresponding density functional is also known exactly [Percus1976].

A model which allows for the construction of an FMT which is even simpler and more transparent than for fluids of hard spheres is furnished by fluids of parallel hard parallelepipeds (cuboids) [Cuesta1996, Cuesta1997/1, Cuesta1997/2, MartinezRaton1999, MartinezRaton2003]. This model is of particular importance for the present work, as a fluid of hard platelike particles modelled by such hard cuboids will be used as a reference system. The corresponding fundamental measure functional can be derived either by requiring correct dimensional crossovers to the zero-dimensional density functional [Cuesta1997/1] or by means of scaled particle theory [Cuesta1997/2].

In principle, integral equation theories are also applicable to inhomogeneous fluids [Oettel2005, Plischke1988, Plischke1989]. However, besides the Ornstein-Zernike equation and the (approximative) closure relation one has to specify a third equation relating the density profiles to the correlation functions or the direct correlation functions. Such an additional equation may be the first Yvon-Born-Green equation [Hansen1986] or the Euler-Lagrange equation of a density functional theory. The major disadvantage of inhomogeneous integral equation theory as compared to density functional theory is the difficult construction of approximative closure relations from physical intuition.

1.3.2 Interfacial structure and wetting

The structure of interfaces between coexisting bulk phases is of importance of both fundamental and applied science: It is intimately related to the interactions between the constituting particles which determine important interfacial quantities such as the interfacial tension.

Van der Waals was the first who calculated the interfacial structure via an expansion of the free energy in gradients of density profiles [Rowlinson1979, vanderWaals1894]. Later Cahn and Hillard reintroduced essentially the same formalism [Cahn1958/1, Cahn1958/2, Cahn1959]. Within the van der Waals-Cahn-Hillard approach the interfacial structure is represented by a smoothly varying profile with translational symmetry parallel to the interface. This description is in contrast to the capillary wave picture introduced by Buff, Lovett, and Stillinger [Buff1965] which considers a sharp, steplike intrinsic density profile with thermally activated undulations parallel to the interface. Nowadays, both descriptions are considered as extreme cases of a general interfacial theory in which fluctuations of wave lengths smaller than the bulk correlation length are attributed to the intrinsic profile whereas fluctuations of wave lengths larger than the bulk correlation lengths are called capillary waves [Mecke1999, Napiorkowski1993, Weeks1977].

The presence of electrolytes in a fluid phase influences the interfacial tension: Wagner observed that the liquid-vapour interfacial tension increases upon increasing the salt concentration [Wagner1924]. He attributed this phenomenon to the repulsion of the ions from the liquid-vapour interface due to their image forces. Later, Onsager and Samaras developed a considerably simplified theory by assuming, in contrast to Wagner, a spatially homogeneous screening of the surface charge [Onsager1934]. An analytically convenient *canonical* approach has been proposed by Levin [Levin2000, Levin2001]. The interfacial tension of an ionic solution in contact with a charged wall is not only influenced by the salt concentration of the liquid but also by the electrostatic surface potential. This gives rise to *electrocapillarity* [Grahame1947] (or *electrowetting*), which has meanwhile found several applications in lab-on-a-chip devices, micro lenses, fibre optics, or display technology [Mugele2005, Quilliet2001].

Measuring interfacial properties of fluids and solids is a challenge because in most cases the signals due to interfacial fluid particles superimpose onto much stronger signals from particles in the bulk. X-ray and neutron reflectometry, which is sensitive to the *gradient* of the mean scattering length density, offers a rather straightforward method to directly obtain interfacial density profiles [Thomas1996]. Grazing incidence X-ray and neutron scattering provide spatially resolved information on interfacial fluctuations [Dietrich1995]. In contrast, ellipsometry yields only indirect information on the interfacial structure [Bain1998, Keddie2001, Teppner1999]. Very rich interfacial data corresponding to particle orientations and conformations is obtained by means of non-linear optical methods such as *second harmonic generation* (SHG) or *sum-frequency generation* (SFG), which occur only in regions *without* spatial inversion symmetry [Bain1998, Shen1989, Vidal2005]. In particular, the addition of an infrared interface signal to a monochromatic visible light laser beam applying SFG shifts the interface signal into the experimentally advantageous visible light range of the electromagnetic spectrum.

Within a macroscopic description, *wetting* of a substrate in contact with a fluid phase by another fluid phase occurs if the contact angle of the latter phase vanishes. Young's equation relates this contact angle to the interfacial tensions. Microscopic theories, such as density functional theories, enable one to calculate the interfacial tensions in terms of model parameters. In terms of a microscopic point of view, wetting amounts to the formation of a macroscopically large film upon approaching phase coexistence along a thermodynamic path. Under these conditions, substrate potentials compete with fluid-fluid interactions giving rise to an *effective interface potential* of the depinning interface. The wetting behaviour can be completely inferred from monitoring the minimum of the effective interface potential. A brief introduction into the concepts of *wetting theory* to the extent used in this work will be given in Sec. 2.5. Thorough treatments on *wetting phenomena* can be found in Refs. [deGennes1985, Dietrich1988, Schick1990, Sullivan1986] and certain recent trends are reviewed in Ref. [Bonn2001].

1.3.3 Charged substrates

Upon bringing a hydrophilic substrate, such as a container wall or the surface of a colloidal particle, into spatial contact with an electrolyte solution the substrate becomes charged due to adsorption and desorption of charge determining ions. The surface charge density acquired by the substrate depends on the structure of the ion density profiles which in turn are determined by the surface charge density.

The adsorption and desorption processes for given ion distributions are usually modelled in terms of chemical reactions and accompanying reaction constants. Several models have been developed which differ in the number of chemical reactions taken into account. The traditional approach considers two chemical reactions, one adsorption and one desorption reaction, and is termed *2pK model* [Chan1975, Davis1978, Healy1978]. Adsorption and desorption at some mineral surfaces, such as gibbsite ($Al(OH)_3$), takes place at certain binding sites which are either occupied or unoccupied. Within the so-called 1*pK* model [Bolt1982, Hiemstra1987, vanRiemsdijk1986] the charge regulation of such substrates is described by only one adsorption / desorption reaction. Both approaches are special cases of the MUlti SIte Complexation model (MUSIC) [Hiemstra1989] which is able to take into account many types of binding sites of different activities. The challenge within all of these charge regulation models resides in determining the reaction constants which are typically fixed by fits to experimental values of the ζ potential or of the isoelectric point [Hunter1981, Kosmulski2002, Kosmulski2004, Kosmulski2005, Kosmulski2006, Sondi1997]. Nowadays charge regulation models are standard tools in studies of surface properties which serve to relate model parameters to experimentally accessible quantities [Biesheuvel2001, Hecht2006, Rahnemaie2006].

The inverse problem of determining the density profiles of ions in the vicinity of a charged substrate of given charge density has been addressed for more than a century. Intuitively one expects the attraction of oppositely charged ions and the repulsion of like-charged ions by a charged wall. In the 19th century, the structure of electrolytic solutions close to a charged substrate was described by the so-called *electrical double layer* modelled as a capacitor composed of the charged substrate and the Helmholtz layer, which is a planar arrangement of ions located parallel to the substrate exactly neutralising the surface charge [Helmholtz1879]. Later Gouy [Gouy1910] and Chapman [Chapman1913] introduced the alternative picture of a diffuse layer by using the *Poisson-Boltzmann equation*. The latter comprises the Poisson equation of electrostatics with the charge density approximated by a sum of the bulk charge densities of each ion species weighted by a Boltzmann factor corresponding to the electrostatic energy of that ion species in the local electrostatic field. The electrostatic potential for 1:1, 1:2, and 2:1 electrolytes obtained within Gouy-Chapman theory decays exponentially [Gouy1910]. This result is generally expressed as the *screening* of the surface charge by the surrounding mobile ions. The calculated capacity of the Gouy-Chapman electrical double layer did not agree well with experimental data, which Stern attributed to the ability of ions within Gouy-Chapman theory to approach the substrate down to zero distance [Stern1924]. Hence he proposed a gap of molecular width free of ions between the substrate and the so-called Stern layer, which is formed by ions adsorbed to the substrate. In contrast to the Helmholtz layer, the Stern layer does not neutralise the surface charges completely. Beyond the Stern layer a diffuse layer in the spirit of Gouy and Chapman is assumed. Since Stern's unification of Helmholtz and Gouy-Chapman theory, various surface models have been proposed which differ mainly in the number of Stern layers and the presence or absence of a diffuse layer [Westall1980].

An alternative to *proposing* ad hoc models for the ionic structure near charged walls is furnished by density functional theories, which offer the opportunity to *calculate* inhomogeneous structures. Early studies by Evans and Sluckin have been performed within the local density approximation in conjunction with the Poisson equation [Evans1980, Sluckin1981]. Today, more advanced, non-local density functionals, based upon the weighted density functional approach, are in use [MieryTeran1990, Patra1993, Patra1994/1, Patra1994/2, Patra1999, Patra2002/1, Patra2002/2, Tang1990] which are able to reproduce computer simulational results [Torrie1979, Torrie1982] with a high degree of accuracy. Moreover, exact sum rules offer another possibility to assess the reliability of density functional approaches [Blum1981, Carnie1981/1, Carnie1981/2, Gruber1981, Henderson1979, Henderson1981].

Whereas Poisson-Boltzmann theories provide simple and reliable approaches for weakly charged substrates, they become invalid in the strong coupling limit [Netz2001/2]. However, the "apparent" surface charge density at large distances from the substrate is small due to the screening by ions. Hence the application of Poisson-Boltzmann theories is justified provided the surface charge is renormalised properly [Aubouy2003, Netz2003]. Ions condensed onto strongly charged substrates form quasi two-dimensional plasmas [Moreira2000, Moreira2002/1, Moreira2002/2, Rouzina1996, Shklovskii1999]. Two-dimensional plasmas are isomorphic to the xy model for which the Kosterlitz-Thouless transition, a binding-unbinding transition of vortices at low densities, takes place [Kosterlitz1973, Levin2002]. In the language of electrolytes this transition corresponds to an insulator-conductor transition due to the formation of ion pairs. Interestingly, some two-dimensional Coulomb systems are or are expected to be exactly soluble [Samaj2003, Samaj2004, Samaj2005/1, Samaj2005/2, Tellez2005/1, Tellez2005/2]. Analytical solutions of two-dimensional electrolytes are extremely valuable because they offer the possibility of analytical studies of correlations in such systems, which are considered to be responsible for effects such as *like-charge attraction* and *charge inversion* [Levin2002].

An attraction between equal, like-charged particles was reported for experiments on geometrically confinded colloidal suspensions [Kepler1994, Crocker1996, CruzdeLeon1998, Han2003, Grier2000, Grier2004]. These measurements have been performed by means of digital video microscopy which leads to pair distribution functions. Using the zero-order density approximation to the pair distribution functions or integral equation closures, one obtains approximate effective interaction potentials. These investigations stimulated a lively theoretical controversy on the applicability of Poisson-Boltzmann theories close to walls [Goulding1998, Goulding1999, Mateescu2001, Trizac1999, Trizac2000, Trizac2001] which led to, e.g., a general proof of the statement that long-ranged interactions between like-charged particles within Poisson-Boltzmann theory are necessarily repulsive [Neu1999, Sader1999, Sader2000]. Therefore, like-charge attraction is attributed to correlation effects, which are not taken into account by Poisson-Boltzmann theory. However, recent experimental investigations challenge former reports on like-charge attraction by asserting erroneous particle-particle distances due to optical artefacts [Baumgartl2005, Baumgartl2006].

Short-ranged like-charge attraction has been observed in computer simulation studies on bulk colloid-polyelectrolyte mixtures [Messina2002/1, Messina2002/2]. Moreover, the inverse effect, a repulsion between oppositely charged surfaces, has been reported recently [Trulsson2006]. Finally, several theoretical models have been proposed predicting an attraction between equally charged walls enclosing a narrow film of electrolyte [Bohnic2004, Diehl1999, Naji2004, Rouzina1996].

Charge inversion of colloids refers to the condensation of ions such that the surface charge is overcompensated by the total charge of the condensed ions. Theoretical models exist which exhibit this phenomenon for sufficiently large surface charge density and multivalent ions [Pianegonda2005]. The condensed ions are considered to form a strongly correlated, quasi two-dimensional liquid [Perel1999, Shklovskii1999]. Experimental detection of charge inversion is possible [vanderHeyden2006], e.g., by measuring the streaming potential [Hunter1981]. Within a recent study on trivalent La^{3+} ions, charge inversion occurred even for very small ionic strength [Pittler2006]. The model derived within the present work exhibits charge inversion of the surface charge under certain conditions. This charge inversion will be detected by a reversal of the electric field with respect to the surface field. According to the generally expectation, this phenomenon occurs due to correlations between the charged particles which are directly modelled within the present approach.

Chapter 2

Model and general formalism

In this work, inhomogeneities in fluids of charged platelike colloids will be investigated within a particular model. Density functional theory, which is considered as an appropriate general approach to this kind of problems, is recollected first. Next, the model as well as the construction of the corresponding density functional will be explained in detail. Finally, basic concepts of wetting theory are introduced. In particular, an analytical asymptotic expression for the effective interface potential, which is needed in subsequent chapters, will be calculated. This chapter provides all relevant quantities, concepts, and equations to be solved numerically in the following chapters.

2.1 Foundations of density functional theory

In view of the inhomogeneities in fluids of charged platelike colloids to be investigated in this work, density functional theory [Evans1979] is the method of choice [Evans1992]. This approach describes fluids in terms of number density profiles, i.e., number densities as functions of position in space and maybe further degrees of freedom such as particle orientations. In a one-component fluid of, e.g., disclike particles the number density at position $\mathbf{r}$ of particles with disc orientation specified by the normal vector $\mathbf{n}$ is given by $\varrho(\mathbf{r}, \mathbf{n})$. An additional index v describing the particle species is introduced in the case of multi-component fluids of disclike particles:

$\varrho_v(\mathbf{r}, \mathbf{n})$.

Within grandcanonical density functional theory, the equilibrium number density profiles ϱ_v^{eq} minimise a density functional [Evans1979]

$$\Omega[\underline{\varrho}] = \sum_v \int \mathrm{d}^3 r \int \mathrm{d}^2 n \, \varrho_v(\mathbf{r}, \mathbf{n}) \Big(\ln \left(\varrho_v(\mathbf{r}, \mathbf{n}) \Lambda_v^3 \right) - 1 - \mu_v + V_v(\mathbf{r}, \mathbf{n}) \Big) + F^{\mathrm{ex}}[\underline{\varrho}], \tag{2.1}$$

where $\underline{\varrho}$ denotes the set of all density profiles ϱ_v. Λ_v and μ_v describe the thermal de Broglie wavelength and the chemical potential of particle species v, respectively. V_v is the external potential exerted on particles of species v, e.g., due to walls. F^{ex} denotes the free energy in excess over the ideal gas contribution to Ω. It depends only on the interaction between fluid particles and not on external fields. Throughout this work energies (e.g., Ω, μ_v, V_v, and F^{ex}) are expressed in units of the thermal energy $k_B T$ and are therefore taken to be dimensionless.

The stationarity condition of $\Omega[\underline{\varrho}]$ at $\underline{\varrho} = \underline{\varrho}^{\mathrm{eq}}$ amounts to the *Euler-Lagrange equation*:

$$\left. \frac{\delta \Omega}{\delta \varrho_v(\mathbf{r}, \mathbf{n})} \right|_{\underline{\varrho}^{\mathrm{eq}}} = 0. \tag{2.2}$$

For the density functional in Eq. (2.1) one readily finds

$$\ln \left(\varrho_v^{\mathrm{eq}}(\mathbf{r}, \mathbf{n}) \Lambda_v^3 \right) - \mu_v + V_v(\mathbf{r}, \mathbf{n}) - c_v(\mathbf{r}, \mathbf{n}, [\underline{\varrho}^{\mathrm{eq}}]) = 0, \tag{2.3}$$

where the one-particle direct correlation function

$$c_v(\mathbf{r}, \mathbf{n}, [\underline{\varrho}]) := - \left. \frac{\delta F^{\mathrm{ex}}}{\delta \varrho_v(\mathbf{r}, \mathbf{n})} \right|_{\underline{\varrho}} \tag{2.4}$$

has been introduced.

The minimal value $\Omega[\underline{\varrho}^{\mathrm{eq}}]$ equals the grand potential $\Omega^{\mathrm{eq}}(T, V, \underline{\mu})$ [Evans1979], from which all thermodynamic quantities can be derived. The type of excess free energy functional $F^{\mathrm{ex}}[\underline{\varrho}]$ used within the present study corresponds to a *mean field theory*. One therefore expects classical critical exponents close to critical points [Binney1992, Goldenfeld1992, leBellac1991, Plischke1994, Stanley1971].

If the density functional Ω in Eq. (2.1) were exactly known, the corresponding equilibrium number density profiles $\underline{\varrho}^{\mathrm{eq}}$ would also be exact [Evans1979]. In practice, however, Ω, or equivalently F^{ex}, is *not* known exactly but only approximately. There are some formally exact relations between the excess free energy functional F^{ex} and quantities such as pair distribution functions, interaction potentials, external potentials, or two-particle direct correlation functions which might be exploited in order to determine F^{ex} approximately [Evans1979]. One such relation [Evans1979] relates F^{ex} to the interaction potential $U_{vw}(\mathbf{r},\mathbf{n},\mathbf{r}',\mathbf{n}')$ between two particles of species v and w at positions $\mathbf{r}$ and $\mathbf{r}'$ and orientations $\mathbf{n}$ and $\mathbf{n}'$, respectively, and the pair distribution function $g_{vw}(\mathbf{r},\mathbf{n},\mathbf{r}',\mathbf{n}')$ [Hansen1986]:

$$\frac{\delta F^{\mathrm{ex}}}{\delta U_{vw}(\mathbf{r},\mathbf{n},\mathbf{r}',\mathbf{n}')} = \frac{1}{2}\varrho_v(\mathbf{r},\mathbf{n})\varrho_w(\mathbf{r}',\mathbf{n}')g_{vw}(\mathbf{r},\mathbf{n},\mathbf{r}',\mathbf{n}'). \tag{2.5}$$

Upon decomposing the total particle-particle interaction $U = U^{\mathrm{ref}} + U^{\mathrm{per}}$ into a reference part U^{ref} and a perturbation part U^{per} one finds along the path in function space $U^{(\eta)} := U^{\mathrm{ref}} + \eta U^{\mathrm{per}}, \eta \in [0,1]$

$$\begin{aligned}\frac{\mathrm{d}F^{\mathrm{ex},(\eta)}}{\mathrm{d}\eta} &= \sum_{vw}\int \mathrm{d}^5x \int \mathrm{d}^5x'\ \frac{\delta F^{\mathrm{ex}}}{\delta U_{vw}(\mathbf{x},\mathbf{x}')}\bigg|_{U^{(\eta)}} \frac{\mathrm{d}U^{(\eta)}_{vw}(\mathbf{x},\mathbf{x}')}{\mathrm{d}\eta} \qquad (2.6)\\ &= \frac{1}{2}\sum_{vw}\int \mathrm{d}^5x \int \mathrm{d}^5x'\ \varrho_v(\mathbf{x})\varrho_w(\mathbf{x}')g^{(\eta)}_{vw}(\mathbf{x},\mathbf{x}')U^{\mathrm{per}}_{vw}(\mathbf{x},\mathbf{x}'),\end{aligned}$$

where the abbreviation $\mathbf{x} := (\mathbf{r},\mathbf{n})$ has been introduced. Using the fact that $F^{\mathrm{ex},(0)} = F^{\mathrm{ex,ref}}$ and $F^{\mathrm{ex},(1)} = F^{\mathrm{ex}}$ leads to

$$\begin{aligned}F^{\mathrm{ex}} &= F^{\mathrm{ex,ref}} + \int_0^1 \mathrm{d}\eta\ \frac{\mathrm{d}F^{\mathrm{ex},(\eta)}}{\mathrm{d}\eta}\\ &= F^{\mathrm{ex,ref}} \qquad (2.7)\\ &\quad +\frac{1}{2}\sum_{vw}\int \mathrm{d}^5x \int \mathrm{d}^5x'\ \varrho_v(\mathbf{x})\varrho_w(\mathbf{x}')U^{\mathrm{per}}_{vw}(\mathbf{x},\mathbf{x}') \int_0^1 \mathrm{d}\eta\ g^{(\eta)}_{vw}(\mathbf{x},\mathbf{x}').\end{aligned}$$

Given approximations for $F^{\mathrm{ex,ref}}$ and $g^{(\eta)}$ lead to expressions for F^{ex}. The simplest choices $F^{\mathrm{ex,ref}} = 0$ and $g^{(\eta)} = 1$, i.e., an ideal gas reference system ($U^{\mathrm{ref}} = 0$) and vanishing correlations between the particles, yields the density functional analogue of the high-temperature expansion [Hansen1986]. By substituting the pair distribution function $g^{(\eta)}_{vw}(\mathbf{x},\mathbf{x}') := \exp(-\eta U^{\mathrm{per}}_{vw}(\mathbf{x},\mathbf{x}'))$, on the other hand, one obtains the analogue of a virial expansion up to second order [Hansen1986]. Within the current work, a more elaborated fundamental measure excess free energy $F^{\mathrm{ex,ref}}$ (Sec. 2.2) and a pair distribution function $g^{(\eta)}$ similar to the one known from Debye-Hückel theory (Sec. 2.3) will be used. These concepts will be introduced next.

2.2 Zwanzig model and reference functional

The model fluid considered in this work is a ternary mixture of charged platelike colloids and salt dissolved in a dielectric solvent (e.g., water) with dielectric constant ε. The solvent is treated as a continuum.

Throughout this work dimensionless charges will be expressed in units of the elementary charge e. Due to the electrical charges involved, one length scale of the system is given by the *Bjerrum length* $\ell_B := \dfrac{e^2}{4\pi\varepsilon_0\varepsilon k_B T}$, which describes the distance between two isolated elementary charges e whose Coulomb interaction energy equals the thermal energy k_BT. For $T = 300\,\mathrm{K}$ and $\varepsilon = 78$ (water) one has $\ell_B \approx 0.72\,\mathrm{nm}$. Henceforth lengths are given in units of the Bjerrum length ℓ_B and are taken to be dimensionless. Dimensional and dimensionless quantities are denoted by the same symbol in order to avoid a clumsy notation — they can be distinguished by the presence or absence of units.

For technical convenience, an approximation due to Zwanzig [Zwanzig1963] concerning the orientational degrees of freedom, which in the previous section have been described by the continuously varying platelet normal vector $\mathbf{n}$, will be applied: the particles are restricted to take one out of only three mutually perpendicular orientations. These allowed orientations are chosen to be parallel to the Cartesian axes. Hence the integrals $\int \mathrm{d}^2n$ in Eqs. (2.1), (2.6), and (2.7) can be replaced by sums $\sum_{\mathbf{n}}$. Enumerating the finite set of pairs $(v, \mathbf{n})$ (Sec. 2.1) by the *type* index i, the double summation $\sum_v \sum_{\mathbf{n}}$ over all species and orientations is accounted for by the single summation $\sum_i$ over all types $i \in \{M_x, M_y, M_z, S, C\}$ (see Fig. 2.1). In terms of this nomenclature Eq. (2.1) reads

$$\Omega[\underline{\varrho}] = \sum_i \int \mathrm{d}^3r\ \varrho_i(\mathbf{r})\Big(\ln\big(\varrho_i(\mathbf{r})\big) - 1 - \mu_i^* + V_i(\mathbf{r})\Big) + F^{\mathrm{ex}}[\underline{\varrho}], \qquad (2.8)$$

where the reduced chemical potentials $\mu_i^* := \mu_i - 3\ln\Lambda_i$ have been introduced.

All particles are modelled as square cuboids with their edges parallel to the Cartesian axes. For simplicity, the charges are fixed, monodisperse, and concentrated at the centres of the particles. The particles of the first species represent the macroions M of size $D_M \times D_M \times L_M$, $D_M > L_M$, and charge Q_M. The three different macroion orientations possible within the Zwanzig model give rise to the three types M_x, M_y, and M_z corresponding to whether the L_M-edges are parallel to the x-, y-, or z-axis, respectively (see Fig. 2.1). The second species consists of salt ions S modelled as

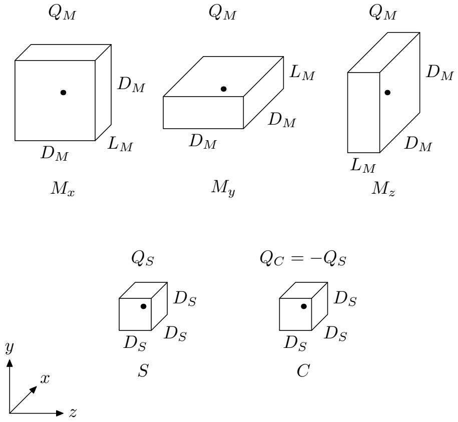

Figure 2.1: Macroions M are square cuboids of size $D_M \times D_M \times L_M$, $D_M > L_M$ with the effective charge Q_M whereas salt ions S and counterions C are cubes of side length D_S with charges Q_S and $-Q_S$, respectively. The pointlike charges (•) are localised at the centres of the cuboids. The macroions can adopt three possible orientations M_x, M_y, and M_z corresponding to the L_M-edges being parallel to the x-, y-, and z-axis, respectively.

cubes of side length D_S and charge Q_S. Since cubes can adopt only one orientation within the Zwanzig model, the species S is identical with the type S (see Fig. 2.1). The salt ion charge Q_S is chosen to have the same sign as the macroion charge Q_M if the latter does not vanish. Finally, the third species consists of counterions C guaranteeing overall charge neutrality. They are also described by cubes with the same side length D_S but opposite charge $Q_C := -Q_S$. The corresponding type is also termed C (see Fig. 2.1). Due to the choice of the same sign for Q_M and Q_S, ions of species C are counterions in the usual sense for both the macroions M and the salt ions S. $\varrho_i(\mathbf{r}), i \in \{M_x, M_y, M_z, S, C\}$, denotes the number density at point $\mathbf{r}$ of the centres of macroions with orientation along the x-, y-, and z-axis, salt ions, and counterions, respectively. If type i corresponds to species v and orientation $\mathbf{n}$, it is $\varrho_i(\mathbf{r}) = \varrho_v(\mathbf{r}, \mathbf{n})$ (Sec. 2.1). The abbreviation $\underline{\varrho}(\mathbf{r}) := (\varrho_{M_x}(\mathbf{r}), \ldots, \varrho_C(\mathbf{r}))$ is introduced for later convenience.

In this work the reference excess free energy functional $F^{\mathrm{ex,ref}}$ to be substituted into Eq. (2.7) corresponds to the model fluid just described with all particle charges vanishing ($Q_M = Q_S = 0$). The particles of this reference fluid hence interact only via the hard-core interactions which prevent the particles from overlapping. A *fundamental measure theory* of hard cuboids within the Zwanzig model which reproduces the exact second and third order virial coefficients has been derived in Refs. [Cuesta1997/1, Cuesta1997/2]. *Fundamental measure theory* refers to the approximation [Rosenfeld1989]

$$F^{\mathrm{ex,ref}}[\underline{\varrho}] := \int \mathrm{d}^3 r \; \Phi\big(\underline{n}(\mathbf{r})\big) \tag{2.9}$$

with appropriately chosen weighted densities

$$n_\alpha(\mathbf{r}) = \sum_i \int \mathrm{d}^3 r' \; \omega_{\alpha,i}(\mathbf{r}-\mathbf{r}')\varrho_i(\mathbf{r}') \tag{2.10}$$

and an excess free energy density Φ which is a *function* of the weighted densities. The weight functions ω used in Eq. (2.10) are given by [Cuesta1997/1, Cuesta1997/2]

$$\begin{aligned}
\omega_{0,i}(\mathbf{r}) &= a(x,S_i^x)a(y,S_i^y)a(z,S_i^z) \\
\omega_{1x,i}(\mathbf{r}) &= b(x,S_i^x)a(y,S_i^y)a(z,S_i^z) \\
\omega_{1y,i}(\mathbf{r}) &= a(x,S_i^x)b(y,S_i^y)a(z,S_i^z) \\
\omega_{1z,i}(\mathbf{r}) &= a(x,S_i^x)a(y,S_i^y)b(z,S_i^z) \\
\omega_{2x,i}(\mathbf{r}) &= a(x,S_i^x)b(y,S_i^y)b(z,S_i^z) \\
\omega_{2y,i}(\mathbf{r}) &= b(x,S_i^x)a(y,S_i^y)b(z,S_i^z) \\
\omega_{2z,i}(\mathbf{r}) &= b(x,S_i^x)b(y,S_i^y)a(z,S_i^z) \\
\omega_{3,i}(\mathbf{r}) &= b(x,S_i^x)b(y,S_i^y)b(z,S_i^z)
\end{aligned} \tag{2.11}$$

with $S_i^d, d \in \{x,y,z\}$, denoting the extension of cuboids of type i in direction d and with the abbreviations $a(d,S) := \frac{1}{2}\big(\delta(S/2-d)+\delta(S/2+d)\big)$ and $b(d,S) := \Theta(S/2-|d|)$. Spatial integrals of the weight functions Eq. (2.11) can be interpreted as characteristic one-particle quantities such as number, side lengths, cross-sectional areas, and occupied volume; hence the notion *fundamental measure*. Requiring exact second and third order virial coefficients as well as the property of dimensional crossover [Cuesta1997/1, Cuesta1997/2] the excess free energy density reads

$$\Phi(\underline{n}) = -n_0 \ln(1-n_3) + \frac{n_{1x}n_{2x}+n_{1y}n_{2y}+n_{1z}n_{2z}}{1-n_3} + \frac{n_{2x}n_{2y}n_{2z}}{(1-n_3)^2}. \tag{2.12}$$

One part of the investigations done in this work have been devoted to the fluid in contact with a charged substrate. The charged wall, which confines the fluid from one side, is modelled as impenetrable for the fluid particles. Moreover, it carries a fixed homogeneously distributed surface charge of areal density σ which, depending on the sign of σ, can be assumed to have been generated by releasing an appropriate amount of ions of either type S or type C into the fluid.

The system under consideration is coupled to two particle reservoirs: One supplies neutralised macroions (chemical formula $C_kM, k := \frac{Q_M}{Q_S} \geq 0$) and the other neutral salt (chemical formula CS); μ_{C_kM} and μ_{CS} denote the corresponding chemical potentials. The "molecules" dissociate upon entering the system:

$$\begin{aligned} C_kM &\longrightarrow kC^{Q_C} + M^{Q_M}, \\ CS &\longrightarrow C^{Q_C} + S^{Q_S}. \end{aligned} \tag{2.13}$$

These equilibrium chemical reactions lead to the following relations between the reservoir chemical potentials (μ_{C_kM} and μ_{CS}) and the particle chemical potentials ($\mu_i, i \in \{M_x, M_y, M_z, S, C\}, \mu_{M_x} = \mu_{M_y} = \mu_{M_z} =: \mu_M$):

$$\begin{aligned} \mu_{C_kM} &= k\mu_C + \mu_M \\ \mu_{CS} &= \mu_C + \mu_S. \end{aligned} \tag{2.14}$$

Defining the *reduced reservoir chemical potentials* ($\Lambda_{M_x} = \Lambda_{M_y} = \Lambda_{M_z} =: \Lambda_M$)

$$\begin{aligned} \mu^*_{C_kM} &:= \mu_{C_kM} - 3(k \ln \Lambda_C + \ln \Lambda_M) \\ \mu^*_{CS} &:= \mu_{CS} - 3(\ln \Lambda_C + \ln \Lambda_S), \end{aligned} \tag{2.15}$$

Eq. (2.14) is equivalent to

$$\begin{aligned} \mu^*_{C_kM} &= k\mu^*_C + \mu^*_M \\ \mu^*_{CS} &= \mu^*_C + \mu^*_S. \end{aligned} \tag{2.16}$$

Upon solving the Euler-Lagrange equations corresponding to the density functional Eq. (2.8) for mixtures of platelike macroions and monovalent salt under the constraint of *global charge neutrality*, the equilibrium state of this system is obtained in terms of density profiles $\underline{\varrho}$. In order to identify various structures of the fluid it is advantageous to express the macroion densities ϱ_{M_x}, ϱ_{M_y}, and ϱ_{M_z} in terms of the *total macroion density* $\varrho_M := \varrho_{M_x} + \varrho_{M_y} + \varrho_{M_z}$, the *nematic order parameter* along the z-axis

$$s_M := \frac{3}{2}\frac{\varrho_{M_z}}{\varrho_M} - \frac{1}{2} \in \left[-\frac{1}{2}, 1\right], \tag{2.17}$$

and the *biaxiality order parameter* perpendicular to the z-axis

$$q_M := \frac{\varrho_{\mathrm{M_x}} - \varrho_{\mathrm{M_y}}}{\varrho_{\mathrm{M}}}. \tag{2.18}$$

The definition of s_M coincides with the well-known scalar liquid-crystal order parameter [deGennes1993] $S = \langle P_2(\cos\vartheta)\rangle = \frac{3}{2}\langle(\cos\vartheta)^2\rangle - \frac{1}{2}$ for the special case of a Zwanzig model, within which the only possible macroion orientations are parallel (M_z, $\cos\vartheta = 1$) and perpendicular ($M_{x,y}$, $\cos\vartheta = 0$) to the z-axis. Therefore, structures with $s_M = 0$ and $s_M > 0$ are called *isotropic* and *nematic*, respectively. The biaxiality order parameter q_M vanishes if there is no preference of either macroion orientation perpendicular to the z-axis. Structures with $q_M = 0$ and $q_M \neq 0$ will be called *uniaxial* and *biaxial*, respectively.

2.3 Debye-Hückel theory and perturbation functional

In the previous section the reference fluid has been chosen as a mixture of hard cuboids whose excess free energy functional $F^{\mathrm{ex,ref}}$ entering in Eq. (2.7) has been approximated within fundamental measure theory (Eqs. (2.9)–(2.12)). In this section an approximate pair distribution function $g^{(\eta)}$ in Eq. (2.7) corresponding to the particle-particle interaction $U^{(\eta)} = U^{\mathrm{ref}} + \eta U^{\mathrm{per}}, \eta \in [0,1]$, will be defined. Here $U^{\mathrm{ref}}_{ij}(\mathbf{r})$ — the reference hard-core interaction — is infinite if two particles of types i and j, respectively, with centre-centre distance $\mathbf{r}$ overlap and zero otherwise. The perturbation interaction $U^{\mathrm{per}}_{ij}(\mathbf{r})$ describes the Coulomb interactions between two particles of types i and j at distance $\mathbf{r}$ with charges Q_i and Q_j, respectively. Dispersion forces are not taken into account. For technical convenience the following approximation is applied:

$$U^{\mathrm{per}}_{ij}(\mathbf{r}) := \frac{Q_i Q_j}{\|\mathbf{r}\|_\infty}, \tag{2.19}$$

where the usual Euclidean norm $\|\mathbf{r}\|_2 = \sqrt{x^2+y^2+z^2}$ is replaced by the supremum norm $\|\mathbf{r}\|_\infty = \max(|x|,|y|,|z|)$ because of computational advantages. Since these two norms are topologically equivalent, i.e., $\|\mathbf{r}\|_\infty \leq \|\mathbf{r}\|_2 \leq \sqrt{3}\,\|\mathbf{r}\|_\infty$, it is not expected that the results change qualitatively due to this approximation. Furthermore, $\|\cdot\|_\infty$-spheres are cubes with their edges parallel to the Cartesian axes; therefore, the supremum norm is the most natural and adapted norm in the context of a Zwanzig model for cuboids.

Since $U^{(\eta)}$ includes Coulomb interactions a simple and sensible choice for $g^{(\eta)}$ might be of the form obtained within the Debye-Hückel theory for electrolytes [Debye1923, McQuarrie2000]. This theory calculates the electrostatic potential $\varphi_{\mathrm{DH},p}(r)$ around an ion of species p in a comoving frame by solving the *linearised radial Poisson-Boltzmann equation*

$$\frac{1}{r^2}\frac{\mathrm{d}}{\mathrm{d}r}\Big(r^2\frac{\mathrm{d}}{\mathrm{d}r}\varphi_{\mathrm{DH},p}(r)\Big) = \kappa_{\mathrm{DH}}^2\varphi_{\mathrm{DH},p}(r) \tag{2.20}$$

with the *screening factor* $\kappa_{\mathrm{DH}}^2 = 4\pi\sum_{p'} q_{p'}^2 n_{p'}$, where $q_{p'}$ and $n_{p'}$ are the valency and the bulk number density of ion species p', respectively. The solution for a charge neutral system and vanishing electrostatic potential infinitely far from the origin, i.e., $\varphi_{\mathrm{DH},p}(\infty) = 0$, is given by [Debye1923, McQuarrie2000]

$$\varphi_{\mathrm{DH},p}(r) = \frac{q_p}{r}\exp(-\kappa_{\mathrm{DH}}r). \tag{2.21}$$

Ultimately, this expression yields the pair distribution function within Debye-Hückel theory

$$g_{\mathrm{DH},pp'}(r) = 1 - \frac{q_p q_{p'}\exp(-\kappa_{\mathrm{DH}}r)}{r}. \tag{2.22}$$

The linearisation approximation which leads to Eq. (2.20) is justified only for distances with small values of $\varphi_{\mathrm{DH},p}(r)$, i.e., for $r \to \infty$. Moreover, $g_{\mathrm{DH},pp'}$ in Eq. (2.22) is only meaningful for large distances r, because otherwise it can become negative, which is impossible for pair distribution functions. On the other hand, the functional form of $g_{\mathrm{DH},pp'}(r)$ is *asymptotically exact* [McQuarrie2000] except for the "amplitude" $q_p q_{p'}$, because the linearisation approximation of Eq. (2.20) does not influence the asymptotic behaviour of $\varphi_{\mathrm{DH},p}$. The "amplitudes" in front of $\exp(-\kappa_{\mathrm{DH}}r)/r$ within given exact asymptotic pair distribution functions may serve to infer *effective* valencies q_p^*, which in general differ from the *bare* valencies q_p entering in Eq. (2.22) [Aubouy2003].

Motivated by Eq. (2.22) the pair distribution function $g^{(\eta)}$ corresponding to the particle-particle interaction $U^{(\eta)}$ is approximated by

$$\begin{aligned} g_{ij}^{(\eta)}(\mathbf{r},\mathbf{r}') \quad := \quad & \exp\big(-U_{ij}^{\mathrm{ref}}(\mathbf{r}-\mathbf{r}')\big)\max\Big[0, \qquad (2.23)\\ & 1 - U_{ij}^{\mathrm{per}}(\mathbf{r}-\mathbf{r}')\eta\exp\big(-\sqrt{\eta}\kappa(\mathbf{r},\mathbf{r}';[\underline{\varrho}])\,\|\mathbf{r}-\mathbf{r}'\|_{\infty}\big)\Big]. \end{aligned}$$

The *screening factor* in Eq. (2.23) is chosen as

$$\kappa(\mathbf{r},\mathbf{r}';[\underline{\varrho}]) := \frac{1}{2}\big(\tilde{\kappa}(\mathbf{r};[\underline{\varrho}]) + \tilde{\kappa}(\mathbf{r}';[\underline{\varrho}])\big) \tag{2.24}$$

where only anions and cations contribute to the screening [Warren2000]:

$$\tilde{\kappa}(\mathbf{r};[\underline{\varrho}]) := \sqrt{4\pi Q_{\mathrm{S}}^2(\varrho_{\mathrm{A}}(\mathbf{r}) + \varrho_{\mathrm{C}}(\mathbf{r}))}. \tag{2.25}$$

This pair distribution function has non-negative values, it vanishes within the hard-core, and it approaches unity at infinitely large distances. Again, here the Euclidean norm $\|\cdot\|_2$ has been replaced by the supremum norm $\|\cdot\|_\infty$. The factor $\sqrt{\eta}$ in Eq. (2.23) is introduced because ηU^{per} is equivalent to Eq. (2.19) with Q_i replaced by $\sqrt{\eta}Q_i$, and κ in Eq. (2.24) scales linearly with the charges. Furthermore, the charge parameters Q_i have to be interpreted as *effective charges* in order to reproduce the actual effective interactions between charged particles within Debye-Hückel theory [Aubouy2003]. The relation between Q_i and actual charges remains undetermined within the present work.

The analysis rendered that, for a *spatially constant* screening factor κ, the above model does *not* yield stable interfacial profiles. This led to introduce the spatially varying expression in Eq. (2.24). Alternative expressions for inhomogeneous screening factors are known from the theory of electrolytes: In Ref. [Lee1997] non-symmetric screening factors are provided whereas in Ref. [Groh1998] κ is calculated from the mean salt density. Here the definition in Eqs. (2.24) and (2.25) is preferred because it is symmetric and the screening is determined by the salt concentration *at* the actually investigated positions.

With Eq. (2.23), the innermost integral in Eq. (2.7) can be evaluated leading to an expression

$$\int_0^1 \mathrm{d}\eta\, g_{ij}^{(\eta)}(\mathbf{r},\mathbf{r}') = \exp\big(-U_{ij}^{\mathrm{ref}}(\mathbf{r}-\mathbf{r}')\big)\big(1 + G_{ij}(\kappa(\mathbf{r},\mathbf{r}';[\underline{\varrho}]), \|\mathbf{r}-\mathbf{r}'\|_\infty)\big) \tag{2.26}$$

with functions

$$G_{ij}(\kappa,s) := -\int_0^1 \mathrm{d}\eta\ \min\big[1, U_{ij}^{\mathrm{per}}(s)\eta\exp(-\sqrt{\eta}\kappa s)\big] \tag{2.27}$$

which decay for $s \longrightarrow \infty$ as

$$\begin{aligned} G_{ij}(\kappa, s) &\simeq -\int\limits_0^1 \mathrm{d}\eta \, U_{ij}^{\mathrm{per}}(s)\eta \exp(-\sqrt{\eta}\kappa s) \\ &= -\frac{Q_iQ_j}{s}\int\limits_0^1 \mathrm{d}\eta \, \eta \exp(-\sqrt{\eta}\kappa s) \\ &= -\frac{Q_iQ_j}{s}\int\limits_0^1 \mathrm{d}\zeta \, 2\zeta^3 \exp(-\zeta\kappa s) \\ &= -\frac{2Q_iQ_j}{\kappa^4 s^5}\gamma(4, \kappa s) \\ &\simeq -\frac{12Q_iQ_j}{\kappa^4 s^5}, \end{aligned} \tag{2.28}$$

where γ denotes the incomplete gamma function [Abramowitz1972, Gradshteyn1980]. Therefore, the integrand in Eq. (2.7) vanishes at small distances $\|\mathbf{r}-\mathbf{r}'\|_\infty$ due to U_{ij}^{ref}, whereas it decays as $\|\mathbf{r}-\mathbf{r}'\|_\infty^{-1}$ for $\|\mathbf{r}-\mathbf{r}'\|_\infty \longrightarrow \infty$. In order to isolate the $\|\mathbf{r}-\mathbf{r}'\|_\infty^{-1}$ asymptotics, unity has been added and subtracted on the right-hand side of Eq. (2.26), which, after insertion into Eq. (2.7), leads to the following decomposition of the perturbation excess free energy functional

$$F^{\mathrm{ex,per}} = F_{\mathrm{el}}^{\mathrm{ex,per}} + F_{\mathrm{corr}}^{\mathrm{ex,per}} \tag{2.29}$$

with the *electrostatic* part

$$F_{\mathrm{el}}^{\mathrm{ex,per}}[\underline{\varrho}] := \frac{1}{2}\sum_{ij}\int \mathrm{d}^3r \int \mathrm{d}^3r' \; \varrho_i(\mathbf{r})\varrho_j(\mathbf{r}')U_{ij}^{\mathrm{per}}(\mathbf{r},\mathbf{r}') \tag{2.30}$$

and the *correlation* part

$$\begin{aligned} F_{\mathrm{corr}}^{\mathrm{ex,per}}[\underline{\varrho}] := \frac{1}{2}\sum_{ij}\int \mathrm{d}^3r \int \mathrm{d}^3r' \; \varrho_i(\mathbf{r})\varrho_j(\mathbf{r}')U_{ij}^{\mathrm{per}}(\mathbf{r},\mathbf{r}')\Big[\exp\big(-U_{ij}^{\mathrm{ref}}(\mathbf{r},\mathbf{r}')\big) \\ -1 + \exp\big(-U_{ij}^{\mathrm{ref}}(\mathbf{r},\mathbf{r}')\big)G_{ij}\big(\kappa(\mathbf{r},\mathbf{r}';[\underline{\varrho}]), \|\mathbf{r}-\mathbf{r}'\|_\infty\big)\Big]. \end{aligned} \tag{2.31}$$

Note that, although the integrands in Eqs. (2.30) and (2.31) are undefined for $\mathbf{r} = \mathbf{r}'$, the *three-dimensional* integrals exist due to the $\|\mathbf{r}-\mathbf{r}'\|_\infty^{-1}$

asymptotics for $\|\mathbf{r}-\mathbf{r}'\|_\infty \longrightarrow 0$. Since the integrand in Eq. (2.31) decays as $\|\mathbf{r}-\mathbf{r}'\|_\infty^{-6}$ for $\|\mathbf{r}-\mathbf{r}'\|_\infty \longrightarrow \infty$, $F_{\mathrm{corr}}^{\mathrm{ex,c}}$ is well-defined for all finite system volumes V and the thermodynamic limit of the ratio $\frac{1}{V}F_{\mathrm{corr}}^{\mathrm{ex,c}}$ exists. This decay is the same as in models of non-retarded isotropic dispersion forces [Dietrich1988, Dietrich1991, Schick1990].

In Ch. 3 bulk phase diagrams of *spatially homogeneous* phases will be determined by solving the Euler-Lagrange equation corresponding to density functional Eq. (2.8) in the subspace of spatially homogeneous density profiles $\underline{\varrho}^{(\mathrm{bulk})}$. In order to assess the stability of such spatially homogeneous states, one has to check whether the second order term of a functional Taylor expansion of $\Omega[\underline{\varrho} = \underline{\varrho}^{(\mathrm{bulk})} + \delta\underline{\varrho}]$ around $\underline{\varrho}^{(\mathrm{bulk})}$ in powers of perturbations $\delta\underline{\varrho}$ is non-negative. Consider the particular perturbations $\delta\varrho_{M_x}(\mathbf{r}) := A(\delta(\mathbf{r}-\mathbf{v}) - \delta(\mathbf{r}-\mathbf{u}))$ and $\delta\varrho_{M_y,\dots,C}(\mathbf{r}) := 0$ which correspond to the translation of an amount A of particles of type M_x from position $\mathbf{u}$ to position $\mathbf{v}$. According to Eqs. (2.8), (2.7), (2.9), (2.26), and (2.19), one obtains for $\|\mathbf{v}-\mathbf{u}\|_\infty > D_M$

$$
\begin{aligned}
&\frac{1}{2}\sum_{ij}\int \mathrm{d}^3r \int \mathrm{d}^3r' \left.\frac{\delta^2\,\Omega}{\delta\varrho_i(\mathbf{r})\delta\varrho_j(\mathbf{r}')}\right|_{\underline{\varrho}^{(\mathrm{bulk})}} \delta\varrho_i(\mathbf{r})\delta\varrho_j(\mathbf{r}') \\
&= \frac{1}{2}\sum_{ij}\int \mathrm{d}^3r \int \mathrm{d}^3r'\ \delta\varrho_i(\mathbf{r})\delta\varrho_j(\mathbf{r}') \\
&\quad\Bigg(\frac{1}{\varrho_i^{(\mathrm{bulk})}(\mathbf{r})}\delta_{ij}\delta(\mathbf{r}-\mathbf{r}') \\
&\quad + \int \mathrm{d}^3r'' \sum_{\alpha,\alpha'} \frac{\partial^2\Phi}{\partial n_\alpha \partial n_{\alpha'}}(\underline{n}^{(\mathrm{bulk})}(\mathbf{r}''))\omega_{\alpha,i}(\mathbf{r}-\mathbf{r}'')\omega_{\alpha',j}(\mathbf{r}'-\mathbf{r}'') \\
&\quad + U_{ij}^{\mathrm{per}}(\mathbf{r}-\mathbf{r}')\exp\big(-U_{ij}^{\mathrm{ref}}(\mathbf{r}-\mathbf{r}')\big)\big(1+G_{ij}(\kappa(\mathbf{r},\mathbf{r}';[\underline{\varrho}]),\|\mathbf{r}-\mathbf{r}'\|_\infty)\big)\Bigg) \\
&= A^2\Bigg(\sum_{\alpha,\alpha'} \frac{\partial^2\Phi}{\partial n_\alpha \partial n_{\alpha'}}(\underline{n}^{(\mathrm{bulk})}) \int \mathrm{d}^3r''\ \omega_{\alpha,M_x}(\mathbf{r}'')\omega_{\alpha',M_x}(\mathbf{r}'') \\
&\qquad - Q_M^2 \frac{1+G_{M_xM_x}(\kappa(\mathbf{v},\mathbf{u};[\underline{\varrho}]),\|\mathbf{v}-\mathbf{u}\|_\infty)}{\|\mathbf{v}-\mathbf{u}\|_\infty}\Bigg). \qquad (2.32)
\end{aligned}
$$

Whereas the first term is positive, the second term is negative (see Eq. (2.27)) and its absolute value increases proportional to Q_M^2. Hence the expression in Eq. (2.32) becomes negative, i.e., the spatially homogeneous state $\underline{\varrho}^{(\text{bulk})}$ is unstable with respect to spatial variations, if the macroion charge $|Q_M|$ is sufficiently large. Thus, the choice for $g^{(\eta)}$ in Eq. (2.23) leads to spatially *inhomogeneous* bulk phases if the effective macroion charge $|Q_\text{M}|$ is larger than some threshold value which, for the parameters used within the present work, is approximately $1.2|Q_S|$. As already mentioned, the threshold value in terms of actual charges is undetermined. In this work only sufficiently small effective macroion charges are considered, such that stable spatially *homogeneous* bulk phases exist. Such small effective macroion charges occur for pH values close to the point of zero charge [Kosmulski2002, Kosmulski2004, Kosmulski2005, Kosmulski2006].

2.4 Substrate, electrostatic, and Donnan potentials

By imposing suitable boundary conditions, only systems with translational symmetry in the lateral x and y directions are considered. Hence, in the absence of spontaneous symmetry breaking, all densities ϱ_i depend at most on the z coordinate. Since the thermodynamic limit of globally charge neutral systems of Coulomb interacting hard particles exists [Lebowitz1969, Lieb1972], i.e., the bulk free energy density depends neither on the shape nor on the boundaries of the system volume V, the following system volumes $V(L) := A(L) \times [\hat{z}(L), \hat{z}(L) + L]$ of size $2L \times 2L \times L$ are considered in the limit $L \longrightarrow \infty$, where $A(L)$ is a square in the xy plane of side length $2L$ with (lateral) periodic boundary conditions and $\hat{z}(L)$ denotes an arbitrary real function of the extention L. In order to ensure that the strongly varying parts of the density profiles $\underline{\varrho}(z)$ are located in the vicinity of position $z = 0$ upon $L \to \infty$, the choice $\hat{z}(L) := -\frac{L}{2}$ is made for the investigation of free interfaces (Sec. 4.1) whereas $\hat{z}(L) := 0^-$ is set for charged substrates (Secs. 4.2–4.4). The notation 0^- in the latter case is used in order to emphasise that the wall charges belong *entirely* to the system volume.

If a charged hard wall is present at $z = 0$, a corresponding substrate potential V_i is exerted on particles of type i. This substrate potential can be decomposed as $V_i = V_i^\text{h} + V_i^\text{c}$ with the hard wall contribution

$$V_i^\text{h}(\mathbf{r}) := \begin{cases} \infty & , z \leq \frac{S_i^z}{2} \\ 0 & , z > \frac{S_i^z}{2} \end{cases} , \tag{2.33}$$

where S_i^z is the z-extension of particles of type i, and the contribution due to the surface charge

$$V_i^{\mathrm{c}}(\mathbf{r}) := \int\limits_V \mathrm{d}^3r' \, \frac{Q_i \sigma \delta(z')}{\|\mathbf{r} - \mathbf{r}'\|_\infty}. \tag{2.34}$$

The electrostatic self energy of the wall is given by

$$U^{\mathrm{self}}(\sigma) := \frac{1}{2} \int\limits_V \mathrm{d}^3r \int\limits_V \mathrm{d}^3r' \, \frac{\sigma\delta(z)\sigma\delta(z')}{\|\mathbf{r} - \mathbf{r}'\|_\infty}. \tag{2.35}$$

In the absence of a charged hard wall $V_i(z)$ as well as $U^{\mathrm{self}}(\sigma)$ vanish.

Introducing the local charge density

$$\varrho^Q(\mathbf{r}, [\underline{\varrho}]) := \sum_i Q_i \varrho_i(\mathbf{r}) + \sigma\delta(z) \tag{2.36}$$

and the electrostatic potential

$$\psi(\mathbf{r}, [\underline{\varrho}]) := \int\limits_V \mathrm{d}^3r' \, \frac{\varrho^Q(\mathbf{r}', [\underline{\varrho}])}{\|\mathbf{r} - \mathbf{r}'\|_\infty} \tag{2.37}$$

one readily finds (see Eqs. (2.30), (2.34), and (2.35))

$$\begin{aligned} &F_{\mathrm{el}}^{\mathrm{ex,per}}[\underline{\varrho}] + \sum_i \int\limits_V \mathrm{d}^3r \, \varrho_i(\mathbf{r}) V_i^{\mathrm{c}}(\mathbf{r}) + U^{\mathrm{self}}(\sigma) \\ &= \frac{1}{2} \int\limits_V \mathrm{d}^3r \int\limits_V \mathrm{d}^3r' \, \frac{\varrho^Q(\mathbf{r}, [\underline{\varrho}])\varrho^Q(\mathbf{r}', [\underline{\varrho}])}{\|\mathbf{r} - \mathbf{r}'\|_\infty} \\ &= \frac{1}{2} \int\limits_V \mathrm{d}^3r \, \varrho^Q(\mathbf{r}, [\underline{\varrho}])\psi(\mathbf{r}, [\underline{\varrho}]). \end{aligned} \tag{2.38}$$

For systems with translational invariance perpendicular to the z-axis, the electrostatic potential in Eq. (2.37) can be expressed as

$$\psi(z, [\underline{\varrho}]) = \int\limits_{\hat{z}(L)}^{\hat{z}(L)+L} \mathrm{d}z' \, \varrho^{\mathrm{Q}}(z', [\underline{\varrho}]) \int\limits_{A(L)} \mathrm{d}^2a' \, \frac{1}{\|(\mathbf{a}', z - z')\|_\infty}, \tag{2.39}$$

where $\mathbf{a}'$ denotes a two-dimensional vector in the x-y plane. The inner integral in Eq. (2.39) leads to

$$\begin{aligned}\int\limits_{A(L)} \mathrm{d}^2a' \, \frac{1}{\|(\mathbf{a}', z-z')\|_\infty} &= \int\limits_{0}^{|z-z'|} \mathrm{d}a' \, 8a' \frac{1}{|z-z'|} + \int\limits_{|z-z'|}^{L} \mathrm{d}a' \, 8a' \frac{1}{a'} \\ &= -4|z-z'| + 8L. \end{aligned} \tag{2.40}$$

Global charge neutrality

$$\int\limits_{\hat{z}(L)}^{\hat{z}(L)+L} \mathrm{d}z \; \varrho^Q(z, [\underline{\varrho}]) = 0 \tag{2.41}$$

reduces Eq. (2.39) to

$$\psi(z, [\underline{\varrho}]) = -4 \int\limits_{\hat{z}(L)}^{\hat{z}(L)+L} \mathrm{d}z' \; \varrho^{\mathrm{Q}}(z', [\underline{\varrho}])|z-z'|. \tag{2.42}$$

By differentiating twice, one finds that ψ fulfils the *Poisson equation*

$$\psi'' = -8\varrho^Q. \tag{2.43}$$

Furthermore, due to Eq. (2.41) one obtains

$$\begin{aligned}\psi(\hat{z}(L), [\underline{\varrho}]) &= -4 \int\limits_{\hat{z}(L)}^{\hat{z}(L)+L} \mathrm{d}z' \; \varrho^{\mathrm{Q}}(z', [\underline{\varrho}])(z' - \hat{z}(L)) \\ &= -4 \int\limits_{\hat{z}(L)}^{\hat{z}(L)+L} \mathrm{d}z' \; \varrho^{\mathrm{Q}}(z', [\underline{\varrho}])z' \\ &= 4 \int\limits_{\hat{z}(L)}^{\hat{z}(L)+L} \mathrm{d}z' \; \varrho^{\mathrm{Q}}(z', [\underline{\varrho}])(\hat{z}(L) + L - z') \\ &= -\psi(\hat{z}(L) + L, [\underline{\varrho}]). \end{aligned} \tag{2.44}$$

Combined with Eqs. (2.29) and (2.38), the density functional in Eq. (2.8) takes the final form

$$\Omega[\underline{\varrho}] = 4L^2 \Bigg(\sum_i \int\limits_{\hat{z}(L)}^{\hat{z}(L)+L} \mathrm{d}z \; \varrho_i(z) \Big(\ln(\varrho_i(z)) - 1 - \mu_i^* + V_i^{\mathrm{h}}(z) + \frac{1}{2} Q_i \psi(z, [\underline{\varrho}]) \Big)$$

$$+\frac{1}{2}\sigma\psi(\hat{z}(L),[\underline{\varrho}])\Bigg) + F^{\text{ex,ref}}[\underline{\varrho}] + F^{\text{ex,per}}_{\text{corr}}[\underline{\varrho}] - U^{\text{self}}(\sigma) \quad (2.45)$$

which has to be minimised under the constraint of global charge neutrality Eq. (2.41). The corresponding Euler-Lagrange equations read

$$\ln(\varrho_i(z)) - \mu_i^* + V_i^{\text{h}}(z) + Q_i\psi(z,[\underline{\varrho}]) - c_i^{\text{ref}}(z,[\underline{\varrho}]) - c^{\text{per}}_{\text{corr},i}(z,[\underline{\varrho}]) = 0. \quad (2.46)$$

In the isotropic and the nematic bulk fluid, the densities $\underline{\varrho}$ are spatially constant. In this case, the Euler-Lagrange equations Eq. (2.46) comprise five coupled equations:

$$\ln(\varrho_i^{(\text{bulk})}) - \mu_i^{*(\text{bulk})} - c_i^{\text{ref},(\text{bulk})} - c^{\text{per},(\text{bulk})}_{\text{corr},i} = 0, \quad (2.47)$$

where the chemical potentials $\mu_i^{*(\text{bulk})}$ fulfil Eq. (2.16) and the *local* charge neutrality condition $\sum_i Q_i\varrho_i^{(\text{bulk})} = 0$. The electrostatic contribution $-c^{\text{per},(\text{bulk})}_{\text{el},i} = Q_i\psi^{(\text{bulk})}$ is absent in Eq. (2.47) because the electrostatic potential ψ vanishes in locally charge neutral systems (see Eq. (2.37)).

For determining the number density profiles at free interfaces between coexisting bulk phases $\mathcal{B}_1$ and $\mathcal{B}_2$, the Euler-Lagrange equations

$$\ln\big(\varrho_i(z)\big) - \mu_i^* + Q_i\psi(z,[\underline{\varrho}]) - c_i^{\text{ref}}(z,[\underline{\varrho}]) - c^{\text{per}}_{\text{corr},i}(z,[\underline{\varrho}]) = 0 \quad (2.48)$$

are to be solved with the boundary conditions

$$\varrho_i(\hat{z}(L)) = \varrho_i^{(\mathcal{B}_1)}, \qquad \varrho_i(\hat{z}(L)+L) = \varrho_i^{(\mathcal{B}_2)}. \quad (2.49)$$

In order that for $z = \hat{z}(L)$ and $z = \hat{z}(L) + L$ Eq. (2.48) reduces to Eq. (2.47) for $\mathcal{B}_1$ and $\mathcal{B}_2$, respectively, one has to require

$$\begin{aligned} -\mu_i^* + Q_i\psi(\hat{z}(L),[\underline{\varrho}]) &= -\mu_i^{*(\mathcal{B}_1)}, \\ -\mu_i^* + Q_i\psi(\hat{z}(L)+L,[\underline{\varrho}]) &= -\mu_i^{*(\mathcal{B}_2)}. \end{aligned} \quad (2.50)$$

Using Eq. (2.44), one readily concludes

$$\mu_i^* = \frac{1}{2}(\mu_i^{*(\mathcal{B}_1)} + \mu_i^{*(\mathcal{B}_2)}) \quad (2.51)$$

and

$$\psi_D := \psi(\hat{z}(L)+L,[\underline{\varrho}]) - \psi(\hat{z}(L),[\underline{\varrho}]) = \frac{1}{Q_i}(\mu_i^{*(\mathcal{B}_1)} - \mu_i^{*(\mathcal{B}_2)}). \quad (2.52)$$

ψ_D is known as *Donnan potential* [Adamson1973] between the two bulk phases $\mathcal{B}_1$ and $\mathcal{B}_2$. It maintains a density gradient of the mobile particles at the interface between two coexisting bulk phases. Its definition given above is unique, i.e., the rightmost expression is in fact independent of i due to Eq. (2.16), e.g.,

$$\frac{\mu_{\mathrm{S}}^{*(\mathcal{B}_1)} - \mu_{\mathrm{S}}^{*(\mathcal{B}_2)}}{Q_{\mathrm{S}}} = \frac{(\mu_{CS}^{*} - \mu_{\mathrm{C}}^{*(\mathcal{B}_1)}) - (\mu_{CS}^{*} - \mu_{\mathrm{C}}^{*(\mathcal{B}_2)})}{-Q_{\mathrm{C}}} = \frac{\mu_{\mathrm{C}}^{*(\mathcal{B}_1)} - \mu_{\mathrm{C}}^{*(\mathcal{B}_2)}}{Q_{\mathrm{C}}}. \tag{2.53}$$

2.5 Theory of wetting

The purpose of this section is to introduce the basic concepts of wetting theory to the extent necessary for Ch. 4. Thorough reviews can be found in Refs. [deGennes1985, Dietrich1988, Schick1990, Sullivan1986].

A fluid deep within the one-phase region of the phase diagram in contact with a substrate exhibits the structure of the stable bulk phase down to microscopic distances from the substrate. Upon approaching two-phase coexistence along a thermodynamic path can lead to the formation of a macroscopic film at the substrate with a fluid structure corresponding to the (previously) metastable bulk phase; this phenomenon is called *complete wetting*. In contrast, *partial wetting* occurs if only films of finite thickness of the metastable bulk phase are attained. *Wetting transitions* occur at state points of two-phase coexistence lines where complete wetting is separated from partial wetting. Upon approaching a wetting transition along two-phase coexistence from the partial wetting side, the film thickness either is bounded from above close to the wetting transition and jumps to infinity at the wetting transition, or it increases continuously to infinity. The former case is called *first-order wetting transition* whereas the latter case is called *critical wetting transition*.

In principle, the asymptotic wetting behaviour can be completely inferred from the *effective interface potential* $\Omega^{\mathrm{eff}}(\zeta) := (\Omega[\underline{\varrho}_{\zeta}]-\Omega^{\mathrm{bulk}})/(4L^2)$ where Ω is the density functional Eq. (2.45), Ω^{bulk} denotes the *bulk* contribution to the grand potential and the density profiles $\underline{\varrho}_{\zeta}$ are the solutions of the Euler-Lagrange equations Eq. (2.46) under the *constraint* of a prescribed film thickness ζ characterised by the position of the isotropic-nematic interface [Dietrich1988]. The effective interface potential Ω^{eff} resembles the thermodynamic potential within Landau theory [Binney1992, Goldenfeld1992, Landau1979, leBellac1991, Plischke1994, Stanley1971] from which all stable and metastable states as well as the order of phase transitions can be inferred. $\Omega^{\text{eff}}(\zeta)$ takes its global minimum at the equilibrium interface position ζ^*; the corresponding density profiles $\underline{\varrho}_{\zeta^*}$ are the *unconstraint* minima of Eq. (2.45). Local minima of Ω^{eff} are related to interface locations which are only metastable. $\zeta^* = \infty$ and $\zeta^* < \infty$ at two-phase coexistence correspond to complete and partial wetting, respectively. If $\zeta^* \to \infty$ continuously upon approaching a wetting transition point along coexistence critical wetting occurs. A first-order wetting transition, on the other hand, is identified if $\Omega^{\text{eff}}(\zeta)$ at the wetting transition exhibits two global minima, one at $\zeta < \infty$ and another one at $\zeta = \infty$, with a maximum in between [Dietrich1988].

In the following, the asymptotic behaviour of the effective interface potential $\Omega^{\text{eff}}(\zeta)$ for $\zeta \to \infty$ will be determined analytically for the case of a wall in contact with an *isotropic* bulk fluid (compare Sec. 4.2). The analogous expressions for the case of a wall in contact with a *nematic* bulk fluid (compare Sec. 4.3) can be obtained by interchanging the terms "isotropic" and "nematic".

Since exact solutions are out of reach for the present model, $\Omega^{\text{eff}}(\zeta)$ is approximated by considering the following subspace of density profiles [Dietrich1991]:

$$\tilde{\varrho}_{i,\zeta}(z) := \begin{cases} \varrho_i^{\text{wn}}(z) & , z \leq \zeta/2 \\ \varrho_i^{\text{ni}}(z-\zeta) & , z > \zeta/2 \end{cases}, \tag{2.54}$$

where $\underline{\varrho}^{\text{wn}}(z)$ and $\underline{\varrho}^{\text{ni}}(z)$ correspond to solutions of the Euler-Lagrange equations Eq. (2.46) with wall-nematic and nematic-isotropic boundary conditions, respectively. The interfaces for $\underline{\varrho}^{\text{wn}}(z)$ and $\underline{\varrho}^{\text{ni}}(z)$ are located at $z = 0$. Therefore, in the interval $z \in (-\infty, \zeta/2]$ the trial density profile $\underline{\tilde{\varrho}}_{\zeta}$ is described by the wall-nematic profile whereas in the interval $z \in (\zeta/2, \infty)$ it is given by the free nematic-isotropic profile shifted to position ζ. Due to $\varrho_i^{\text{wn}}(\infty) = \varrho_i^{\text{ni}}(-\infty)$, the discontinuity of $\underline{\tilde{\varrho}}_{\zeta}$ at $z = \zeta/2$ vanishes in the limit $\zeta \to \infty$. The leading asymptotic terms of $\Omega^{\text{eff}}(\zeta \to \infty)$ are independent of the actual form of the density profiles $\underline{\tilde{\varrho}}_{\zeta}(z)$ within the transition regime around $z = \zeta/2$ [Dietrich1991].

Except for the electrostatic term Eq. (2.38), the density functional in Eq. (2.45) is identical to the one in Ref. [Dietrich1991] modelling isotropic nonretarded van der Waals forces, because the integrand $\Phi(\underline{n}(\mathbf{r}))$ of $F^{\text{ex,ref}}$ (Eq. (2.9)) represents interactions of only finite range and the integral kernel $U_{ij}^{\text{per}}(\mathbf{r})G_{ij}(\kappa, \mathbf{r})$ of $F_{\text{corr}}^{\text{ex,per}}$ (Eq. (2.31)) as a function of $\mathbf{r}$ decays proportional to $\|\mathbf{r}\|_{\infty}^{-6}$ (Eqs. (2.19) and (2.28)). Using the results of

Ref. [Dietrich1991] for this part of the effective interface potential along thermodynamic paths with *constant* salt reservoir chemical potential μ^*_{CS} leads to

$$\begin{aligned}\tilde{\Omega}^{\mathrm{eff}}(\zeta \to \infty) &= \gamma^{\mathrm{wn}} + \gamma^{\mathrm{ni}} - (\varrho^{\mathrm{ni}}_M(-\infty) - \varrho^{\mathrm{ni}}_M(\infty))\Delta\mu^*_{C_k M}\zeta \\ &\quad + a_2\zeta^{-2} + a_3\zeta^{-3} + \mathcal{O}(\zeta^{-4}) \qquad (2.55)\end{aligned}$$

with the wall-nematic and nematic-isotropic interfacial tensions γ^{wn} and γ^{ni}, respectively, the difference $\Delta\mu^*_{C_k M}$ of the macroion reservoir chemical potential with respect to the value at isotropic-nematic coexistence, and the amplitudes [Dietrich1991]

$$a_2 = \frac{1}{2}\sum_{ij} T_{ij} \qquad (2.56)$$

and

$$a_3 = \sum_{ij} T_{ij}(d_{i,\mathrm{wn}} - d_{j,\mathrm{ni}}) \qquad (2.57)$$

where the abbreviation

$$T_{ij} := -\frac{24 Q_i^2 Q_j^2}{\kappa^4}\varrho^{\mathrm{ni}}_i(-\infty)\big(\varrho^{\mathrm{ni}}_j(-\infty) - \varrho^{\mathrm{ni}}_j(\infty)\big) \qquad (2.58)$$

has been introduced. The quantities

$$d_{i,\mathrm{wn}} := \int_0^\infty \mathrm{d}z \left(1 - \frac{\varrho^{\mathrm{wn}}_i(z)}{\varrho^{\mathrm{wn}}_i(\infty)}\right) \qquad (2.59)$$

and

$$d_{j,\mathrm{ni}} := \frac{\displaystyle\int_{-\infty}^{0} \mathrm{d}z\big(\varrho^{\mathrm{ni}}_j(z) - \varrho^{\mathrm{ni}}_j(-\infty)\big) + \int_0^\infty \mathrm{d}z\big(\varrho^{\mathrm{ni}}_j(z) - \varrho^{\mathrm{ni}}_j(\infty)\big)}{\varrho^{\mathrm{ni}}_j(-\infty) - \varrho^{\mathrm{ni}}_j(\infty)} \qquad (2.60)$$

are related to excess adsorptions of the wall-nematic and the free nematic-isotropic interface, respectively.

In order to calculate the contribution of the electrostatic term Eq. (2.38) to the asymptotic behaviour of $\tilde{\Omega}^{\mathrm{eff}}(\zeta)$ for $\zeta \to \infty$, the asymptotic behaviour of the density profiles $\underline{\varrho}^{\mathrm{wn}}(z)$ and $\underline{\varrho}^{\mathrm{ni}}(z)$ at distances far from the substrate and interface, respectively, has to be determined. Expanding the

Euler-Lagrange equations (Eq. (2.46)) for $z \to \infty$ around the bulk values provides the number density deviations $\Delta\underline{\varrho}(z) := \underline{\varrho}(z) - \underline{\varrho}(\infty)$ with

$$\Delta\varrho_i(z \to \infty) = \varrho_i(\infty)\big(- \Delta V_i^{\mathrm{h}}(z) - Q_i \Delta\psi(z) + \Delta c_i^{\mathrm{ref}}(z) + \Delta c_{\mathrm{corr},i}^{\mathrm{per}}(z)\big). \tag{2.61}$$

The electrostatic potential difference $\Delta\psi$ depends on $\Delta\underline{\varrho}$ via the local charge density ϱ^Q (see Eqs. (2.36) and (2.37)). However, this dependence will not be used for the derivation of, c.f., Eq. (2.68). Inserting Eqs. (2.9) and (2.31) into Eq. (2.4) leads to

$$\Delta c_i^{\mathrm{ref}}(z \to \infty) = -\sum_j \Delta\varrho_j(z) A_{ij} \tag{2.62}$$

and

$$\Delta c_{\mathrm{corr},i}^{\mathrm{per}}(z \to \infty) = \sum_j \big(t_{ij}(z) - \Delta\varrho_j(z) B_{ij}\big), \tag{2.63}$$

where $t_{ij}(z) := -24 Q_i^2 Q_j^2 \varrho_j(\infty) \tilde{\kappa}(\infty)^{-4} z^{-3}$. The spatially constant 5×5-matrices A_{ij} and B_{ij} depend only on model parameters (particle sizes and charges) and bulk quantities: The 5×5-matrix A_{ij} in Eq. (2.62) is given by

$$A_{ij} = -\int\limits_{-\infty}^{\infty} \mathrm{d}z \; c_{ij}^{\mathrm{ref}}\big(z, [\underline{\varrho}(\infty)]\big), \tag{2.64}$$

where $\underline{\varrho}(\infty)$ is the set of *constant* bulk density profiles. By introducing

$$\begin{aligned} w_{ij}(z) \quad := \quad & \int\limits_{A(L)} \mathrm{d}^2 a \; U_{ij}^{\mathrm{per}}(\mathbf{a}, z)\big(\exp(-U_{ij}^{\mathrm{ref}}(\mathbf{a}, z)) - 1 \\ & + \exp(-U_{ij}^{\mathrm{ref}}(\mathbf{a}, z)) G_{ij}(\kappa, \|\mathbf{a}, z\|_\infty)\big), \end{aligned} \tag{2.65}$$

which renders Eq. (2.31) in the form

$$F_{\mathrm{corr}}^{\mathrm{ex,per}}[\underline{\varrho}] = \frac{1}{2} 4L^2 \sum_{ij} \int\limits_{0^-}^{\infty} \mathrm{d}z \int\limits_{0^-}^{\infty} \mathrm{d}z' \; \varrho_i(z) \varrho_j(z') w_{ij}(z - z'), \tag{2.66}$$

the 5×5-matrix B_{ij} in Eq. (2.63) can be expressed as

$$B_{ij} = \int\limits_{-\infty}^{\infty} \mathrm{d}z \; w_{ij}(z). \tag{2.67}$$

Defining $M_{ij} := \delta_{ij}/\varrho_i(\infty) + A_{ij} + B_{ij}$ and since $V_i^{\mathrm{h}}(z) = 0$ for $z > \frac{1}{2}\max_i(S_i^z)$ (Eq. (2.33)), Eq. (2.61) is equivalent to

$$\sum_j M_{ij}\Delta\varrho_j(z \to \infty) = -Q_i\Delta\psi(z) + \sum_j t_{ij}(z). \tag{2.68}$$

Firstly, Eq. (2.68) implies an asymptotic decay of $\Delta\varrho_i(z)$ *not faster* than proportional to z^{-3}; otherwise $\Delta\psi(z \to \infty) = Kz^{-3}$ with some spatially constant amplitude K would fulfil the relation $K + 24Q_i\tilde{\kappa}(\infty)^{-4}\sum_j Q_j^2\varrho_j(\infty) = 0$ *simultaneously* for *all* i which is impossible because the second term depends on i whereas the first does not. Moreover, it can be shown that the deviations $\Delta\varrho_i(z)$ exhibit a purely algebraic decay in leading order. One is led to the conclusion that the asymptotic Euler-Lagrange equations (2.68) in conjunction with the Poisson equation (2.43) lead to the properties $\Delta\varrho_i(z \to \infty) = \mathcal{O}(z^{-3})$, $\Delta\psi(z \to \infty) = \mathcal{O}(z^{-3})$, and $\varrho^Q(z \to \infty) = \mathcal{O}(z^{-5})$. Note that on the right-hand side of Eq. (2.36) for $z \to \infty$ the leading and the next to leading order contributions to the density profiles $\underline{\varrho}$ cancel.

Interestingly, the asymptotic decay proportional to z^{-3} of $\Delta\varrho_i(z)$ within the current model for charged particles equals the corresponding one for systems governed by non-retarded isotropic dispersion forces in Ref. [Dietrich1991]. This behaviour is in sharp contrast to the results obtained within multicomponent Poisson-Boltzmann theories which give rise to exponentially decaying density profiles [Grahame1947].

Substituting the trial density profiles $\underline{\tilde{\varrho}}_\zeta$ into the electrostatic term Eq. (2.38) and using the asymptotic behaviour of $\Delta\psi$ and ϱ^Q one obtains after some manipulations

$$\frac{1}{2}\int_V \mathrm{d}^3r\ \varrho^Q(\mathbf{r}, [\underline{\tilde{\varrho}}_\zeta])\psi(\mathbf{r}, [\underline{\tilde{\varrho}}_\zeta]) = \mathrm{const.} + \mathcal{O}(\zeta^{-4}). \tag{2.69}$$

Hence the electrostatic term Eq. (2.38) does *not contribute* to the leading and next-to-leading non-constant terms of the effective interface potential $\tilde{\Omega}^{\mathrm{eff}}(\zeta)$ in Eq. (2.55).

By inspection one recognises the *same* leading asymptotic decay of $\tilde{\Omega}^{\mathrm{eff}}(\zeta)$ in Eq. (2.55) as for systems governed by *non-retarded isotropic dispersion forces* [Dietrich1988, Schick1990]. This is regarded as a surprising result because the model (Sec. 2.3) does *not* include dispersion forces. The asymptotic behaviour $\mathcal{O}(\zeta^{-2})$ in Eq. (2.55) is ultimately generated by using a pair distribution function g_{ij} which decays asymptotically with a

Debye-Hückel (screened Coulomb) form (Sec. 2.3). This assumption concerning the pair distribution function g_{ij} is valid because the linearisation approximation underlying the Debye-Hückel theory is justified at large distances.

The parameters $\varrho^{\mathrm{ni}}(-\infty) - \varrho^{\mathrm{ni}}(\infty)$, a_2, and a_3 in Eq. (2.55), which will be calculated numerically in Chs. 3 and 4, determine the asymptotic functional form of the effective interface potential $\Omega^{\mathrm{eff}}(\zeta \to \infty)$, the derivative of which with respect to ζ is given by

$$\frac{\mathrm{d}\,\Omega^{\mathrm{eff}}(\zeta \to \infty)}{\mathrm{d}\zeta} \simeq -(\varrho^{\mathrm{ni}}_M(-\infty) - \varrho^{\mathrm{ni}}_M(\infty))\Delta\mu^*_{C_kM} - 2a_2\zeta^{-3} - 3a_3\zeta^{-4}. \quad (2.70)$$

For $\Delta\mu^*_{C_kM} \nearrow 0$, and hence $\varrho^{\mathrm{ni}}(-\infty) - \varrho^{\mathrm{ni}}(\infty) > 0$, the minimum of $\Omega^{\mathrm{eff}}(\zeta)$ at $\zeta = \zeta^*$ fulfils the equation

$$-(\varrho^{\mathrm{ni}}_M(-\infty) - \varrho^{\mathrm{ni}}_M(\infty))\Delta\mu^*_{C_kM} = 2a_2(\zeta^*)^{-3}. \quad (2.71)$$

The left-hand side of Eq. (2.71) is positive and decreases as $\Delta\mu^*_{C_kM} \nearrow 0$. Thus, ζ^* tends to ∞, i.e., *complete wetting* occurs, if and only if $a_2 > 0$. In this case an asymptotic behaviour

$$\zeta^* = \left(\frac{-(\varrho^{\mathrm{ni}}_M(-\infty) - \varrho^{\mathrm{ni}}_M(\infty))\Delta\mu^*_{C_kM}}{2a_2}\right)^{-\frac{1}{3}} = \mathcal{O}(|\Delta\mu^*_{C_kM}|^{-\frac{1}{3}}) \quad (2.72)$$

is found.

If $\Delta\mu^*_{C_kM} = 0$ and $a_2 \nearrow 0$, the equilibrium interface position ζ^* is given by

$$\zeta^* = \frac{3a_3}{-2a_2}. \quad (2.73)$$

ζ^* diverges continuously to ∞, i.e., *critical wetting* occurs, if $a_3 > 0$. In the case $a_3 < 0$ the interface position $\zeta = \infty$ for $a_2 < 0$ corresponds to a relative *maximum* of Ω^{eff} and ζ^* approaches a finite limit as $a_2 \nearrow 0$. At the wetting transition $a_2 = 0$ for $a_3 < 0$ the equilibrium interface position ζ^* exhibits a discontinuous divergence, i.e., first-order wetting occurs.

Chapter 3

Bulk and surface phase diagrams

Having introduced a density functional theory for a model fluid of charged platelike colloids in the previous chapter, a first investigation will be devoted to the bulk properties, particularly to the bulk phase diagrams. Although this work aims at interfaces knowledge about the bulk structure is important in a least three respects: First, one has to ensure that the model fluid in which inhomogeneities should be investigated exhibits physically acceptable behaviours in homogeneous configurations. Second, bulk phase diagrams may serve as a guide which surface phase transitions can occur and under which conditions. Finally, coexistence conditions and the corresponding bulk structure have to be determined precisely in order to calculate equilibrium interfacial profiles. Afterwards, the bulk phase diagrams augmented by surface phase transition lines will be described in order to provide a general overview of the wetting and drying phenomena occurring within the model considered here. The anticipated surface phase behaviour will be justified in detail in the next chapter.

3.1 Bulk phase diagrams

As a first step in the investigation of the density functional developed in the last chapter, bulk phase diagrams are determined for various effective macroion charges Q_{M} by solving the bulk Euler-Lagrange equations (2.47) numerically.

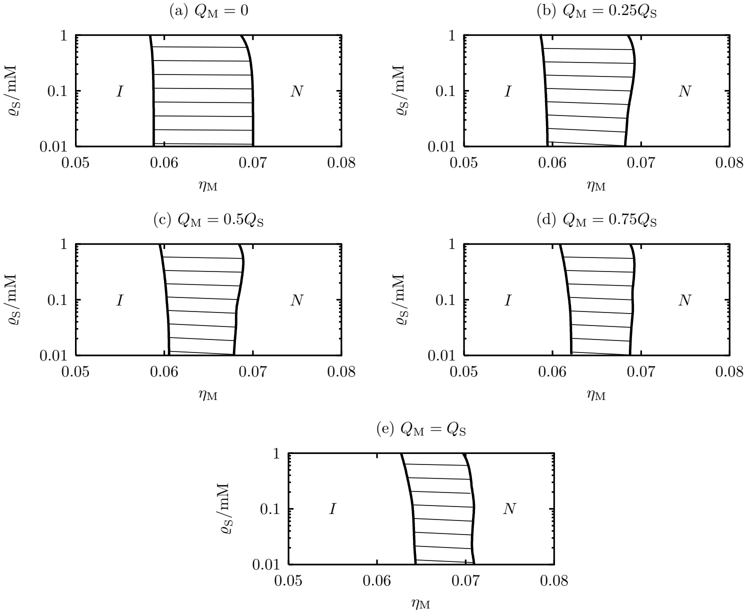

Figure 3.1: Bulk phase diagrams of mixtures of plate-like macroions ($D_\mathrm{M} = 14\,\mathrm{nm}$, $L_\mathrm{M} = 0.72\,\mathrm{nm}$) and monovalent salt ($D_\mathrm{S} = 0.72\,\mathrm{nm}$, $Q_\mathrm{S} = -e$) for effective macroion charges $Q_\mathrm{M} = 0$ (a), $Q_\mathrm{M} = 0.25Q_\mathrm{S}$ (b), $Q_\mathrm{M} = 0.5Q_\mathrm{S}$ (c), $Q_\mathrm{M} = 0.75Q_\mathrm{S}$ (d), and $Q_\mathrm{M} = Q_\mathrm{S}$ (e) in terms of the platelet packing fraction $\eta_\mathrm{M} = \varrho_\mathrm{M} D_\mathrm{M}^2 L_\mathrm{M}$ and the salt density ϱ_S. Note that $\varrho_\mathrm{S} = 1\,\mathrm{mM}$ for $D_\mathrm{S} = 0.72\,\mathrm{nm}$ corresponds to a salt packing fraction $\varrho_\mathrm{S} D_\mathrm{S}^3 = 2.2 \cdot 10^{-4}$. Coexisting states are connected by (non-horizontal) tie lines. The model exhibits one isotropic (I) and one nematic (N) phase separated by first-order phase transitions. The salt density of coexisting phases is higher in the isotropic and lower in the nematic phase (Donnan effect) as can be inferred from the negative slope of the tie lines. For increasing effective macroion charge, the isotropic and the nematic binodals are shifted to larger macroion packing fractions η_M. With increasing salt density ϱ_S, the isotropic-nematic binodals for systems of charged macroions bend towards lower values of the macroion packing fraction.

It turned out that the biaxial order parameter q_M (Eq. 2.18) vanishes throughout the whole inspected range of chemical potentials $\mu^*_{\mathrm{C_k M}}$ and μ^*_CS, whereas the nematic order parameter s_M (Eq. 2.17) indicates either an isotropic fluid ($s_\mathrm{M} = 0$) or a nematic fluid ($s_\mathrm{M} > 0$).

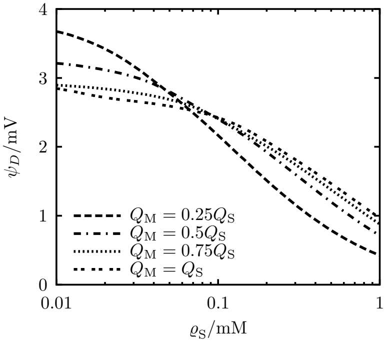

Figure 3.2: Donnan potential ψ_D (see Eq. (2.52)) between the coexisting nematic (N) and isotropic (I) bulk phases in mixtures of platelike macroions and salt (see Fig. 3.1). For fixed effective macroion charge Q_M, the Donnan potential decreases with increasing salt density ϱ_S. For salt densities $\varrho_\mathrm{S} \approx 0.01\,\mathrm{mM}$, ψ_D decreases upon increasing $|Q_\mathrm{M}|$, whereas for salt densities $\varrho_\mathrm{S} \approx 1\,\mathrm{mM}$, ψ_D increases with increasing $|Q_\mathrm{M}|$.

Figure 3.1 displays phase diagrams for the parameters (compare Fig. 2.1) $D_\mathrm{M} = 14\,\mathrm{nm}$, $L_\mathrm{M} = 0.72\,\mathrm{nm}$, $D_\mathrm{S} = 0.72\,\mathrm{nm}$, $Q_\mathrm{S} = -e$ with $Q_\mathrm{M} = 0$, $Q_\mathrm{M} = 0.25Q_\mathrm{S}$, $Q_\mathrm{M} = 0.5Q_\mathrm{S}$, $Q_\mathrm{M} = 0.75Q_\mathrm{S}$, and $Q_\mathrm{M} = Q_\mathrm{S}$ in terms of the macroion packing fraction $\eta_\mathrm{M} = \varrho_\mathrm{M} D_\mathrm{M}^2 L_\mathrm{M}$ and the salt density ϱ_S. Dimensional salt number densities are given in units of $1\,\mathrm{mM} = 1\,\mathrm{mol/m^3} \approx 6 \times 10^{23}\,\mathrm{m^{-3}}$.

One isotropic phase (I) and one nematic phase (N) are found separated by first-order phase transitions. Whereas for coexisting phases η_M is always smaller in the isotropic phase than in the nematic phase, ϱ_S of coexisting phases is higher in the isotropic and lower in the nematic phase. A similar displacement of salt from regions of large concentrations of charged macroions is known as Donnan effect [Adamson1973, Donnan1911, Donnan1924]. Whereas the original Donnan effect has been discovered in systems subdivided by membranes which are impermeable for macroions, here the density difference of the macroions occurs due to two coexisting bulk phases. As for the case of membrane equilibrium, here a Donnan potential ψ_D (Eq. (2.52)) maintains the density gradients between the coexisting phases. Figure 3.2 depicts its dependence on the effective macroion charge Q_M and the salt density ϱ_S. ψ_D decreases with increasing salt density ϱ_S. This tendency is intuitively expected as the

Donnan effect becomes less pronounced upon increasing the screening of the macroion charge by increasing the salt density. For fixed salt density ϱ_{S} well below $\approx 0.1\,\mathrm{mM}$, ψ_D decreases with increasing $|Q_{\mathrm{M}}|$, whereas this behaviour is reversed for fixed salt density ϱ_{S} above $\approx 0.1\,\mathrm{mM}$.

Upon an increase of the effective macroion charge $|Q_{\mathrm{M}}|$, the isotropic and the nematic binodals in Fig. 3.1 are shifted to larger values of the macroion packing fraction η_{M}. This may be qualitatively understood by introducing the notion of an effective shape, which, in the present case, for macroions is given by a hard core surrounded by a soft $\|\cdot\|_\infty$-sphere, i.e., a cube, with its linear extension proportional to Q_{M}^2 due to the pairwise Coulomb repulsion. For small macroion charges, the effective shape is still platelike whereas for highly charged colloids, the effective shape tends towards a cube leading to a shift of the two-phase region to larger macroion packing fractions.

For fixed effective macroion charge as well as particle shape and increasing salt density ϱ_{S}, the isotropic-nematic binodals in Fig. 3.1 bend towards smaller macroion packing fractions. This behaviour is expected intuitively, because high ionic strength causes strong screening which in turn leads to effectively quasi-hard platelets (see Fig. 3.1(a)).

3.2 Bulk and surface phase diagram

Having calculated the bulk states at coexistence (see Sec. 3.1), the Euler-Lagrange equations (Eq. (2.46)) for mixtures of platelike macroions and monovalent salt in contact with a charged hard wall can be solved. Changes in the wetting behaviour of the substrate by films of (meta)stable structures different from the bulk structure upon changing model parameters are reflected by *surface phase transitions*. These surface phase transitions are represented by additional points and lines in the phase diagrams (see Fig. 3.3). Although details of the wetting behaviour of charged substrates will be discussed in Ch. 4, the resulting surface phase diagram will be described already here.

The equilibrium states are calculated as function of the chemical potential $\mu^*_{C_kM}$, the effective macroion charge Q_M, and the surface charge density σ. The remaining parameters of the model have been fixed as (see Fig. 2.1) $D_M = 14\,\mathrm{nm}$, $L_M = 0.72\,\mathrm{nm}$, $D_S = 0.72\,\mathrm{nm}$, $|Q_S| = e$, and salt density $\varrho_S = 0.1\,\mathrm{mM}$ in the bulk. As discussed in Sec. 2.3, the current model yields spatially homogeneous bulk phases only in the range $|Q_M| \lesssim e$.

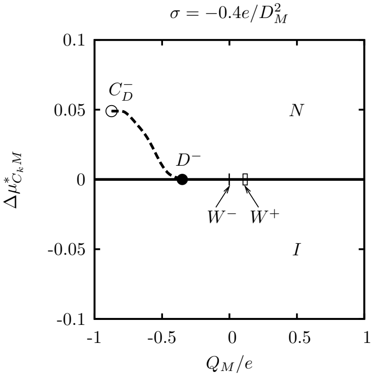

Figure 3.3: Bulk and surface phase diagram of mixtures of platelike macroions ($D_M = 14\,\mathrm{nm}, L_M = 0.72\,\mathrm{nm}$) and monovalent salt ($D_S = 0.72\,\mathrm{nm}, |Q_S| = e$) for salt density $\varrho_S = 0.1\,\mathrm{mM}$ in contact with a charged hard wall of surface charge density $\sigma = -0.4e/D_M^2$ in terms of effective macroion charge Q_M and chemical potential difference $\Delta\mu^*_{C_kM}$. The bulk equilibrium states for $\Delta\mu^*_{C_kM} < 0$ and $\Delta\mu^*_{C_kM} > 0$ are isotropic (I) and nematic (N), respectively. Isotropic-nematic bulk coexistence corresponds to $\Delta\mu^*_{C_kM} = 0$ (solid line). For isotropic boundary conditions in the bulk ($z \to \infty$) at isotropic-nematic coexistence ($\Delta\mu^*_{C_kM} = 0^-$), two first-order wetting transition points W^- (at $Q_M^{W^-} \in [-2 \times 10^{-3}e, 0]$) and W^+ (at $Q_M^{W^+} \in [0.1e, 0.132e]$) have been found. The tolerance intervals are indicated by frames of corresponding widths. Complete wetting by the nematic phase occurs for $Q_M \in (Q_M^{W^-}, Q_M^{W^+})$ upon approaching coexistence from the isotropic side. For nematic boundary conditions in the bulk at isotropic-nematic coexistence ($\Delta\mu^*_{C_kM} = 0^+$), a first-order drying transition point D^- (at $Q_M^{D^-} = -0.35e$) has been found. The accompanying predrying line (dashed line) terminates at a critical point C_D^- (at $Q_M^{C_D^-} = -0.87e, \Delta\mu^{*C_D^-}_{C_kM} = 0.049$). Complete drying by the isotropic phase occurs upon approaching coexistence from the nematic side for $Q_M < Q_M^{D^-}$. This implies that for $Q_M^{D^-} < Q_M < Q_M^{W^-}$ or $Q_M^{W^-} < Q_M < e$ there is neither complete wetting (by the nematic phase) nor complete drying (by the isotropic phase). A (not shown) second drying transition point D^+ appears for Q_M sufficiently large and σ sufficiently small so that there is reentrance of complete drying for large positive values of Q_M.

Figure 3.3 displays the bulk and surface phase diagram for the surface charge density $\sigma = -0.4e/D_M^2$ in terms of the effective macroion charge Q_M and the chemical potential difference $\Delta\mu^*_{C_kM} := \mu^*_{C_kM} - \mu^{*IN}_{C_kM}$. The solid line ($\Delta\mu^*_{C_kM} = 0$) denotes the states of bulk coexistence between the isotropic (I) phase and the nematic (N) phase, corresponding to the chemical potential $\mu^{*IN}_{C_kM}$ at coexistence. The bulk equilibrium states for $\Delta\mu^*_{C_kM} < 0$ and $\Delta\mu^*_{C_kM} > 0$ are isotropic and nematic, respectively.

At isotropic-nematic bulk coexistence with isotropic boundary conditions in the bulk ($\Delta\mu^*_{C_kM} = 0^-$), two first-order wetting transition points W^- and W^+ have been found which could be located only within the intervals of the coexistence line indicated by frames of corresponding widths: Whereas W^- ($Q_M^{W^-} \in [-2 \times 10^{-3}e, 0]$) is known rather precisely, there remains some uncertainty with respect to the location of W^+ ($Q_M^{W^+} \in [0.1e, 0.132e]$). The corresponding prewetting lines [Dietrich1988] are so close to the coexistence line such that they could not be resolved numerically.

Complete wetting by the nematic phase, i.e., the formation of an infinitely thick film of nematic structure upon approaching isotropic-nematic bulk coexistence from the isotropic side (see Sec. 2.5 or Refs. [Dietrich1988, Schick1990]), occurs exclusively for $Q_M \in (Q_M^{W^-}, Q_M^{W^+})$. The phenomenon that *partial wetting* (see Sec. 2.5 or Refs. [Dietrich1988, Schick1990]), i.e., a nematic film of finite thickness, is found for sufficiently large effective macroion charges $|Q_M|$ may be qualitatively understood as follows: The macroion number density profiles ϱ_{M_x}, ϱ_{M_y}, and ϱ_{M_z} close to the substrate are influenced by the hard-core interactions — which give rise to a preference of nematic order close to the wall —, the macroion-substrate Coulomb interactions proportional to $|Q_M|$, and the macroion-macroion Coulomb repulsion proportional to $|Q_M|^2$. The latter dominates for large effective macroion charges $|Q_M|$ leading to a depression of the values of the macroion number densities near the wall which in turn prevents the growth of a nematic film. For small effective macroion charges $|Q_M|$, ϱ_{M_x}, ϱ_{M_y}, and ϱ_{M_z} near the substrate are determined by the balance between the hard-core interactions and the macroion-substrate interactions which lead to complete wetting for attractive walls. Details on the wetting behaviour will be given in Sec. 4.2.

In Fig. 3.3, a first-order drying transition point D^- at $Q_M^{D^-} = -0.35e$ is found for isotropic-nematic bulk coexistence with nematic boundary conditions in the bulk fixing the director to be parallel to the interface normal ($\Delta\mu^*_{C_kM} = 0^+$). The first-order character of the drying transition at state point D^- implies the existence of a predrying line (dashed line in

Fig. 3.3), along which the excess adsorption of macroions

$$\Gamma_M := \int\limits_0^\infty \mathrm{d}z\ (\varrho_M(z) - \varrho_M(\infty)), \tag{3.1}$$

which is proportional to the thickness of the emerging film, exhibits a finite discontinuity. The predrying line is expected to meet the isotropic-nematic bulk coexistence line tangentially [Hauge1983]. The numerical data are consistent with this behaviour but not definitely conclusive due to the numerical difficulties arising from the large thickness of drying films very close to isotropic-nematic bulk coexistence. The predrying line terminates at a critical point C_D^- located at state point $(Q_M^{C_D^-} = -0.87e, \Delta\mu_{C_kM}^{*C_D^-} = 0.049)$. Complete drying by the isotropic phase occurs for $Q_M < Q_M^{D^-}$ upon approaching isotropic-nematic bulk coexistence from the nematic side.

As for the wetting scenario discussed above, the macroion-macroion repulsion will prevail over the macroion-substrate interactions for a sufficiently large effective macroion charges $|Q_M|$. Therefore, for large $|Q_M|$, the formation of an isotropic film is initiated by the strongly depressed macroion number density close to the substrate. Hence one expects complete drying for sufficiently large effective macroion charges $|Q_M|$. For a surface charge density $\sigma = -0.4e/D_M^2$ (see Fig. 3.3), *partial* drying is found for $Q_M \in (Q_M^{D^-}, e]$, i.e., an expected second drying transition point D^+ is located in the range $Q_M > e$. For smaller surface charge densities σ, indeed *two* drying transition points have been found within the range $Q_M \in [-e, e]$. More details of the first-order drying transition and the corresponding predrying line can be found in Sec. 4.3.

Within the intervals $Q_M \in [Q_M^{D^-}, Q_M^{W^-}]$ and $Q_M \in [Q_M^{W^+}, Q_M^{D^+}]$ only partial wetting and drying occurs. In order to validate the topology of the bulk and surface phase diagram in Fig. 3.3, a modified version of the density functional (Eq. (2.45)) has been investigated in which the correlation term $F_{\mathrm{corr}}^{\mathrm{ex,per}}[\underline{\varrho}]$ is omitted. An asymptotic analysis analogous to Sec. 2.5 leads to exponentially decaying profiles of $\Delta\underline{\varrho}$, $\Delta\psi$, and ϱ^Q. The corresponding phase diagram is qualitatively the same as in Fig. 3.3. In particular, there are also first-order wetting and drying transition points which are separated by intervals of only partial wetting *and* drying. Due to the exponentially decaying electrostatic potential, this modified model is similar to a recently investigated model of hard rods interacting with an exponentially decaying wall potential [Shundyak2006]. Whereas the authors of Ref. [Shundyak2006] relied entirely on a numerical approach which provided them only with *evidences* of first-order wetting transitions, within the present work it is *analytically* shown that the wetting and the drying transitions displayed in Fig. 3.3 are of first order (Secs. 4.2 and 4.3).

Chapter 4

Free and fluid-substrate interfaces

The isotropic and nematic structures at two phase coexistence, which have been numerically determined in the previous chapter, are used as boundary conditions for the Euler-Lagrange equations of spatially varying density profiles. A first investigation is devoted to the structure of free interfaces between a semi-infinite isotropic bulk system coexisting with a semi-infinite nematic bulk system. Next, the structure of a semi-infinite isotropic or nematic bulk system in contact with a charged hard wall will be addressed. In particular *wetting* of the substrate in contact with an isotropic bulk by a nematic film and *drying* of the substrate in contact with a nematic bulk by an isotropic film gives rise to several surface phase transitions. Moreover, the electrostatic potential profiles at free and fluid-substrate interfaces will be studied.

4.1 Free interface and interfacial electrostatic potential

Based on the bulk properties provided in the previous chapter, one is now able to calculate the density profiles at the free interface between coexisting isotropic and nematic phases by solving the spatially varying Euler-Lagrange equations (Eq. (2.48)). The interfacial structure and hence quantities such as the interfacial tension and the interfacial width depend on the orientation of the director of the nematic bulk phase with respect

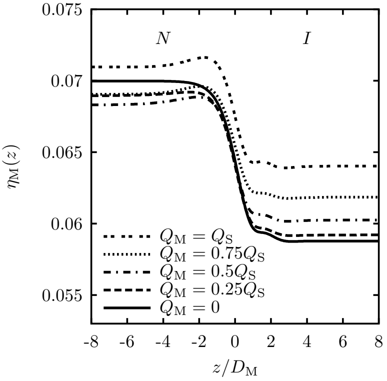

Figure 4.1: Macroion density profiles at the free interface between coexisting isotropic (I) and nematic (N) phases for the mixtures of platelike macroions and salt as studied in Fig. 3.1 at nematic bulk salt density $\varrho_S^{(N)} = 0.1\,\text{mM}$. The interface position $z = 0$ is chosen such that $\varrho_M(0) = \frac{1}{2}\left(\varrho_M^{(I)} + \varrho_M^{(N)}\right)$. The interface width τ^{ni}, inferred from the slope of the density profiles at the interface position $z = 0$ (see main text), and the Debye length κ^{-1} decrease monotonically upon increasing the effective macroion charge $|Q_M|$. The same behaviour is found for the interfacial tension γ^{ni}. See also Fig. 4.2.

to the interface normal. Within the Zwanzig model (see Sec. 2.2) only two different director orientations, parallel and perpendicular to the interface normal, have to be distinguished. However, as the present work is not primarily concerned with the dependence of the interfacial structure on the director orientation relative to the interface, the nematic bulk phase is chosen to be exclusively oriented *parallel* to the interface normal.

The density and order parameter profiles corresponding to the parameters of Sec. 3.1 and a nematic bulk salt density $\varrho_S^{(N)} = 0.1\,\text{mM}$ are depicted in Figs. 4.1 and 4.2, respectively. The interface position $z = 0$ is chosen such that $\varrho_M(0) = \frac{1}{2}\left(\varrho_M^{(I)} + \varrho_M^{(N)}\right)$.

First, and most important, the formalism described in Ch. 2 renders stable free interfaces between coexisting bulk phases. This should be regarded as an accomplishment which can be traced back to using the *spatially varying* screening factor κ introduced in Eq. (2.24); previous attempts with spatially constant κ were not successful.

For a given density profile $\varrho_M(z)$ (Fig. 4.1), the corresponding interface

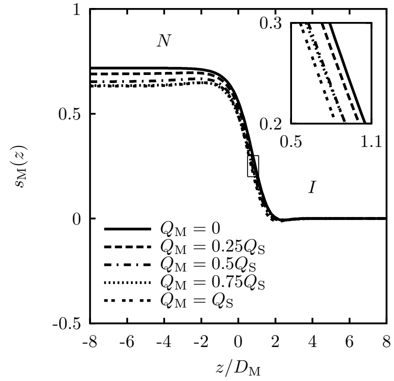

Figure 4.2: Macroion nematic order parameter profiles s_M (Eq. (2.17)) at the free interface between coexisting isotropic (I) and nematic (N) phases for mixtures of platelike macroions and salt as shown in Fig. 3.1 at nematic bulk salt density $\varrho_S^{(N)} = 0.1\,\text{mM}$. The position $z = 0$ is fixed by the choice $\varrho_M(0) = \frac{1}{2}\left(\varrho_M^{(I)} + \varrho_M^{(N)}\right)$ (see Fig. 4.1). On the nematic side of the free interface, most of the macroions lie parallel to the interface. For $z < 0$, $s_M(z)$ decreases upon increasing the effective macroion charge $|Q_M|$. The inset shows a detailed view of the steepest portions of the nematic order parameter profiles in the range $s_M(z) \in [0.2, 0.3]$ indicated by the frame.

width τ^{ni} is defined as the spatial distance between the loci, where the tangent at the density profile at position $z = 0$ reaches the values of the nematic bulk density $\varrho_M^{(N)}$ and the isotropic bulk density $\varrho_M^{(I)}$, respectively. This interface width τ^{ni} decreases monotonically with increasing effective macroion charge from $\tau^{\text{ni}} = 1.8D_M$ for $Q_M = 0.25Q_S$ to $\tau^{\text{ni}} = 1.3D_M$ for $Q_M = Q_S$ (see Fig. 4.1). In parallel, the Debye length κ^{-1} decreases monotonically from $\kappa^{-1} = 1.5D_M$ for $Q_M = 0.25Q_S$ to $\kappa^{-1} = D_M$ for $Q_M = Q_S$.

The nematic order parameter profiles $s_M(z)$ (Fig. 4.2) interpolate almost monotonically between $s_M(\infty) > 0$ in the nematic bulk phase (N) and $s_M(\infty) = 0$ in the isotropic bulk phase (I). Note that s_M has been defined for a director in z-direction, i.e., platelets on the nematic side ($z < 0$) are preferably oriented parallel to the free interface. At a fixed position on the nematic side ($z < 0$), $s_M(z)$ decreases with increasing effective macroion charge $|Q_M|$. This behaviour is consistent with the picture of an increasingly isotropic effective shape, introduced in Sec 3.1.

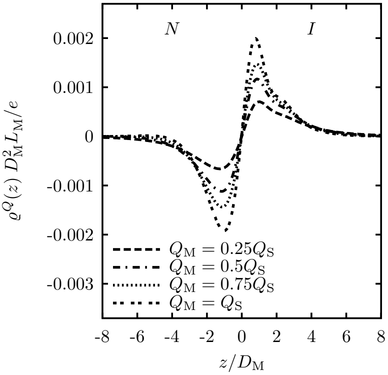

Figure 4.3: Local charge density profiles (Eq. (2.36)) at the free isotropic-nematic interfaces shown in Figs. 4.1 and 4.2 using the same parameters and line code. Whereas *global* charge neutrality holds, deviations from *local* charge neutrality occur near the interface with a negative charge density on the nematic side (N) and a positive charge density on the isotropic side (I). The corresponding electrostatic potential profile is shown in Fig. 4.4.

The charge density profiles $\varrho^Q(z)$ (Eq. (2.36)) displayed in Fig. 4.3 exhibit deviations from local charge neutrality within the interfacial region $-4D_\mathrm{M} \lesssim z \lesssim 4D_\mathrm{M}$. An electrical double layer with a negative charge density on the nematic side (N) and a positive charge density on the isotropic side (I) occurs. Such a local charging is an inevitable consequence of the non-vanishing Donnan potentials ψ_D shown in Fig. 3.2. The full electrostatic potential profiles $\psi(z)$ are depicted in Fig. 4.4. They increase monotonically from the macroion-rich nematic phase N to the macroion-poor isotropic phase I, maintaining the density gradients occurring in the interface region. The potential difference $\psi(\infty) - \psi(-\infty)$ equals the Donnan potential ψ_D (see Eq. (2.52) and Fig. 3.2).

The interfacial tensions γ^ni of the interfaces shown in Fig. 4.1 decrease monotonically from $\gamma^\mathrm{ni} = 108\,\mathrm{nN}\cdot\mathrm{m}^{-1}$ for $Q_\mathrm{M} = 0.25Q_\mathrm{S}$ to $\gamma^\mathrm{ni} = 5\,\mathrm{nN}\cdot\mathrm{m}^{-1}$ for $Q_\mathrm{M} = Q_\mathrm{S}$, which are comparable to experimental findings for gibbsite suspensions [vanderKooij2001]. The corresponding wetting parameters $\omega = (4\pi\gamma\kappa^{-2})^{-1}$ [Schick1990], where the bulk correlation length has been approximated by the Debye length κ^{-1} (see Eq. (2.23)), are in the range $6\ldots340$. If the values for γ^ni are indeed so small, the free isotropic-nematic interfaces are expected to be strongly affected by capil-

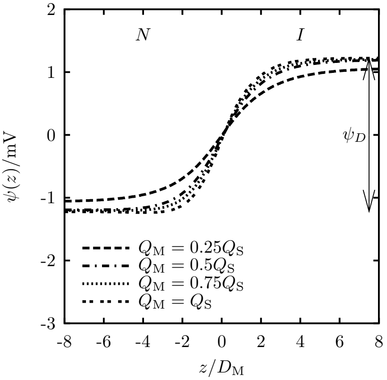

Figure 4.4: Electrostatic potential profiles at the free isotropic-nematic interfaces shown in Figs. 4.1-4.3. The potential difference between the nematic and the isotropic bulk is given by the Donnan potential ψ_D displayed in Fig. 3.2; it is indicated for $Q_{\rm M} = Q_{\rm S}$.

lary wavelike fluctuations which are not captured by the present theory.

Calculating bulk phase diagrams and density profiles for effective macroion charges $|Q_{\rm M}| \geq 1.25|Q_{\rm S}|$ along the lines described above lead to unphysical results like, e.g., negative interfacial tensions. The reason for this phenomenon is that the bulk phases determined in Ch. 3 are assumed to be spatially homogeneous, whereas it has been shown in Sec. 2.3 that the equilibrium bulk states are spatially inhomogeneous for sufficiently large effective macroion charges.

4.2 Isotropic-substrate interface

In this section, the wetting of a charged hard wall in contact with the isotropic model fluid of platelike macroions and salt by a film of nematic structure is discussed. For such wetting scenarios, the boundary conditions imposed on the solutions of the Euler-Lagrange equations (Eq. (2.46)) require the isotropic bulk structure far from the wall. Isotropic-nematic coexistence with such boundary conditions is denoted as $\Delta\mu^*_{C_kM} = 0^-$. Since the macroion density in nematic wetting films is larger than in the isotropic bulk (see Fig. 3.1), the scenario considered here is simply referred to as *wetting* — in contrast to *drying* to be introduced in Sec. 4.3.

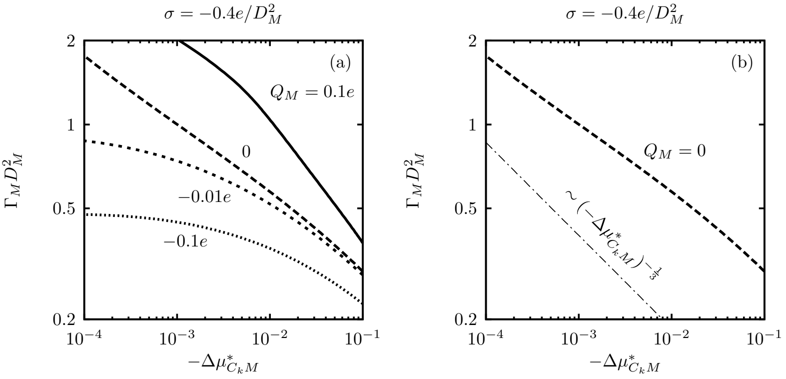

Figure 4.5: Excess adsorption Γ_M of platelike macroions along vertical thermodynamic paths in Fig. 3.3 characterised by fixed effective macroion charges Q_M and parameterised by the chemical potential difference $\Delta\mu^*_{C_k M} < 0$, which measures the thermodynamic distance from isotropic-nematic bulk coexistence. (a) The numerically determined excess adsorption Γ_M remains finite upon $\Delta\mu^*_{C_k M} \nearrow 0$ for $Q_M \leq -0.01e$ (see also Fig. 4.6), whereas a divergence is suggested for the effective macroion charges $Q_M = 0$ and $Q_M = 0.1e$, i.e., there is complete wetting of the substratee by a nematic film. (b) The comparison of the numerical solution for $Q_M = 0$ (dashed line) with the analytical asymptotic power law behaviour $\Gamma_M \sim (-\Delta\mu^*_{C_k M})^{-\frac{1}{3}}$ (dash-dotted line) (see main text) indicates that the asymptotic regime is not yet reached within the numerically accessible range of undersaturations.

Minimising the effective interface potential $\Omega^{\text{eff}}(\zeta)$ in Eq. (2.55) with respect to the interface position ζ leads to the (equilibrium) excess adsorption $\Gamma_M \sim (-\Delta\mu^*_{C_k M})^{-\frac{1}{3}} \nearrow \infty$ for $\Delta\mu^*_{C_k M} \nearrow 0$ as long as $a_2 > 0$ (see Sec. 2.5). Evaluating the analytic expression for a_2 along the isotropic-nematic coexistence line, which depends only on bulk quantities (see Sec. 2.5), one finds two wetting transition points — corresponding to W^- and W^+ in Fig. 3.3 — with complete wetting, i.e., $a_2 > 0$, in between.

Figure 4.5 displays the excess adsorption Γ_M (Eq. (3.1)) as a function of the chemical potential difference $\Delta\mu^*_{C_k M} < 0$ for fixed effective macroion charges Q_M. For $\Delta\mu^*_{C_k M} \nearrow 0$, isotropic-nematic bulk coexistence is approached along vertical thermodynamic paths in Fig. 3.3. In Fig. 4.5(a) the curves for $Q_M = 0$ and $Q_M = 0.1e$ suggest a divergence of Γ_M in this limit, i.e., *complete wetting* of the substrate by a nematic phase occurs for these effective macroion charges. On the other hand, for $Q_M \leq -0.01e$ the excess adsorption remains finite, i.e., *partial wetting* occurs. The complete wetting curves for $Q_M = 0$ and $Q_M = 0.1e$ in Fig. 4.5(a) exhibit *no discontinuity* in the shown range. Thus, the prewetting lines attached to the first-order wetting transition points W^- and W^+ must be closer to the isotropic-nematic coexistence line than the numerically accessible values of $\Delta\mu^*_{C_kM}$.

Figure 4.5(b) compares the analytically obtained asymptotic behaviour for the case $Q_M = 0$ (dash-dotted line) with the corresponding numerical solution (dashed line). The differences between these curves indicate that the ultimate asymptotic regime is not yet reached within the numerically accessible range of undersaturations.

The order of the wetting transitions at state points W^- and W^+ in Fig. 3.3 is determined by $\tilde{\Omega}^{\text{eff}}(\zeta)$ for $\Delta\mu^*_{C_kM} = 0$ (see Sec. 2.5). Critical wetting occurs for $a_2 = 0$, provided $a_3 > 0$; if $a_3 < 0$ the wetting transition is of first order and does not necessarily occur at the point given by $a_2 = 0$ [Dietrich1988, Dietrich1991]. According to Sec. 2.5 the analytical expression for a_3 contains a contribution due to the wall-nematic excess adsorption, which is influenced by the surface charge density σ. Therefore, there is the possibility that the order of the wetting transition depends on the surface charge density σ. For the values of σ used in the present study, however, $a_3 < 0$ is found throughout, i.e., the wetting transitions at W^- and W^+ are of first order.

Whereas the asymptotical analysis above is reliable with respect to the *order* of the wetting transitions at W^- and W^+, this is not the case concerning the *location* of W^- and W^+, because the wetting transitions are of first order [Dietrich1988]. Therefore, numerical methods have to be applied.

In Fig. 4.6 the numerically determined excess adsorption at coexistence is shown as a function of the surface charge density σ. Without loss of generality, only curves for negative effective macroion charges Q_M are displayed: since the density functional described in Ch. 2 is invariant under the simultaneous inversion of the signs of all charges (Q_M, Q_S, and σ), the curve for $Q_M = \overline{Q}_M$ is mapped onto the curve for $Q_M = -\overline{Q}_M$ by reflecting it at the axis $\sigma = 0$.

As expected, the excess adsorption Γ_M of the macroions increases with increasing surface charge density σ for fixed effective macroion charge $Q_M < 0$, because the surface becomes increasingly attractive (or decreasingly repulsive) for the macroions. However, for a fixed surface charge density σ and sufficiently large effective macroion charges $|Q_M|$, Γ_M de-

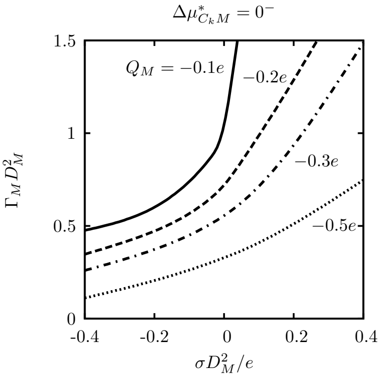

Figure 4.6: Excess adsorption Γ_M of platelike macroions at isotropic-nematic coexistence with isotropic boundary conditions in the bulk ($\Delta\mu^*_{C_kM} = 0^-$) (see Fig. 3.3) in terms of the surface charge density σ. Curves for $Q_M = \overline{Q}_M$ and $Q_M = -\overline{Q}_M$ can be mapped upon each other by reflecting them at the axis $\sigma = 0$. For fixed effective macroion charge, the excess adsorption increases with increasing surface charge density. For fixed surface charge density, the excess adsorption *decreases* upon increasing $|Q_M|$, even for attractive walls.

creases upon increasing $|Q_M|$, irrespective of the sign of Q_M, i.e., even for $\sigma Q_M < 0$, for which the wall attracts macroions. This depression of the macroion number density near the substrate occurs because the macroion-macroion repulsion dominates the macroion-substrate interactions (see Ch. 3.2). From Fig. 4.6 one can indeed infer that there is *partial* wetting for sufficiently large effective macroion charges $|Q_M|$.

The variation of the macroion excess adsorption Γ_M upon $Q_M \nearrow 0$ along isotropic-nematic coexistence for a surface charge density $\sigma = -0.4e/D_M^2$ is shown in Fig. 4.7. Γ_M is finite for $-Q_M \geq 2\times10^{-3}e$. On the other hand, $Q_M = 0$ corresponds to hard colloidal platelets for which the occurrence of complete wetting is well known [Harnau2002/3]. Hence the lower wetting transition point W^- in Fig. 3.3 is located within the range $Q_M^{W^-} \in [-2\times 10^{-3}e, 0]$. In order to locate the upper wetting transition point W^+ one may use the fact that the true wetting transitions points $W^\pm$ can only be located *within* the interval $Q_M \in [-Q_M^*, Q_M^*]$, $Q_M^* = 0.1317165(5)e$, where $\pm Q_M^*$ are the locations of the wetting transition points inferred from the asymptotic analysis of Sec. 2.5. This statement follows from the observation that $|Q_M| > Q_M^*$ leads to $a_2 < 0$ which renders $\zeta = \infty$ as a

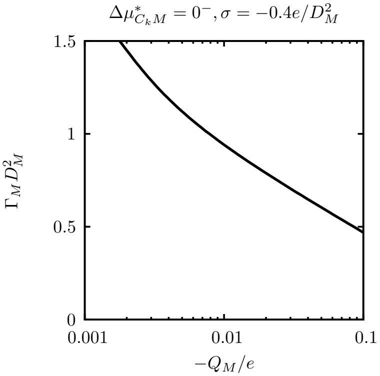

Figure 4.7: Excess adsorption Γ_M of platelike macroions at isotropic-nematic coexistence with isotropic boundary conditions in the bulk ($\Delta\mu^*_{C_kM} = 0^-$) for a surface charge density $\sigma = -0.4e/D_M^2$ (see Fig. 3.3) as function of the effective macroion charge Q_M. It is finite within the range $-Q_M \geq 2 \times 10^{-3}e$ which implies the location of the lower wetting transition point W^- (Fig. 3.3) to be within the range $Q_M \in [-2 \times 10^{-3}e, 0]$.

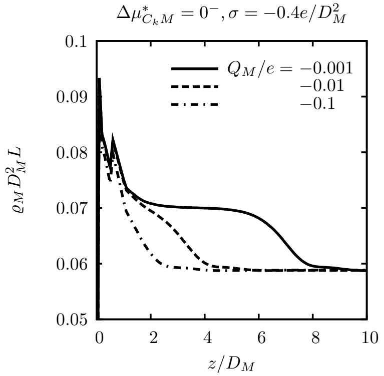

Figure 4.8: Macroion density profiles ϱ_M of a mixture of platelike macroions and salt at isotropic-nematic coexistence with isotropic boundary conditions in the bulk ($\Delta\mu^*_{C_kM} = 0^-$) for a surface charge density $\sigma = -0.4e/D_M^2$ (see Fig. 3.3). Upon decreasing $|Q_M|$, i.e., upon approaching the wetting transition point W^- in Fig. 3.3, a nematiclike film forms at the substrate.

local *maximum* of $\Omega^{\text{eff}}(\zeta)$ (see Sec. 2.5). Together with the numerically found complete wetting for $Q_M = 0.1e$ one concludes that the location of the upper wetting transition point W^+ lies within the range $Q_M^{W^+} \in [0.1e, 0.132e]$.

Finally, Fig. 4.8 displays the increase of the nematic film thicknesses upon increasing $Q_M < 0$ in terms of the macroion density profiles ϱ_M.

4.3 Nematic-substrate interface

In this section the fluid composed of platelike macroions and salt in contact with a charged hard substrate for nematic boundary conditions at large distances from the wall is studied. According to the free isotropic-nematic interface (see Sec. 4.1), the director of the nematic bulk phase, i.e., the preferred macroion orientation, is chosen to be parallel to the interface normal. Isotropic-nematic coexistence with these nematic boundary conditions in the bulk will be denoted as $\Delta\mu^*_{C_kM} = 0^+$. Films forming in between the substrate and the nematic bulk will be isotropic. Since the macroion density of an isotropic film is smaller than within the nematic bulk (see Fig. 3.1), this scenario is called *drying*.

An asymptotic analysis of the effective interface potential for drying along the lines of Sec. 2.5 predicts two first-order drying transition points D^- and D^+. Due to the first-order character of the drying transitions, the loci of D^- and D^+ have been determined numerically (see Sec. 2.5). Note that the upper drying transition point D^+ is not visible in Fig. 3.3 because it is located at $Q_M^{D^+} > e$. However, for sufficiently small surface charge densities $|\sigma|$ both drying transition points have been found within the interval $Q_M \in [-e, e]$. In contrast to the wetting scenario in Sec. 4.2, the discontinuity of the excess adsorption at the *drying* transitions could have been detected numerically. Moreover, the locations of the predrying lines in the phase diagrams (e.g., the dashed line in Fig. 3.3) can be numerically determined.

Figure 4.9 displays the macroion excess adsorption Γ_M close to a charged hard wall with surface charge density $\sigma = -0.4e/D_M^2$ as a function of the effective macroion charge $Q_M \leq 0$. For $-0.35e = Q_M^{D^-} < Q_M \leq 0$, the excess adsorption is finite and bounded from below. It jumps to $-\infty$ at $Q_M = Q_M^{D^-}$. The wall-nematic interfacial tensions of the numerical solutions with finite excess adsorption are smaller than the sums of the corresponding wall-isotropic and the isotropic-nematic interfacial tensions. Therefore, these numerical solutions indeed describe equilibrium structures

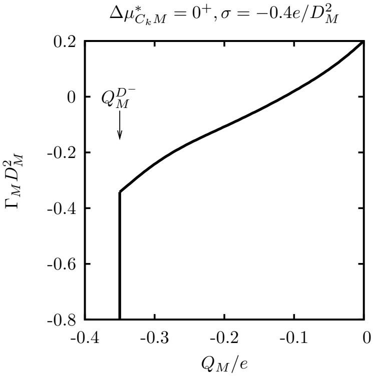

Figure 4.9: Excess adsorption Γ_M of platelike macroions at isotropic-nematic coexistence with nematic boundary conditions ($\Delta\mu^*_{C_kM} = 0^+$) for surface charge density $\sigma = -0.4e/D_M^2$ (see Fig. 3.3) in terms of the effective macroion charge Q_M. The excess adsorption is finite and bounded from below for $Q_M > Q_M^{D^-} = -0.35e$, whereas at $Q_M = Q_M^{D^-}$ it jumps to $-\infty$. It has been verified by a comparison of interfacial tensions that the numerical solutions with finite excess adsorption correspond to equilibrium structures and not only to metastable states. The *discontinuity* of Γ_M at $Q_M^{D^-}$ identifies state point D^- in Fig. 3.3 as a *first-order* drying transition point. The latter conclusion can also be drawn from an asymptotic analysis of the effective interface potential (see main text).

and not only metastable states. The *discontinuity* of Γ_M corresponds to the occurrence of a first-order drying transition at $Q_M^{D^-}$, which is displayed as state point D^- in Fig. 3.3.

A first-order drying transition is accompanied by a *predrying line* in the surface phase diagram (see the dashed line in Fig. 3.3), which connects the drying transition point D^- with a critical point C_D^-, located at $(Q_M^{C_D^-} = -0.87e, \Delta\mu^{*C_D^-}_{C_kM} = 0.049)$. The predrying line may be parameterised in terms of, e.g., the effective macroion charge: $\Delta\mu^{*PD}_{C_kM}(Q_M)$ for $Q_M \in [Q_M^{C_D^-}, Q_M^{D^-})$ denotes the chemical potential difference $\Delta\mu^*_{C_kM}$ for which the excess adsorption Γ_M as a function of Q_M and $\Delta\mu^*_{C_kM}$ exhibits a *finite* discontinuity $\Delta\Gamma_M$. Figure 4.10 displays this discontinuity as a function of the effective macroion charge Q_M (solid line). It vanishes according to a power law $\Delta\Gamma_M \sim (Q_M - Q_M^{C_D^-})^\beta$ with the mean field critical exponent $\beta = \frac{1}{2}$ (dashed line). *Beyond* mean field theory, one expects an

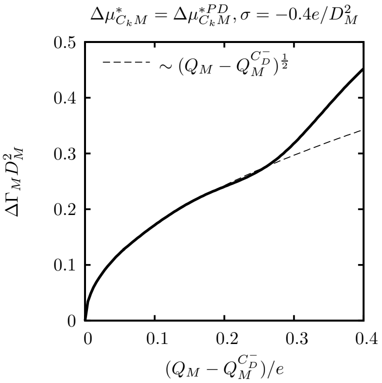

Figure 4.10: Excess adsorption discontinuity $\Delta\Gamma_M$ (solid line) of a mixture of platelike macroions and salt at the predrying line parameterised by the effective macroion charge Q_M for a surface charge density $\sigma = -0.4e/D_M^2$ (see Fig. 3.3). The excess adsorption difference vanishes for $Q_M \searrow Q_M^{C_D^-} = -0.87e$ according to a power law $\Delta\Gamma_M \sim (Q_M - Q_M^{C_D^-})^\beta$ with the mean field critical exponent $\beta = \frac{1}{2}$ (dashed line).

exponent $\beta = \frac{1}{8}$, corresponding to the two-dimensional Ising universality class.

Figure 4.11 depicts the formation of an isotropic film upon approaching isotropic-nematic coexistence for $\Delta\mu^*_{C_kM} > 0$ with effective macroion charge $Q_M = -0.6e$ and surface charge density $\sigma = -0.4e/D_M^2$. A *finite* discontinuity of the film thickness upon crossing the predrying line at $\Delta\mu^*_{C_kM} \approx 0.03$ can be inferred.

Figure 4.12 displays the salt ion density profile ϱ_S and the counter ion density profile ϱ_C for the case of effective macroion charge $Q_M = -0.1e$ and surface charge density $\sigma = -0.4e/D_M^2$ at isotropic-nematic bulk coexistence with nematic boundary conditions in the bulk ($\Delta\mu^*_{C_kM} = 0^+$). The positive counter ions C are attracted by and the negative salt ions S are repelled from the negatively charged wall. This behaviour is found to be qualitatively independent of the chemical potential difference $\Delta\mu^*_{C_kM}$ and the boundary conditions (isotropic or nematic) in the bulk. Attraction and repulsion are reversed upon reversing the sign of σ. As discussed in Sec. 3.2, the number densities close to the charged hard wall follow from a balance between entropic contributions due to the hard cores as well as

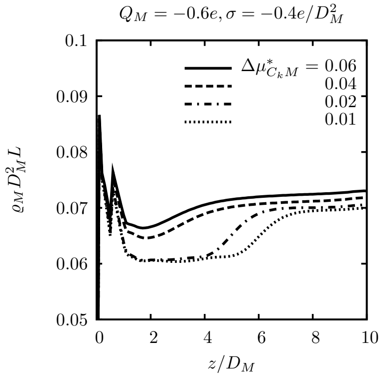

Figure 4.11: Macroion density profiles ϱ_M of a mixture of platelike macroions with $Q_M = -0.6e$ and salt in contact with a substrate of charge density $\sigma = -0.4e/D_M^2$ upon crossing the predrying line at $\Delta\mu^*_{C_kM} \approx 0.03$ (Fig. 3.3). At the predrying line, a quasi-isotropic film with *finite* thickness appears at the substrate.

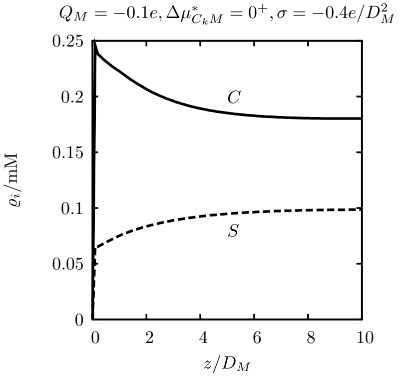

Figure 4.12: Salt ion (S) and counter ion (C) density profile in a mixture of platelike macroions with $Q_M = -0.1e$ and salt at isotropic-nematic bulk coexistence with nematic boundary conditions in the bulk ($\Delta\mu^*_{C_kM} = 0^+$) in contact with a charged substrate at $z \leq 0$ with surface charge density $\sigma = -0.4e/D_M^2$ (see Fig. 3.3).

energetic contributions due to the Coulomb interaction. Hence it is not necessarily the ion species of maximal charge and minimal size which accumulates at the substrate (compare the first peaks in Figs. 4.8, 4.11, and 4.12).

The rather strong variation of the salt and counter ion density profiles close to a strongly charged wall reveals limitations of the approximation of a *fixed* effective macroion charge Q_M within the current model because actually macroion charges adapt according to the local electrolytic environment by means of charge regulation mechanisms. Therefore, macroion charges close to and far from a charged wall are expected to differ considerably. However, no charge regulation model [Bolt1982, Chan1975, Davis1978, Healy1978, Hiemstra1987, Hiemstra1989, vanRiemsdijk1986] is included into the formalism described in Ch. 2 in order to gain much needed technical advantages.

4.4 Electrostatic surface potential

Whereas the two preceding sections have been focused on the fluid *structure* close to charged substrats, this section addresses the *electrostatic* properties of the substrate due to the contact with the fluid of charged particles.

The electrostatic potential profile difference $\Delta\psi(z) := \psi(z) - \psi(\infty)$ (see Eq. (2.42)) relative to the electrostatic bulk potential $\psi(\infty)$ for $Q_M = -0.5e$ at isotropic-nematic bulk coexistence with isotropic boundary conditions in the bulk ($\Delta\mu^*_{C_kM} = 0^-$) is shown in Fig. 4.13. For large distances z from the substrate, $\Delta\psi(z)$ decays proportional to z^{-3} (see Sec. 2.5). Upon increasing the surface charge density σ a crossover from monotonic to non-monotonic electrostatic potential profiles occurs at $\sigma = 0$. According to Eq. (2.43), the slope of the electrostatic potential difference at the wall is given by the surface charge density: $\Delta\psi'(0^+) = -8\sigma$. On the other hand, an electrical double layer is formed with a negatively charged layer on the nematic side and a positively charged layer on the isotropic side if a quasi-free interface between the isotropic bulk and a nematic film of finite thickness is present (see Sec. 4.1). Thus $\Delta\psi$ approaches its bulk value 0 from below, i.e., $\Delta\psi'(z) > 0$ for large distances z from the substrate. Therefore, for $\sigma > 0$, i.e., $\Delta\psi'(0^+) < 0$, $\Delta\psi(z)$ is minimal at some finite distance $0 < z_0 < \infty$, whereas for $\sigma < 0$, i.e., $\Delta\psi'(0^+) > 0$, $\Delta\psi$ attains its minimal value at $z = 0$.

In the aforementioned case, a quasi-free isotropic-nematic interface is

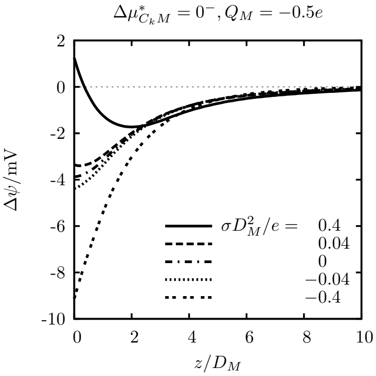

Figure 4.13: Electrostatic potential difference profiles $\Delta\psi$ relative to the electrostatic bulk potential in a mixture of platelike macroions with $Q_M = -0.5e$ and salt at isotropic-nematic bulk coexistence with isotropic boundary conditions in the bulk ($\Delta\mu^*_{C_kM} = 0^-$) (see Fig. 3.3). The slope of $\Delta\psi$ at the substrate ($z = 0$) is governed by the surface charge density σ whereas the bulk value $\Delta\psi(\infty) = 0$ is approached proportional to z^{-3} from below. Hence upon increasing the surface charge, a crossover from monotonic to non-monotonic electrostatic potential profiles occurs.

formed at isotropic-nematic coexistence with isotropic boundary conditions in the bulk. Quasi-free isotropic-nematic interfaces also occur for nematic boundary conditions in the bulk close to complete drying. In the latter case, the electrostatic potential *decreases* upon approaching the bulk because $Q_M < 0$. Moreover, it is found that the electrostatic potential is a *monotonic* function of the distance from the substrate if *no* isotropic-nematic interface form, e.g., for nematic boundary conditions in the bulk and $Q_M = 0$.

Since the spatial derivative of the electrostatic potential is proportional to the electric field, the occurrence of non-monotonic electrostatic potential profiles is equivalent to the phenomenon of *charge inversion*, i.e., the local inversion of the direction of the electric field with respect to the surface field. Charge inversion [Levin2002] is possible within the present formalism as correlations beyond the random phase approximation (RPA) are taken into account (see Sec. 2.3).

Figure 4.14 displays the electrostatic substrate potential $\Delta\psi(0)$ as a function of the surface charge density σ at isotropic-nematic coexistence

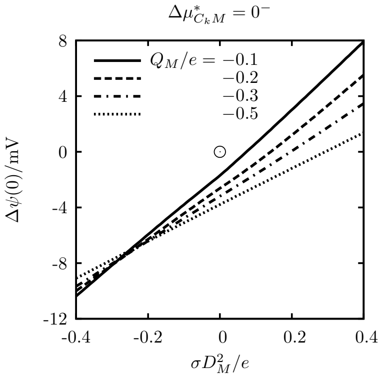

Figure 4.14: Electrostatic surface potential $\Delta\psi(0) = \psi(0) - \psi(\infty)$ as a function of the surface charge density σ in a mixture of platelike macroions and salt at isotropic-nematic coexistence with isotropic boundary conditions in the bulk ($\Delta\mu^*_{C_kM} = 0^-$) (see Fig. 3.3). All curves are monotonically increasing but they do *not* pass through the origin ($\odot$) at ($\sigma = 0, \Delta\psi(0) = 0$) if $Q_M \neq 0$. Thus, the point of zero (surface) charge ($\sigma = 0$) does *not* coincide with the isoelectric point ($\Delta\psi(0) = 0$). Note that curves for $Q_M = \overline{Q}_M$ and $Q_M = -\overline{Q}_M$ can be mapped upon each other by reflecting them at the origin.

with isotropic boundary conditions in the bulk ($\Delta\mu^*_{C_kM} = 0^-$). Curves for $Q_M = \overline{Q}_M$ and $Q_M = -\overline{Q}_M$ can be mapped upon each other by reflecting them at the origin ($\odot$). As expected, the surface potential increases monotonically with the surface charge. However, the points of zero charge ($\sigma = 0$) do *not* coincide with the isoelectric points ($\Delta\psi(0) = 0$), i.e., the curves in Fig. 4.14 do *not* pass through the origin ($\odot$), in contrast to Poisson-Boltzmann theories [Grahame1947]. This behaviour arises from the hard-core interaction of the particles [Messina2002/3], which leads to a depletion attraction of the larger macroions towards the wall on purely entropic grounds. Therefore, for a hard and uncharged wall ($\sigma = 0$), negatively charged macroions ($Q_M < 0$) are accumulated close to the substrate leading to a negative electrostatic surface potential ($\Delta\psi(0) < 0$).

It has been checked that the sign of the electrostatic substrate potential $\Delta\psi(0)$ for vanishing surface charge density $\sigma = 0$ depends only on the sign of the effective macroion charge and not on the boundary conditions in the bulk or the chemical potential difference $\Delta\mu^*_{C_kM}$.

Chapter 5

Conclusions and outlook

In this work a density functional theory of fluids of charged platelike colloids has been developed (Ch. 2) and intensively investigated with respect to spatially homogeneous (Ch. 3) as well as inhomogeneous (Ch. 4) systems.

Within this density functional theory bulk fluids, free interfaces, and charged substrates are described on the same footing. On the one hand, bulk structures are used as boundary conditions for interfacial profiles. Hence in order to achieve numerical consistency a unified description is required. On the other hand, the bulk description within the theory of the present work, which proved to be in good agreement with intuitive expectations (Sec. 3.1), compared with other bulk theories of charged platelike colloids may serve to assess the reliability and degree of sophistication of the results gained within this study. Additional advantages of the present approach are analytically accessible asymptotic expressions for the effective interface potential, which are required for the model studied here because of otherwise inconclusive numerical data.

Bulk and surface phase diagrams of fluids of charged platelike colloids have been analysed by a combination of analytical and numerical tools. Bulk phase transitions have been determined by numerically solving the spatially homogeneous Euler-Lagrange equations. The resulting bulk structures served as boundary conditions to numerical solutions of spatially inhomogeneous Euler-Lagrange equations. The inhomogeneous solutions have been used to calculate the asymptotic form of the effective interface potential which have led to analytical predictions of first-order surface phase transitions such as wetting and drying which imply the existence of corresponding prewetting and predrying lines. Whereas the order of the surface phase transitions can be inferred from the asymptotic effective interface potential, the location of the phase transitions had to be determined numerically. This combination of numerical and analytical methods turned out to be very effective. Moreover, it is generally applicable and not limited to the present model.

The analyses in Chs. 3 and 4 led to numerous qualitative results concerning, e.g., the location and width of the isotropic-nematic coexistence region, the occurrence of a Donnan effect, the width and interfacial tension of free interfaces, the formation of electrical double layers at free interfaces, the existence of first-order surface phase transitions, the asymptotic growth behaviour of complete wetting and drying films, and the occurrence of charge inversion. These phenomena are expected to be directly accessible in experiments if stable suspensions of charged platelike colloids close to the point of zero effective colloid charge become available.

A theoretically interesting finding within the formalism of this work is an effective interface potential of the same asymptotic form as for non-retarded isotropic dispersion forces. This is a remarkable result as the present model does *not* include dispersion forces. It is ultimately generated by the application of a pair distribution function which agrees with the asymptotically correct Debye-Hückel form. An interesting future problem is the inclusion of dispersion forces into the model introduced within this work. However, only the dynamic components contribute to the leading asymptotic terms of the effective interface potential because the static van der Waals interactions decay exponentially [Mahanty1976, Russel1989, Netz2001/1].

Within the model described in Ch. 2 the particle orientations are restricted to three mutually perpendicular directions (Zwanzig model) and the values of particle charges, in particular those of the macroions, are kept fixed and are concentrated in the particle centres. These simplifications are introduced in order to gain technical advantages, and the results are expect not to change *qualitatively* upon relaxing these approximate constraints. Moreover, the present model furnishes only a qualitative approach because the relation between actual macroion charges and the model parameter describing the effective macroion charge remains undetermined. Deriving such a relation is an important problem which deserves to be addressed in the future.

A further challenge related to the choice of the pair distribution functions in Ch. 2 appears if, as within the present study, the effective shape of the macroions becomes more and more isotropic upon increasing the macroion charge: In this case, any anisotropy of the interactions is due to the hard cores only and the two-phase region between isotropic and anisotropic phases is shifted to unrealistically large packing fractions. In order to cure this deficiency of the present model, the pair distribution functions must be chosen properly to yield *anisotropic* effective macroion shapes up to large macroion charges. Unfortunately, deriving *analytical* expressions for pair distribution functions of platelike particles with inhomogeneous charge distributions is still a big challenge. One promising idea could be to approximate the pair distribution function by the leading far-field contribution of the effective pair-potential [Trizac2002]. Within that approach, the effective interactions between two particles can be expressed as the product of the well-known isotropic Debye-Hückel potential and two one-particle anisotropy functions [Trizac2002, Agra2004]. According to these anisotropy functions, the effective shapes of platelike macroions become increasingly anisotropic with increasing ionic strength and they remain anisotropic for large macroion charges. However, within the range of parameters used in the present work, the anisotropy functions yield values close to unity for all directions. Therefore it can be expected that the *distribution* of the charges on the macroions plays an important role for high charges but not for small charges.

In conclusion, the density functional theory developed in this work can be regarded as a first step to qualitatively understand free interfaces and charged substrates in suspensions of charged platelike colloids. It leads to various definite qualitative predictions for the bulk and surface phase behaviour, the structure of free interfaces, the wetting and drying behaviour of charged substrates, as well as the electrostatics within these complex fluids which are expected to be readily testable in experiments if appropriate model systems become available. Theoretical questions raised by the results of this work about the relation between actual and model charges, the asymptotic form of pair distribution functions for charged platelike particles, or the generality of the asymptotic form of the effective interface potential of electrolyte solutions, which will be addressed in future work, are expected to further improve the understanding of the important material class of fluids of charged platelike colloids.

Bibliography

[Abramowitz1972] M. Abramowitz and I.S. Stegun, *Handbook of mathematical functions* (Dover Publications, New York, 1972).

[Adamson1973] A.W. Adamson, *A Textbook of Physical Chemistry* (Academic Press, New York, 1973).

[Agra2004] R. Agra, E. Trizac, and L. Bocquet, *The interplay between screening properties and colloid anisotropy: Towards a reliable pair potential for disc-like charged particles*, Eur. Phys. J. E **15**, 345 (2004).

[Alexander1984] S. Alexander, P.M. Chaikin, P. Grant, G.J. Morales, and P. Pincus, *Charge renormalization, osmotic pressure, and bulk modulus of colloidal crystals: Theory*, J. Chem. Phys. **80**, 5776 (1984).

[Allen1987] M.P. Allen and D.J. Tildesley, *Computer Simulation of Liquids* (Oxford University Press, Oxford, 1987).

[Arrhenius1887] S. Arrhenius, *Über die Dissociation der in Wasser gelösten Stoffe*, Z. phys. Chem. **1**, 631 (1887).

[Artymov2003] M.N. Artymov, V. Kobelev, and A.B. Kolomeisky, *Lattice models of ionic systems with charge asymmetry*, J. Chem. Phys. **118**, 6394 (2003).

[Asakura1954] S. Asakura and F. Oosawa, *On Interaction between Two Bodies Immersed in a Solution of Macromolecules*, J. Chem. Phys. **22**, 1255 (1954).

[Asakura1958]	S. Asakura and F. Oosawa, *Interaction between Particles Suspended in Solutions of Macromolecules*, J. Polymer Sci. **33**, 183 (1958).
[Aubouy2003]	M. Aubouy, E. Trizac, and L. Bocquet, *Effective charge versus bar charge: an analytical estimate for colloids in the infinite dilution limit*, J. Phys. A **36**, 5835 (2003).
[Bain1998]	C.D. Bain, *Studies of adsorption at interfaces by optical techniques: ellipsometry, second harmonic generation and sum-frequency generation*, Curr. Opin. Colloid Interface Sci. **3**, 287 (1998).
[Barker1967/1]	J.A. Barker and D. Henderson, *Perturbation Theory and Equation of State for Fluids: The Square-Well Potential*, J. Chem. Phys. **47**, 2856 (1967).
[Barker1967/2]	J.A. Barker and D. Henderson, *Perturbation Theory and Equation of State for Fluids: A Successful Theory of Liquids*, J. Chem. Phys. **47**, 4714 (1967).
[Baumgartl2005]	J. Baumgartl and C. Bechinger, *On the limits of digital video microscopy*, Europhys. Lett. **71**, 487 (2005).
[Baumgartl2006]	J. Baumgartl, J.L. Arauz-Lara, and C. Bechinger, *Like-charge attraction in confinement: myth or truth?*, Soft Matter **2**, 631 (2006).
[Baus1980]	M. Baus and J.-P. Hansen, *Statistical mechanics of simple Coulomb systems*, Phys. Rep. **59**, 1 (1980).
[Baus1985]	M. Baus and J.L. Colot, *The freezing of hard spheres. The density functional theory revisited*, Mol. Phys. **55**, 653 (1985).
[Belloni2000]	L. Belloni, *Colloidal interactions*, J. Phys.: Condens. Matter **12**, R549 (2000).
[Bier2004]	M. Bier, L. Harnau, and S. Dietrich, *Bulk and interfacial properties of binary hard-platelet fluids*, Phys. Rev. E **69**, 021506 (2004).

[Bier2005] M. Bier, L. Harnau, and S. Dietrich, *Free isotropic-nematic interfaces in fluids of charged platelike colloids*, J. Chem. Phys. **123**, 114906 (2005).

[Bier2006] M. Bier, L. Harnau, and S. Dietrich, *Surface properties of fluids of charged platelike colloids*, J. Chem. Phys. **125**, 184704 (2006).

[Biesheuvel2001] P.M. Biesheuvel, *Implications of the Charge Regulation Model for the Interaction of Hydrophilic Surface in Water*, Langmuir **17**, 3553 (2001).

[Binney1992] J.J. Binney, N.J. Dowrick, A.J. Fisher, and M.E.J. Newman, *The theory of critical phenomena*, (Oxford University Press, Oxford, 1992).

[Blum1977] L. Blum and J.S. Høye, *Mean Spherical Model for Asymmetric Electrolytes. 2. Thermodynamic Properties and the Pair Correlation Function*, J. Phys. Chem. **81**, 1311 (1977).

[Blum1980] L. Blum, *Solution of the Ornstein-Zernike Equation for a Mixture of Hard Ions and Yukawa Closure*, J. Stat. Phys. **22**, 661 (1980).

[Blum1981] L. Blum, D. Henderson, J.L. Lebowitz, Ch. Gruber, and Ph.A. Martin, *A sum rule for an inhomogeneous electrolyte*, J. Chem. Phys. **75**, 5974 (1981).

[Bocquet2002] L. Bocquet, E. Trizac, and M. Aubouy, *Effective charge saturation in colloidal suspensions*, J. Chem. Phys. **117**, 8138 (2002).

[Bohnic2004] K. Bohnic, A. Iglič, and S. May, *Interaction between macroions mediated by divalent rod-like ions*, Europhys. Lett. **68**, 494 (2004).

[Bolt1982] G.H. Bolt and W.H. van Riemsdijk, *Ion adsorption on inorganic variable charge constituents*, in *Soil Chemistry. B. Physico-chemical Models*, edited by G.H. Bolt (Elsevier, Amsterdam, 1982), p. 459.

[Bonn2001] D. Bonn and D. Ross, *Wetting transitions*, Rep. Prog. Phys. **64**, 1085 (2001).

[Brown1998] A.B.D. Brown, S.M. Clarke, and A.R. Rennie, *Ordered Phase of Platelike Particles in Concentrated Dispersions*, Langmuir **14**, 3129 (1998).

[Brown1999] A.B.D. Brown, C. Ferrero, T. Narayanan, and A.R. Rennie, *Phase separation and structure in a concentrated colloidal dispersion of uniform plates*, Eur. J. Phys. B **11**, 481 (1999).

[Buff1965] F.P. Buff, R.A. Lovett, and F.H. Stillinger, *Interfacial density profile for fluids in the critical region*, Phys. Rev. Lett. **15**, 621 (1965).

[Buining1993] P.A. Buining and H.N.W. Lekkerkerker, *Isotropic-Nematic Phase Separation of a Dispersion of Organophilic Boehmite Rods*, J. Phys. Chem. **97**, 11510 (1993).

[Buining1994] P.A. Buining, A.P. Philipse, and H.N.W. Lekkerkerker, *Phase Behavior of Aqueous Dispersions of Colloidal Boehmite Rods*, Langmuir **10**, 2106 (1994).

[Caccamo1996] C. Caccamo, *Integral equation theory description of phase equilibria in classical fluids*, Phys. Rep. **274**, 1 (1996).

[Cahn1958/1] J.W. Cahn and J.E. Hilliard, *Free Energy of a Nonuniform System. I. Interfacial Free Energy*, J. Chem. Phys. **28**, 258 (1958).

[Cahn1958/2] J.W. Cahn, *Free Energy of a Nonuniform System. II. Thermodynamic Basis*, J. Chem. Phys. **30**, 1121 (1959).

[Cahn1959] J.W. Cahn and J.E. Hillard, *Free Energy of a Nonuniform System. III. Nucleation in a Two-Component Incompressible Fluid*, J. Chem. Phys. **31**, 688 (1959).

[Caillol2001] J.-M. Caillol and J.-L. Raimbault, *Sine-Gordon Theory for the Equation of State of Classical Hard-Core Coulomb Systems. I. Low Fugacity Expansion*, J. Stat. Phys. **103**, 753 (2001).

[Caillol2002] J.-M. Caillol, D. Levesque, and J.-J. Weis, *Critical behavior of the restricted primitive model revisited*, J. Chem. Phys. , (2002).

[Caillol2003] J.-M. Caillol, *Statistical field theory for simple fluids: mean field and Gaussian approximations*, Mol. Phys. **101**, 1617 (2003).

[Caillol2004] J.-M. Caillol, *Sine-Gordon Theory for the Equation of State of Classical Hard-Core Coulomb Systems. III. Loopwise Expansion*, J. Stat. Phys. **115**, 1461 (2004).

[Caillol2005] J.-M. Caillol, *New mean-field theories for the liquid-vapour transition of charged hard spheres*, Mol. Phys. **103**, 1271 (2005).

[Carnahan1969] N.F. Carnahan and K.E. Starling, *Equation of State for Nonattracting Rigid Spheres*, J. Chem. Phys. **51**, 635 (1969).

[Carnie1981/1] S.L. Carnie and D.Y.C. Chan, *The statistical mechanics of the electrical double layer: Stress tensor and contact conditions*, J. Chem. Phys. **74**, 1293 (1981).

[Carnie1981/2] S.L. Carnie and D.Y. Chan, *The Stillinger-Lovett condition for non-uniform electrolytes*, Chem. Phys. Lett. **77** (3), 437 (1981).

[Casey1995] A. Casey and P. Harrowell, *Monte Carlo simulations of a layering transition in hard parallelepipeds*, J. Chem. Phys. **103**, 6143 (1995).

[Chan1975] D. Chan, J.W. Perram, L.R. White, and T.W. Healy, *Regulation of Surface Potential at Amphoteric Surfaces during Particle-Particle Interaction*, J. Chem. Soc.: Faraday Trans. I **71**, 1046 (1975).

[Chandler1972] D. Chandler and H.C. Andersen, *Optimized Cluster Expansions for Classical Fluids. II. Theory of Molecular Liquids*, J. Chem. Phys. **57**, 1930 (1972).

[Chapman1913] D.L. Chapman, *A Contribution to the Theory of Electrocapillarity*, Philos. Mag. **25**, 475 (1913).

[Ciach2000] A. Ciach and G. Stell, *Field-theoretic approach to ionic systems: Criticality and tri-criticality*, J. Mol. Liq. **87**, 253 (2000).

[Ciach2001] A. Ciach and G. Stell, *Why the Ising and continuous-space models of ionic systems exhibit essentially different critical behavior*, J. Chem. Phys. **114**, 382 (2001).

[Ciach2002] A. Ciach and G. Stell, *Criticality and tricriticality in ionic systems*, Physica A **306**, 220 (2002).

[Ciach2003] A. Ciach and G. Stell, *Effect of Space Discretization on Phase Diagrams in Ionic Systems: A Field-Theoretic Approach*, Phys. Rev. Lett. **91**, 060601 (2003).

[Ciach2005] A. Ciach and G. Stell, *Mesoscopic field theory of ionic systems*, Int. J. Mod. Phys. B **19**, 3309 (2005).

[Coalson1992] R.D. Coalson and A. Duncan, *Systematic ionic screening theory of macroions*, J. Chem. Phys. **97**, 5653 (1992).

[Colot1985] J.L. Colot and M. Baus, *The freezing of hard spheres. II. A search for structural (f.c.c-h.c.p) phase transitions*, Mol. Phys. **56**, 807 (1985).

[Colot1986] J.-L. Colot, M. Baus, and H. Xu, *The freezing of hard spheres. III. Testing the approximations*, Mol. Phys. **57**, 809 (1986).

[Crocker1996] J.C. Crocker and D.G. Grier, *When Like Charges Attract: The Effects of Geometrical Confinement on Long-Range Colloidal Interactions*, Phys. Rev. Lett. **77**, 1897 (1996).

[CruzdeLeon1998] G. Cruz de León, J.M. Saucedo-Solorio, and J.L. Arauz-Lara, *Colloidal Interactions in Partially Quenched Suspensions of Charged Particles*, Phys. Rev. Lett. **81**, 1122 (1998).

[Cuesta1996] J.A. Cuesta, *Fluid Mixtures of Parallel Hard Cubes*, Phys. Rev. Lett. **76**, 3742 (1996).

[Cuesta1997/1] J.A. Cuesta and Y. Martínez-Ratón, *Dimensional Crossover of the Fundamental-Measure Functional for Parallel Hard Cubes*, Phys. Rev. Lett. **78**, 3681 (1997).

[Cuesta1997/2] J.A. Cuesta and Y. Martínez-Ratón, *Fundamental measure theory for mixtures of parallel hard cubes. I. General formalism*, J. Chem. Phys. **107**, 6379 (1997).

[Cuesta1999] J.A. Cuesta and R.P. Sear, *Phase transitions in simple models of rod-like and disc-like micelles*, Eur. Phys. J. B **8**, 233 (1999).

[Curtin1985] W.A. Curtin and N.A. Ashcroft, *Weighted-density-functional theory of inhomogeneous liquids and the freezing transition*, Phys. Rev. A **32**, 2909 (1985).

[Curtin1988] W.A. Curtin, *Freezing in the density functional approach: Effect of third-order contribution*, J. Chem. Phys. **88**, 7050 (1988).

[Davidson2005] P. Davidson and J.-C.P. Gabriel, *Mineral liquid crystals*, Curr. Opin. Colloid Interface Sci. **9**, 377 (2005).

[Davis1978] J.A. Davis, R.O. James, and J.O. Leckie, *Surface Ionization and Complexation at the Oxide / Water Interface. I. Computation of Electrical Double Layer Properties in Simple Electrolytes*, J. Colloid Interface Sci. **63**, 480 (1978).

[Debye1923] P. Debye and E. Hückel, *Zur Theorie der Elektrolyte*, Phys. Z. **24**, 185 (1923).

[deDominicis1962] C. de Dominicis, *Variational Formulations of Equilibrium Statistical Mechanics*, J. Math. Phys. **3**, 983 (1962).

[deGennes1985] P.G. de Gennes, *Wetting: statics and dynamics*, Rev. Mod. Phys. **57**, 827 (1985).

[deGennes1993] P.G. de Gennes and J. Prost, *The Physics of Liquid Crystals* (Oxford University Press, Oxford, 1993).

[Dellago1998] C. Dellago, P.G. Bolhuis, F.S. Csajka, and D. Chandler, *Transition path sampling and the calculation of rate constants*, J. Chem. Phys. **108**, 1964 (1998).

[Denton1989] A.R. Denton and N.W. Ashcroft, *Modified weighted-density-functional theory of nonuniform classical liquids*, Phys. Rev. A **39**, 4701 (1989).

[Diehl1999] A. Diehl, M.N. Tamashiro, M.C. Barbosa, and Y. Levin, *Density-functional theory for attraction between like-charged plates*, Physica A **274**, 433 (1999).

[Dietrich1988] S. Dietrich, *Wetting Phenomena*, in *Phase Transitions and Critical Phenomena, Vol. 12*, edited by C. Domb and J.L. Lebowitz (Academic Press, New York, 1988), p. 1.

[Dietrich1991] S. Dietrich and M. Napiórkowski, *Analytic results for wetting transitions in the presence of van der Waals tails*, Phys. Rev. A **43**, 1861 (1991).

[Dietrich1995] S. Dietrich and A. Haase, *Scattering of X-rays and neutrons at interfaces*, Phys. Rep. **260**, 1 (1995).

[Dogic2006] Z. Dogic and S. Fraden, *Phase Behavior of Rod-Like Viruses and Virus-Sphere Mixtures*, in *Soft Matter, Vol. 2: Complex Colloidal Suspensions*, edited by G. Gompper and M. Schick (Wiley, Weinheim, 2006).

[Donnan1911] F.G. Donnan, *Theorie der Membrangleichgewichte und Membranpotentiale bei Vorhandensein von* *nicht dialysierten Elektrolyten. Ein Beitrag zur physikalisch-chemischen Physiologie.*, Z. Elektrochem. **17**, 572 (1911).

[Donnan1924] F.G. Donnan, *The theory of membrane equilibrium*, Chem. Rev. **1**, 73 (1924).

[Ebner1975] C. Ebner and W.F. Saam, *Renormalized density-functional theory of nonuniform superfluid* ^{4}He *at zero temperature*, Phys. Rev. B **12**, 923 (1975).

[Evans1979] R. Evans, *The nature of the liquid-vapour interface and other topics in the statistical mechanics of non-uniform, classical fluids*, Adv. Phys. **28**, 143 (1979).

[Evans1980] R. Evans and T.J. Sluckin, *A density functional theory for inhomogeneous charged fluids. Application to the surfaces of molten salts*, Mol. Phys. **40**, 413 (1980).

[Evans1989] R. Evans, *Microscopic theories of simple fluids and their interfaces*, in *Les Houches, Session XLVIII, 1988 — Liquides aux interfaces / Liquids at interfaces*, edited by J. Charvolin, J.F. Joanny, and J. Zinn-Justin (North-Holland, Amsterdam, 1989), p. 1

[Evans1992] R. Evans, *Density Functionals in the Theory of Nonuniform Fluids*, in *Fundamentals of Inhomogeneous Fluids*, edited by D. Henderson (Marecl Dekker, New York, 1992), p. 85.

[Evans1994] R. Evans, R.J.F. Leote de Carvalho, J.R. Henderson, and D.C. Hoyle, *Asymptotic decay of correlations in liquids and their mixtures*, J. Chem. Phys. **100**, 591 (1994).

[Fisher1993] M.E. Fisher and Y. Levin, *Criticality in Ionic Fluids: Debye-Hückel Theory, Bjerrum, and Beyond*, Phys. Rev. Lett. **71**, 3826 (1993).

[Fisher1994] M.E. Fisher, *The Story of Coulombic Criticality*, J. Stat. Phys. **75**, 1 (1994).

[Forsyth1978] P.A. Forsyth, S. Marčelja, D.J. Mitchell, B.W. Ninham, *Ordering in colloidal systems*, Adv. Colloid Interface Sci. **9**, 37 (1978).

[Fuoss1934] R.M. Fuoss, *Distribution of ions in electrolytic solutions*, Trans. Faraday Soc. **30**, 967 (1934).

[Gabriel1996] J.-C.P. Gabriel, C. Sanchez, and P. Davidson, *Observation of Nematic Liquid-Crystal Textures in Aqueous Gels of Smectite Clays*, J. Phys. Chem. **100**, 11139 (1996).

[Giese2002] R.F. Giese and C.J. van Oss, *Colloid and surface properties of clays and related minerals*, (Marcel Dekker, New York, 2002).

[Goldenfeld1992] N. Goldenfeld, *Lectures on Phase Transitions and the Renormalization Group*, (Westview Press, Boulder, 1992).

[Goulding1998] D. Goulding and J.-P. Hansen, *Effective interaction between charged colloidal particles near a surface*, Mol. Phys. **95**, 649 (1998).

[Goulding1999] D. Goulding and J.-P. Hansen, *Attraction between like-charged colloidal particles induced by a surface: A density-functional analysis*, Europhys. Lett. **46**, 407 (1999).

[Gouy1910] M. Gouy, *Sur la constitution de la charge électrique a la surface d'un électrolyte*, J. de Phys. (4$^{\text{e}}$ série) **9**, 457 (1910).

[Gradshteyn1980] I.S. Gradshteyn and I.M. Ryzhik, *Table of integrals, series, and products* (Academic Press, New York, 1980).

[Grahame1947] D.C. Grahame, *The electrical double layer and the theory of electrocapillarity*, Chem. Rev. **41**, 441 (1947).

[Grier2000] D.G. Grier, *When like charges attract: interactions and dynamics in charge-stabilized colloidal suspensions*, J. Phys.: Condens. Matter **12**, A85 (2000).

[Grier2004] D.G. Grier and Y. Han, *Anomalous interactions in confined charge-stabilized colloid*, J. Phys.: Condens. Matter **16**, S4145 (2004).

[Groh1998] B. Groh, R. Evans, and S. Dietrich, *Liquid-vapor interface of an ionic fluid*, Phys. Rev. E **57**, 6944 (1998).

[Gruber1981] Ch. Gruber, J.L. Lebowitz, and Ph.A. Martin, *Sum rules for inhomogeneous Coulomb systems*, J. Chem. Phys. **75**, 944 (1981).

[Han2003] Y. Han and D.G. Grier, *Confinement-Induced Colloidal Attractions in Equilibrium*, Phys. Rev. Lett. **91**, 038302 (2003).

[Hansen1986] J.-P. Hansen and I.R. McDonald, *Theory of simple liquids* (Academic Press, Amsterdam 1986).

[Hansen2000] J.-P. Hansen and H. Löwen, *Effective Interactions between electric double layers*, Annu. Rev. Phys. Chem. **51**, 209 (2000).

[HansenGoos2006] H. Hansen-Goos and R. Roth, *A new generalization of the Carnahan-Starling equation of state to additive mixtures of hard spheres*, J. Chem. Phys. **124**, 154506 (2006).

[Harnau2001] L. Harnau, D. Costa, and J.-P. Hansen, *A solvable interaction site model for lamellar colloids*, Europhys. Lett. **53**, 729 (2001).

[Harnau2002/1] L. Harnau and S. Dietrich, *Fluids of platelike particles near a hard wall*, Phys. Rev. E **65**, 021505 (2002).

[Harnau2002/2] L. Harnau and J.-P. Hansen, *Colloid aggregation induced by oppositely charged polyions*, J. Chem. Phys. **116**, 9051 (2002).

[Harnau2002/3] L. Harnau and S. Dietrich, *Wetting and capillary nematization of binary hard-platelet and hard-rod fluids*, Phys. Rev. E **66**, 051702 (2002).

[Harnau2002/4] L. Harnau, D. Rowan, and J.-P. Hansen, *Thermodynamics and phase behavior of the lamellar Zwanzig model*, J. Chem. Phys. **117**, 11359 (2002).

[Harrowell1982] P.R. Harrowell and S. Nordholm, *Generalized van der Waals Theory. XI. Gas Solubility in Simple Fluids*, Aust. J. Chem. **35**, 673 (1982).

[Hauge1983] E.H. Hauge and M. Schick, *Continuous and first-order wetting transition from the van der Waals theory of fluids*, Phys. Rev. B **27**, 4288 (1983).

[Haymet1986] A.D.J. Haymet and D.W. Oxtoby, *A molecular theory for freezing: Comparison of theories, and results for hard spheres*, J. Chem. Phys. **84**, 1769 (1986).

[Healy1978] T.W. Healy and L.R. White, *Ionizable surface group models of aqueous interfaces*, Adv. Colloid Interface Sci. **9**, 303 (1978).

[Hecht2006] M. Hecht, J. Harting, M. Bier, J. Reinshagen, and H.J. Herrmann, *Shear viscosity of claylike colloids in computer simulations and experiments*, Phys. Rev. E **74**, 021403 2006).

[Helden2004] L. Helden, J.H. Koenderink, P. Leiderer, and C. Bechinger, *Depletion Potentials Induced by Charged Colloidal Rods*, Langmuir **20**, 5662 (2004).

[Helfand1960] E. Helfand, H. Reiss, H.L. Frisch, and J.L. Lebowitz, *Scaled Particle Theory of Fluids*, J. Chem. Phys. **33**, 1379 (1960).

[Helfand1961] E. Helfand, H.L. Frisch, and J.L. Lebowitz, *Theory of the Two- and One-Dimensional Rigid Sphere Fluids*, J. Chem. Phys. **34**, 1037 (1961).

[Helmholtz1879] H. Helmholtz, *Studien über electrische Grenzschichten*, Ann. Phys. Chem. **7**, 337 (1879).

[Henderson1978] D. Henderson and L. Blum, *Some exact results and the application of the mean spherical approximation to charged hard spheres near a charged hard wall*, J. Chem. Phys. **69**, 5441 (1978).

[Henderson1979] D. Henderson, L. Blum, and J.L. Lebowitz, *An exact formula for the contact value of the density profile of a system of charged hard spheres near a charged wall*, J. Electroanal. Chem. **102**, 315 (1979).

[Henderson1981] D. Henderson and L. Blum, *Some comments regarding the pressure tensor and contact theorem in a nonhomogeneous electrolyte*, J. Chem. Phys. **75**, 2025 (1981).

[Herzfeld1934] K.F. Herzfeld and M. Goeppert-Mayer, *On the States of Aggregation*, J. Chem. Phys. **2**, 38 (1934).

[Hiemstra1987] T. Hiemstra, W.H. van Riemsdijk, and M.G.M. Bruggenwert, *Proton adsorption mechanism at the gibbsite and aluminium oxide solid / solution interface*, Neth. J. Agric. Sci. **35**, 281 (1987).

[Hiemstra1989] T. Hiemstra, W.H. van Riemsdijk, and G.H. Bolt, *Multisite Proton Adsorption Modeling at the Solid / Solution Interface of (Hydr)oxides: A New Approach. I. Model Description and Evaluation of Intrinsic Reaction Constants*, J. Colloid Interface Sci. **133**, 91 (1989).

[Hohenberg1964] P. Hohenberg and W. Kohn, *Inhomogeneous Electron Gas*, Phys. Rev. **136**, B864 (1964).

[Hooper1980] M.A. Hooper and S. Nordholm, *Generalized van der Waals Theory. II. Quantum Effects on the Equation of State*, Aust. J. Chem. **33**, 2029 (1980).

[Hooper1981/1] M.A. Hooper and S. Nordholm, *Generalized van der Waals Theory. IV. Variational Determination of the Hard-Sphere Diameter*, Aust. J. Chem. **34**, 1809 (1981).

[Hooper1981/2] M.A. Hooper and S. Nordholm, *Generalized van der Waals Theory. V. Equation of State of Two-Dimensional Simple Fluid*, Aust. J. Chem. **34**, 1819 (1981).

[Hooper1982] M.A. Hooper and S. Nordholm, *Generalized van der Waals theory. X. Interface profiles and surface tension of simple quantum fluids*, Mol. Phys. **47**, 329 (1982).

[Hoye1974] J.S. Høye, J.L. Lebowitz, and G. Stell, *Generalized mean spherical approximations for polar and ionic fluids*, J. Chem. Phys. **61**, 3253 (1974).

[Hoye1977] J.S. Høye and L. Blum, *Solution of the Yukawa Closure of the Ornstein-Zernike Equation*, J. Stat. Phys. **16**, 1977).

[Hunter1981] R.J. Hunter, *Zeta potential in colloid science* (Academic Press, London, 1981).

[Hunter2001] R.J. Hunter, *Foundations of Colloid Science* (Oxford University Press, Oxford, 2001).

[John2005] B.S. John and F.A. Escobedo, *Phase Behavior of Colloidal Hard Tetragonal Parallelepipeds (Cuboids): A Monte Carlo Simulation Study*, J. Phys. Chem. B **109**, 23008 (2005).

[Johnson1964] J.W. Johnson and D. Cubicciotti, *The Critical Temperature and Coexistence Curve for Bismuth Chloride*, J. Phys. Chem. **68**, 2235 (1964).

[Johnson1981] M. Johnson and S. Nordholm, *Generalized van der Waals Theory. VI. Application to adsorption*, J. Chem. Phys. **75**, 1953 (1981).

[Keddie2001] J.L. Keddie, *Structural analysis of organic interfacial layers by ellipsometry*, Curr. Opin. Colloid Interface Sci. **6**, 102 (2001).

[Kepler1994] G.M. Kepler and S. Fraden, *Attractive Potential between Confined Colloids at Low Ionic Strength*, Phys. Rev. Lett. **73**, 356 (1994).

[Kierlik1990] E. Kierlik and M.L. Rosinberg, *Free-energy density functional for the inhomogeneous hard-sphere fluid: Application to interfacial adsorption*, Phys. Rev. A **42**, 3382 (1990).

[Kirkwood1951] J.G. Kirkwood and F.P. Buff, *The Statistical Mechanical Theory of Solutions. I*, J. Chem. Phys. **19**, 774 (1951).

[Kirkwood1954] J.G. Kirkwood and J.C. Poirier, *The statistical mechanical basis of the Debye-Hückel theory of strong electrolytes*, J. Phys. Chem. **58**, 591 (1954).

[Knaebel2000] A. Knaebel, M. Bellour, J.-P. Munch, V. Viasnoff, F. Lequeux, and J.L. Harden, *Aging behavior of Laponite clay particle suspensions*, Europhys. Lett. **52**, 73 (2000).

[Kobelev2002/1] V. Kobelev, A.B. Kolomeisky, and M.E. Fisher, *Lattice models of ionic systems*, J. Chem. Phys. **116**, 7589 (2002).

[Kobelev2002/2] V. Kobelev and A.B. Kolomeisky, *Anisotropic lattice models of electrolytes*, J. Chem. Phys. **117**, 8879 (2002).

[Kosmulski2002] M. Kosmulski, *The* pH*-Dependent Surface Charging and the Points of Zero Charge*, J. Colloid Interface Sci. **253**, 77 (2002).

[Kosmulski2004] M. Kosmulski, pH*-dependent surface charging and points of zero charge. II. Update*, J. Colloid Interface Sci. **275**, 214 (2004).

[Kosmulski2005] M. Kosmulski, *The Surface Charging at Low Density of Protonable Surface Sites*, Langmuir **21**, 7421 (2005).

[Kosmulski2006] M. Kosmulski, pH*-dependent surface charging and points of zero charge. III. Update*, J. Colloid Interface Sci. **298**, 730 (2006).

[Kosterlitz1973] J.M. Kosterlitz and D.J. Thouless, *Ordering, metastability and phase transitions in two-dimensional systems*, J. Phys. C **6**, 1181 (1973).

[Landau1979] L.D. Landau and E.M. Lifschitz, *Lehrbuch der theoretischen Physik, Bd. V, Statistische Physik Teil 1* (Akademie-Verlag, Berlin, 1979).

[Langmuir1938] I. Langmuir, *The Role of Attractive and Repulsive Forces in the Formation of Tactoids, Thixotropic Gels, Protein Crystals and Coacervates*, J. Chem. Phys. **6**, 873 (1938).

[Leach2005] E.S.H. Leach, A. Hopkinson, K. Franklin, and J.S. van Duijneveldt, *Nonaqueous Suspensions of Laponite and Montmorillonite*, Langmuir **21**, 3821 (2005).

[leBellac1991] M. le Bellac, *Quantum and Statistical Field Theory* (Oxford University Press, Oxford, 1991).

[Lebowitz1964] J.L. Lebowitz, *Exact Solution of Generalized Percus-Yevick Equation for a Mixture of Hard Spheres*, Phys. Rev. **133**, A895 (1964).

[Lebowitz1965] J.L. Lebowitz, E. Helfand, and E. Praestgaard, *Scaled Particle Theory of Fluid Mixtures*, J. Chem. Phys. **43**, 774 (1965).

[Lebowitz1969] J.L. Lebowitz and E.H. Lieb, *Existence of thermodynamics for real matter with Coulomb forces*, Phys. Rev. Lett. **22**, 631 (1969).

[Lee1997] B.P. Lee and M.E. Fisher, *Charge oscillations in Debye-Hückel theory*, Europhys. Lett. **39**, 611 (1997).

[Lekkerkerker1984] H.N.W. Lekkerkerker, Ph. Coulon, and R. van der Haegen, *On the isotroic-liquid crystal phase separation in a solution of rodlike particles of different lengths*, J. Chem. Phys. **80**, 3427 (1984).

[Lekkerkerker1992] H.N.W. Lekkerkerker, W.C.-K. Poon, P.N. Pusey, A. Stroobants, and P.B. Warren, *Phase Behaviour of Colloid + Polymer Mixtures*, Europhys. Lett. **20**, 559 (1992).

[LeotedeCarvalho1994] R.J.F. Leote de Carvalho and R. Evans, *The decay of correlations in ionic fluids*, Mol. Phys. **83**, 619 (1994).

[Levin1994] Y. Levin, X. Li, and M.E. Fisher, *Coulombic Criticality in General Dimensions*, Phys. Rev. Lett. **73**, 2716 (1994).

[Levin1996] Y. Levin and M.E. Fisher, *Criticality in the hard-sphere ionic fluid*, Physica A **225**, 164 (1996).

[Levin1998] Y. Levin, M.C. Barbosa, and M.N. Tamashiro, *Liquid-state theory of charged colloids*, Europhys. Lett. **41**, 123 (1998).

[Levin2000] Y. Levin, *Interfacial tension of electrolyte solutions*, J. Chem. Phys. **113**, 9722 (2000).

[Levin2001] Y. Levin and J.E. Flores-Mena, *Surface tension of strong electrolytes*, Europhys. Lett. **56**, 187 (2001).

[Levin2002] Y. Levin, *Electrostatic correlations: from plasma to biology*, Rep. Prog. Phys. **65**, 1577 (2002).

[Levitz2000] P. Levitz, E. Lécolier, A. Mourchid, A. Delville, and S. Lyonnard, *Liquid-solid transition of Laponite suspensions at very low ionic strength: Long-range electrostatic stabilization of anisotropic colloids*, Europhys. Lett. **49**, 672 (2000).

[Lieb1972] E.H. Lieb and J.L. Lebowitz, *The Constitution of Matter: Existence of Thermodynamics for Systems Composed of Electrons and Nuclei*, Adv. Math. **9**, 316 (1972)

[Liu2003] S. Liu, J. Zhang, N. Wang, W. Liu, C. Zhang, and D. Sun, *Liquid-Crystalline Phases of Colloidal Dispersions of Layered Double Hydroxides*, Chem. Mater. **15**, 3240 (2003).

[Lovett1968] R. Lovett and F.H. Stillinger, *Ion-Pair Theory of Concentrated Electrolytes. II. Approximate Dielectric Response Calculation*, J. Chem. Phys. **48** (9), 3869 (1968).

[Lowen1993] H. Löwen, J.-P. Hansen, and P.A. Madden, *Nonlinear counterion screening in colloidal suspensions*, J. Chem. Phys. **98**, 3275 (1993).

[Lue2006] L. Lue, *A variational field theory for solutions of charged, rigid particles*, Fl. Ph. Equil. **241**, 236 (2006).

[Luijten2002] E. Luijten, M.E. Fisher, and A.Z. Panagiotopoulos, *Universality Class of Criticality in the Restricted Primitive Model Electrolyte*, Phys. Rev. Lett. **88**, 185701 (2002).

[Lutsko1990/1] J.F. Lutsko and M. Baus, *Can the Thermodynamic Properties of a Solid Be Mapped onto Those of a Liquid?*, Phys. Rev. Lett. **64**, 761 (1990).

[Lutsko1990/2] J.F. Lutsko and M. Baus, *Nonperturbative density-functional theories of classical nonuniform systems*, Phys. Rev. A **41**, 6647 (1990).

[Mahanty1976] J. Mahanty and B.W. Ninham, *Dispersion Forces* (Academic Press, London, 1976).

[Mansoori1971] G.A. Mansoori, N.F. Carnahan, K.E. Starling, and T.W. Leland, *Equilibrium Thermodynamic Properties of the Mixture of Hard Spheres*, J. Chem. Phys. **54**, 1523 (1971).

[MartinezRaton1999] Y. Martínez-Ratón and J.A. Cuesta, *Fundamental measure theory for mixtures of parallel hard cubes. II. Phase behavior of the one-component fluid and of the binary mixture*, J. Chem. Phys. **111**, 317 (1999).

[MartinezRaton2003] Y. Martínez-Ratón and J.A. Cuesta, *Phase diagrams of Zwanzig models: The effect of polydispersity*, J. Chem. Phys. **118**, 10164 (2003).

[MartinezRaton2004] Y. Martínez-Ratón, *Bulk inhomogeneous phases of anisotropic particles: A fundamental measure functional study of the restricted orientation model*, Phys. Rev. E **69**, 061712 (2004).

[MartinezRaton2005] Y. Martínez-Ratón, E. Velasco, and L. Mederos, *Demixing behavior in two-dimensional mixtures of anisotropic hard bodies*, Phys. Rev. E **72**, 031703 (2005).

[Mateescu2001] E.M. Mateescu, *Comment on "Long-range electrostatic interactions between like-charged colloids: Steric and confinement effects"*, Phys. Rev. E **64**, 013401 (2001).

[Mayer1958] J.E. Mayer, *Theory of Real Gases*, in *Handbuch der Physik*, Bd. 12, edited by S. Flügge (Springer, Berlin, 1958), p. 73.

[McDonald1978] I.R. McDonald and S.P. O'Gorman, *Graph Theoretic Techniques in the Theory of Classical Fluids*, Phys. Chem. Liq. **8**, 57 (1978).

[McMillan1945] W.G. McMillan and J.E. Mayer, *The Statistical Thermodynamics of Multicomponent Systems*, J. Chem. Phys. **13**, 276 (1945).

[McQuarrie1966] D.A. McQuarrie and J.L. Katz, *High-Temperature Equation of State*, J. Chem. Phys. **44**, 2393 (1966).

[McQuarrie2000] D.A. McQuarrie, *Statistical mechanics* (Universal Science Books, Sausalito, 2000).

[Mecke1999] K.R. Mecke and S. Dietrich, *Effective Hamiltonian for liquid-vapor interfaces*, Phys. Rev. E **59**, 6766 (1999).

[Mermin1965] N.D. Mermin, *Thermal Properties of the Inhomogeneous Electron Gas*, Phys. Rev. **137**, A1441 (1965).

[Messina2002/1] R. Messina, C. Holm, and K. Kremer, *Conformation of a polyelectrolyte complexed to a like-charged colloid*, Phys. Rev. E **65**, 041805 (2002).

[Messina2002/2] R. Messina, C. Holm, and K. Kremer, *Like-charge colloid-polyelectrolyte complexation*, J. Chem. Phys. **117**, 2947 (2002).

[Messina2002/3] R. Messina, E. González-Tovar, M. Lozada-Cassou, and C. Holm, *Overcharging: The crucial role of excluded volume*, Europhys. Lett. **60**, 383 (2002).

[Meyer2001/1] S. Meyer, P. Levitz, and A. Delville, *A (N, V, T) Monte Carlo Study of the Long-range Electrostatic Coupling between a Large Collection of Charged Colloidal Platelets*, J. Phys. Chem. B **105**, 9595 (2001).

[Meyer2001/2] S. Meyer, P. Levitz, and A. Delville, *Influence of the Relative Orientation of Two Charged Anisotropic Colloidal Particles on Their Electrostatic Coupling: A (N, V, T) Monte Carlo Study*, J. Phys. Chem. B **105**, 10684 (2001).

[MieryTeran1990] L. Mier-y-Teran, S.H. Suh, H.S. White, and H.T. Davis, *A nonlocal free-energy density-functional approximation for the electrical double layer*, J. Chem. Phys. **92**, 5087 (1990).

[Moore1992] B.G. Moore and W.E. McMullen, *A Finite-Density Calculation of the Surface Tension of Isotropic-Nematic Interfaces*, J. Phys. Chem. **96**, 3374 (1992).

[Moreira2000] A.G. Moreira and R.R. Netz, *Strong-coupling theory for counter-ion distributions*, Europhys. Lett. **52**, 705 (2000).

[Moreira2002/1] A.G. Moreira and R.R. Netz, *Counterions at charge-modulated substrates*, Europhys. Lett. **57**, 911 (2002).

[Moreira2002/2] A.G. Moreira and R.R. Netz, *Simulations of counterions at charged plates*, Eur. Phys. J E **8**, 33 (2002).

[Morita1958] T. Morita, *Theory of Classical Fluids: Hyper-Netted Chain Approximation. I*, Prog. Theor. Phys. **20**, 920 (1958).

[Morita1959] T. Morita, *Theory of Classical Fluids: Hyper-Netted Chain Approximation. II*, Prog. Theor. Phys. **21**, 361 (1959).

[Morita1960/1] T. Morita, *Theory of Classical Fluids: Hyper-Netted Chain Approximation. IIIa*, Prog. Theor. Phys. **23**, 175 (1960).

[Morita1960/2] T. Morita, *Theory of Classical Fluids: Hyper-Netted Chain Approximation. III*, Prog. Theor. Phys. **23**, 829 (1960).

[Mourchid1995] A. Mourchid, A. Delville, J.Lambard, E. Lécolier, and P. Levitz, *Phase Diagram of Colloidal Dispersions of Anisotropic Charged Particles: Equilibrium Properties, Structure, and Rheology of Laponite Suspensions*, Langmuir **11**, 1942 (1995).

[Mourchid1998] A. Mourchid, E. Lécolier, H. van Damme, and P. Levitz, *On Viscoelastic, Birefringent, and Swelling Properties of Laponite Clay Suspensions: Revisited Phase Diagram*, Langmuir **14**, 4718 (1998).

[Mugele2005] F. Mugele and J.-C. Baret, *Electrowetting: from basics to applications*, J. Phys.: Condens. Matter **17**, R705 (2005).

[Naji2004] A. Naji and R.R. Netz, *Attraction of like-charged macroions in the strong-coupling limit*, Eur. Phys. J. E **13**, 43 (2004).

[Napiorkowski1993] M. Napiórkowski and S. Dietrich, *Structure of the effective Hamiltonian for liquid-vapor interfaces*, Phys. Rev. E **47**, 1836 (1993).

[Netz1999] R.R. Netz and H. Orland, *Field theory for charged fluids and colloids*, Europhys. Lett. **45**, 726 (1999).

[Netz2000/1] R.R. Netz and H. Orland, *One and two-component hard-core plasmas*, Eur. Phys. J. E **1**, 67 (2000).

[Netz2000/2] R.R. Netz and H. Orland, *Beyond Poisson-Boltzmann: Fluctuation effects and correlation functions*, Eur. Phys. J. E **1**, 203 (2000).

[Netz2001/1] R.R. Netz, *Static van der Waals interactions in electrolytes*, Eur. Phys. J. E **5**, 189 (2001).

[Netz2001/2] R.R. Netz, *Electrostatics of couter-ions at and between planer charged walls: From Poisson-Boltzmann to strong-coupling theory*, Eur. Phys. J. E **5**, 557 (2001).

[Netz2003] R.R. Netz and H. Orland, *Variational charge renormalization in charged systems*, Eur. Phys. J. E **11**, 301 (2003).

[Neu1999] J.C. Neu, *Wall-Mediated Forces between Like-Charged Bodies in an Electrolyte*, Phys. Rev. Lett. **82**, 1072 (1999).

[Nicolai2000] T. Nicolai and S. Cocard, *Light Scattering Study of the Dispersion of Laponite*, Langmuir **16**, 8189 (2000).

[Nicolai2001] T. Nicolai and S. Cocard, *Structure of gels and aggregates of disk-like colloids*, Eur. Phys. J. E **5**, 221 (2001).

[Nordholm1980/1] S. Nordholm and A.D.J. Haymet, *Generalized van der Waals Theory. I. Basic Formulation and Application to Uniform Fluids*, Aust. J. Chem. **33**, 2013 (1980).

[Nordholm1980/2] S. Nordholm, M. Johnson, and B.C. Freasier, *Generalized van der Waals Theory. III. The Prediction of Hard Sphere Structure*, Aust. J. Chem. **33**, 2139 (1980).

[Nordholm1981] S. Nordholm and J. Gibson, *Generalized van der Waals Theory. VII. Interface Profiles and Surface Tension*, Aust. J. Chem. **34**, 2263 (1981).

[Nordholm1982/1] S. Nordholm, J. Gibson, and M.A. Hooper, *Generalized van der Waals Theory VIII. An Improved Analysis of the Liquid / Gas Interface*, J. Stat. Phys. **28**, 391 (1982).

[Nordholm1982/2] S. Nordholm, P.R. Harrowell, and K. Cheung, *Generalized van der Waals Theory. IX. Excess Properties of Simple Fluid Mixtures*, Aust. J. Chem. **35**, 247 (1982).

[Nordholm1984] S. Nordholm, *Simple analysis of the thermodynamic properties of the one-component plasma*, Chem. Phys. Lett. **105** (3), 302 (1984).

[Norrish1954] K. Norrish, *The swelling of montmorillonite*, Discuss. Faraday Soc. **18**, 120 (1954).

[Oettel2005] M. Oettel, *Integral equations for simple fluids in a general reference functional approach*, J. Phys.: Condens. Matter **17**, 429 (2005).

[Onsager1933] L. Onsager, *Theories of concentrated electrolytes*, Chem. Rev. **13**, 73 (1933).

[Onsager1934] L. Onsager and N.N.T. Samaras, *The Surface Tension of Debye-Hückel Electrolytes*, J. Chem. Phys. **2**, 528 (1934).

[Onsager1942] L. Onsager, *Anisotropic Solutions of Colloids*, Phys. Rev. **62**, 558 (1942).

[Onsager1949] L. Onsager, *The effects of shape on the interaction of colloidal particles*, Ann. N. Y. Acad. Sci. **51**, 627 (1949).

[Ornstein1914] L.S. Ornstein and F. Zernike, *Accidental Deviations of Density and Opalescence at the Critical Point of a Single Substance*, Proc. Akad. Sci **17**, 793 (1914), see also in *The Equilibrium Theory of Classical Fluids*, edited by H.L. Frisch and J.L. Lebowitz (Benjamin, New York, 1964).

[Oversteegen2005] S.M. Oversteegen and R. Roth, *General methods for free-volume theory*, J. Chem. Phys. **122**, 214502 (2005).

[Padmore1974] T.C. Padmore and M.W. Cole, *Free surface of He II and the electron bubble*, Phys. Rev. A **9**, 802 (1974).

[Panagiotopoulos2005] A.Z. Panagiotopoulos, *Simulations of phase transitions in ionic systems*, J. Phys.: Condens. Matter **17**, S3205 (2005).

[Patra1993] C.N. Patra and S.K. Ghosh, *Weighted-density-functional theory of nonuniform ionic fluids: Application to electric double layers*, Phys. Rev. E **47**, 4088 (1993).

[Patra1994/1] C.N. Patra and S.K. Ghosh, *A nonlocal density functional theory of electric double layer: Symmetric electrolytes*, J. Chem. Phys. **100**, 5219 (1994).

[Patra1994/2] C.N. Patra and S.K. Ghosh, *A nonlocal density-functional theory of electric double layer: Charge-asymmetric electrolytes*, J. Chem. Phys. **101**, 4143 (1994).

[Patra1999] C.N. Patra, *Structure of electric double layers: A simple weighted density functional approach*, J. Chem. Phys. **111**, 9832 (1999).

[Patra2002/1] C.N. Patra and S.K. Ghosh, *A simple weighted-density-functional approach to the structure of inhomogeneous fluids*, J. Chem. Phys. **116**, 8509 (2002).

[Patra2002/2] C.N. Patra and S.K. Ghosh, *Structure of electric double layers: A self-consistent weighted-density-functional approach*, J. Chem. Phys. **117**, 8938 (2002).

[Percus1958] J.K. Percus and G.J. Yevick, *Analysis of Classical Statistical Mechanics by Means of Collective Coordinates*, Phys. Rev. **110**, 1 (1958).

[Percus1962] J.K. Percus, *Approximation methods in classical statistical mechanics*, Phys. Rev. Lett. **8**, 462 (1962).

[Percus1976] J.K. Percus, *Equilibrium State of a Classical Fluid of Hard Rods in an External Field*, J. Stat. Phys. **15**, 505 (1976)

[Perel1999] V.I. Perel and B.I. Shklovskii, *Screening of a macroion by multivalent ions: a new boundary condition for the Poisson-Boltzmann equation and charge inversion*, Physica A **274**, 446 (1999).

[Phan1993] S. Phan, E. Kierlik, M.L. Rosinberg, B. Bildstein, and G. Kahl, *Equivalence of two free-energy models for the inhomogeneous hard-sphere fluid*, Phys. Rev. E **48**, 618 (1993).

[Pianegonda2005] S. Pianegonda, M.C. Barbosa, and Y. Levin, *Charge reversal of colloidal particles*, Europhys. Lett. **71**, 831 (2005).

[Pittler2006] J. Pittler, W. Bu, D. Vaknin, A. Travesset, D.J. McGillivray, and M. Lösche, *Charge Inversion at Minute Electrolyte Concentrations*, Phys. Rev. Lett. **97**, 046102 (2006).

[Pitzer1985] K.S. Pitzer, M.C.P. de Lima, and D.R. Schreiber, *Critical Point and Phase Separation for an Ionic System*, J. Phys. Chem. **89**, 1854 (1985).

[Plischke1988] M. Plischke and D. Henderson, *Pair correlation functions and density profiles in the primitive model of the electric double layer*, J. Chem. Phys. **88**, 2712 (1988).

[Plischke1989] M. Plischke and D. Henderson, *The primitive model of the electric double layer: Nonsymmetric electrolytes*, J. Chem. Phys. **90**, 5738 (1989).

[Plischke1994] M. Plischke and B. Bergersen, *Equilibrium statistical physics*, (World Scientific, Singapore, 1994).

[Poirier1961] J.C. Poirier and J.H. DeLap, *On the Theory of Ion Pairs in Solutions*, J. Chem. Phys. **35**, 213 (1961).

[Porion2001] P. Porion, M. Al Mukhtar, S. Meyer, A.M. Faugère, J.R.C. van der Maarel, and A. Delville, *Nematic Ordering of Suspesions of Charged Anisotropic Colloids Detected by* ^{23}Na *Nuclear Magnetic Resonance*, J. Phys. Chem. B **105**, 10505 (2001).

[Quilliet2001] C. Quilliet and B. Berge, *Electrowetting: a recent outbreak*, Curr. Opin. Colloid Interface Sci. **6**, 34 (2001).

[Rahnemaie2006] R. Rahnemaie, T. Hiemstra, and W.H. van Riemsdijk, *A new surface structural approach to ion adsorption: Tracing the location of electrolyte ions*, J. Colloid Interface Sci. **293**, 312 (2006).

[Raimbault2001] J.-L. Raimbault and J.-M. Caillol, *Sine-Gordon Theory for the Equation of State of Classical Hard-Core Coulomb Systems. II. High-Temperature Expansion*, J. Stat. Phys. **103**, 777 (2001).

[Rand1980] B. Rand, E. Pekenć, J.W. Goodwin, and R.W. Smith, *Investigation into the Existence of Edge-Face Coagulated Structures in* Na-*Montmorillonite Suspensions*, J. Chem. Soc.: Faraday Trans. I **76**, 225 (1980).

[Reiss1956] H. Reiss, *Refined Theory of Ion Pairing. I. Equilibrium Aspects*, J. Chem. Phys. **25**, 400 (1956).

[Reiss1959] H. Reiss, H.L. Frisch, and J.L. Lebowitz, *Statistical Mechanics of Rigid Spheres*, J. Chem. Phys. **31**, 369 (1959).

[Reiss1977] H. Reiss, *Scaled particle theory of hard sphere fluids to 1976*, in *Statistical Mechanics and Statistical Methods in Theory and Application*, edited by U. Landman (Plenum Press, New York, 1977).

[Rosenfeld1989] Y. Rosenfeld, *Free-Energy Model for the Inhomogeneous Hard-Sphere Fluid Mixture and Density-Functional Theory of Freezing*, Phys. Rev. Lett. **63**, 980 (1989).

[Rosenfeld1994] Y. Rosenfeld, *Density functional theory of molecular fluids: Free-energy model for the inhomogeneous hard-body fluid*, Phys. Rev. E **50**, 3318 (1994).

[Rosenfeld1995] Y. Rosenfeld, *Free energy model for the inhomogeneous hard-body fluid: application of the Gauss-Bonnet theorem*, Mol. Phys. **86**, 637 (1995).

[Rosenfeld1996] Y. Rosenfeld, M. Schmidt, H. Löwen, and P. Tarazona, *Dimensional crossover and the freezing transition in density functional theory*, J. Phys.: Condens. Matter **8**, L577 (1996).

[Rosenfeld1997] Y. Rosenfeld, M. Schmidt, H. Löwen, and P. Tarazona, *Fundamental-measure free-energy density functional for hard spheres: Dimensional crossover and freezing*, Phys. Rev. E **55**, 4245 (1997).

[Roth2000] R. Roth, R. Evans, and S. Dietrich, *Depletion potential in hard-sphere mixtures: Theory and applications*, Phys. Rev. E **62**, 5360 (2000).

[Roth2002] R. Roth, R. Evans, A. Lang, and G. Kahl, *Fundamental measure theory for hard-sphere mixtures revisited: the White Bear version*, J. Phys.: Condens. Matter **14**, 12063 (2002).

[Roth2003] R. Roth, *Depletion potentials in colloidal mixtures of spheres and rods*, J. Phys.: Condens. Matter **15**, S277 (2003).

[Roth2006] R. Roth and M. Kinoshita, *Depletion potential between large spheres immersed in a multicomponent mixture of small spheres*, J. Chem. Phys. **125**, 084910 (2006).

[Rouzina1996] I. Rouzina and V.A. Bloomfield, *Macroion Attraction Due to Electrostatic Correlation between Screening Counterions. 1. Mobile Surface-Adsorbed Ions and Diffuse Ion Cloud*, J. Phys. Chem. **100**, 9977 (1996).

[Rowan2002] D.G. Rowan and J.-P. Hansen, *Salt-Induced Ordering in Lamellar Colloids*, Langmuir **18**, 2063 (2002).

[Rowlinson1979] J.S. Rowlinson, *Translation of J.D. van der Waals' "The Thermodynamic Theory of Capillarity Under the Hypothesis of a Continuous Variation of Density"*, J. Stat. Phys. **20**, 197 (1979).

[Russel1989] W.B. Russel, D.A. Saville, and W.R. Schowalter, *Colloidal Dispersions* (Cambridge University Press, Cambridge, 1989).

[Saam1975] W.F. Saam and C. Ebner, *Surface-Mode Renormalized Density-Functional Theory of the Free Surface of* ^{4}He, Phys. Rev. Lett. **34**, 253 (1975).

[Sader1999] J.E. Sader and D.Y.C. Chan, *Long-Range Electrostatic Attractions between Identically Charged Particles in Confined Geometries: An Unresolved Problem*, J. Colloid Interface Sci. **213**, 268 (1999).

[Sader2000] J.E. Sader and D.Y.C. Chan, *Long-Range Electrostatic Attractions between Identically Charged Particles in Confined Geometries and the Poisson-Boltzmann Theory*, Langmuir **16**, 324 (2000).

[Samaj2003] L. Šamaj, *The statistical mechanics of the classical two-dimensional Coulomb gas is exactly solved*, J. Phys. A **36**, 5913 (2003).

[Samaj2004] L. Šamaj, *Is the Two-Dimensional One-Component Plasma Exactly Solvable?*, J. Stat. Phys. **117**, 131 (2004).

[Samaj2005/1] L. Šamaj, *Anomalous Effects of "Guest" Charges Immersed in Electrolyte: Exact 2D Results*, J. Stat. Phys. **120**, 125 (2005).

[Samaj2005/2] L. Šamaj and Z. Bajnok, *Exactly solvable model of the two-dimensional electric double layer*, Phys. Rev. E **72**, 061503 (2005).

[Schick1990] M. Schick, *Introduction to wetting phenomena*, in *Les Houches, Session XLVIII, 1988 — Liquides aux interfaces / Liquids at interfaces*, edited by J. Charvolin, J.F. Joanny, and J. Zinn-Justin (Elsevier, Amsterdam, 1990), p. 415.

[Schroer2006] W. Schröer, M. Wagner, and O. Stanga, *Apparent mean-field criticality of liquid-liquid phase transitions in ionic solutions*, J. Mol. Liq. **127**, 2 (2006).

[Shaw1980] D.J. Shaw, *Introduction to Colloid and Surface Chemistry* (Butterworths, London, 1980).

[Shen1989] Y.R. Shen, *Optical second harmonic generation at interfaces*, Annu. Rev. Phys. Chem. **40**, 327 (1989).

[Shklovskii1999] B.I. Shklovskii, *Screening of a macroion by multivalent ions: Correlation-induced inversion of charge*, Phys. Rev. E **60**, 5802 (1999).

[Shundyak2001] K. Shundyak and R. van Roij, *Isotropic-nematic interfaces of hard-rod fluids*, J. Phys.: Condens. Matter **13**, 4789 (2001).

[Shundyak2002] K. Shundyak and R. van Roij, *Entropy-Driven Triple Point Wetting in Hard-Rod Mixtures*, Phys. Rev. Lett. **88**, 205501 (2002).

[Shundyak2003] K. Shundyak and R. van Roij, *Free planar isotropic-nematic interfaces in binary hard-rod fluids*, Phys. Rev. E **68**, 061703 (2003).

[Shundyak2004] K. Shundyak and R. van Roij, *Isotropic-nematic transition in hard-rod fluids: Relation between continuous and restricted-orientation models*, Phys. Rev. E **69**, 041703 (2004).

[Shundyak2006] K. Shundyak and R. van Roij, *Hard colloidal rods near a soft wall: Wetting, drying, and symmetry breaking*, Europhys. Lett. **74**, 1039 (2006).

[Singh2000] S. Singh, *Phase transitions in liquid crystals*, Phys. Rep. **324**, 107 (2000).

[Sluckin1981] T.J. Sluckin, *Applications of the Density-functional Theory of Charged Fluids*, J. Chem. Soc.: Faraday Trans. II **77**, 575 (1981).

[Sogami1984] I. Sogami and N. Ise, *On the electrostatic interaction in macroionic solutions*, J. Chem. Phys. **81**, 6320 (1984).

[Sondi1997] I. Sondi, O. Milat, and V. Pravdić, *Electrokinetic Potentials of Clay Surfaces Modified by Polymers*, J. Colloid Interface Sci. **189**, 66 (1997).

[Stanley1971] H.E. Stanley, *Introduction to Phase Transitions and Critical Phenomena*, (Oxford University Press, New York, 1971).

[Stell1976] G. Stell, K.C. Wu, and B. Larsen, *Critical Point in a Fluid of Charged Hard Spheres*, Phys. Rev. Lett. **37**, 1369 (1976).

[Stell1992] G. Stell, *Critical behavior of ionic-fluid models*, Phys. Rev. A **45**, 7628 (1992).

[Stell1995] G. Stell, *Criticality and Phase Transitions in Ionic Fluids*, J. Stat. Phys. **78**, 197 (1995).

[Stern1924] O. Stern, *Zur Theorie der elektrolytischen Doppelschicht*, Z. Elektrochem. **30**, 508 (1924).

[Stillinger1968/1] F.H. Stillinger and R. Lovett, *Ion-Pair Theory of Concentrated Electrolytes. I. Basic Concepts*, J. Chem. Phys. **48**, 3858 (1968).

[Stillinger1968/2] F.H. Stillinger and R. Lovett, *General Restriction on the Distribution of Ions in Electrolytes*, J. Chem. Phys. **49** (5), 1991 (1968).

[Stringari1987] S. Stringari and J. Treiner, *Surface properties of liquid* ^{3}He *and* ^{4}He*: A density-functional approach*, Phys. Rev. B **36**, 8369 (1987).

[Sullivan1986] D.E. Sullivan and M.M. Telo da Gama, *Wetting Transitions and Multilayer Adsorption at Fluid Interfaces*, in *Fluid Interfacial Phenomena*, edited by C.A. Croxton (John Wiley, Chichester, 1986), p. 45.

[Tamashiro1998] M.N. Tamashiro, Y. Levin, and M.C. Barbosa, *Debye-Hückel-Bjerrum theory for charged colloids*, Physica A **258**, 341 (1998).

[Tamashiro1999] M.N. Tamashiro, Y. Levin, and M.C. Barbosa, *The one-component plasma: a conceptual approach*, Physica A **268**, 24 (1999).

[Tamashiro2003] M.N. Tamashiro and H. Schiessel, *Where the linearized Poisson-Boltzmann cell model fails: Spurious phase separation in charged colloidal suspensions*, J. Chem. Phys. **119**, 1855 (2003).

[Tang1990] Z. Tang, L. Mier-y-Teran, H.T. Davis, L.E. Scriven, and H.S. White, *Non-local free energy density-functional theory applied to the electrical double layer. I. Symmetrical electrolytes*, Mol. Phys. **71**, 369 (1990).

[Tarazona1984] P. Tarazona, *A density functional theory of melting*, Mol. Phys. **52**, 81 (1984).

[Tarazona1985] P. Tarazona, *Free-energy density functional for hard spheres*, Phys. Rev. A **31**, 2672 (1985) [Erratum: Phys. Rev. A **32**, 3148 (1985)].

[Tarazona1997] P. Tarazona and Y. Rosenfeld, *From zero-dimension cavities to free-energy functionals for hard disks and hard spheres*, Phys. Rev. E **55**, 4873 (1997).

[Tellez2005/1] G. Téllez, *Debye-Hückel theory for two-dimensional Coulomb systems living on a finite surface without boundaries*, Physica A **349**, 155 (2005).

[Tellez2005/2] G. Téllez, *Guest Charges in an Electrolyte: Renormalized Charge, Long- and Short-Distance Behavior of the Electric Potential and Density Profiles*, J. Stat. Phys. **122**, 787 (2005).

[Teppner1999] R. Teppner, S. Bae, K. Haage, and H. Motschmann, *On the Analysis of Ellipsometric Measurements of Adsorption Layers at Fluid Interfaces*, Langmuir **15**, 7002 (1999).

[Thiele1963] E. Thiele, *Equation of State for Hard Spheres*, J. Chem. Phys. **39**, 474 (1963).

[Thomas1996] R.K. Thomas and J. Penfold, *Neutron and x-ray relectometry of interfacial systems in colloid and* *polymer chemistry*, Curr. Opin. Colloid Interface Sci. **1**, 23 (1996).

[Tonks1936] L. Tonks, *The Complete Equation of State of One, Two and Three-Dimensional Gases of Hard Elastic Spheres*, Phys. Rev. **50**, 955 (1936).

[Torrie1979] G.M. Torrie and J.P. Valleau, *A Monte Carlo study of an electrical double layer*, Chem. Phys. Lett. **65** (2), 343 (1979).

[Torrie1982] G.M. Torrie and J.P. Valleau, *Electrical Double Layers. 4. Limitations of the Gouy-Chapman Theory*, J. Phys. Chem. **86**, 3251 (1982).

[Trizac1997] E. Trizac and J.-P. Hansen, *Wigner-Seitz model of charged lamellar colloidal dispersions*, Phys. Rev. E **56**, 3137 (1997).

[Trizac1999] E. Trizac and J.-L. Raimbault, *Long-range electrostatic interactions between like-charged colloids: Steric and confinement effects*, Phys. Rev. E **60**, 6530 (1999).

[Trizac2000] E. Trizac, *Effective interactions between like-charged macromolecules*, Phys. Rev. E **62**, 1465 (2000).

[Trizac2001] E. Trizac and J.-L. Raimbault, *Reply to "Comment on 'Long-range electrostatic interactions between like-charged colloids: Steric and confinement effects' "*, Phys. Rev. E **64**, 043401 (2001).

[Trizac2002] E. Trizac, L. Bocquet, R. Agra, J.-J. Weis, and A. Aubouy, *Effective interactions and phase behaviour for a model clay suspension in an electrolyte*, J. Phys.: Condens. Matter **14**, 9339 (2002).

[Trulsson2006] M. Trulsson, B. Jönsson, T. Åkesson, J. Forsman, *Repulsion between Oppositely Charged Surfaces in Multivalent Electrolytes*, Phys. Rev. Lett. **97**, 068302 (2006).

[Uhlenbeck1962] G.E. Uhlenbeck and G.W. Ford, *The theory of linear graphs with applications to the theory of the virial development of the properties of gases*, in *Studies in Statistical Mechanics*, Vol. 1, edited by J. de Boer and G.E. Uhlenbeck (North-Holland Publishing, Amsterdam, 1962), p. 119.

[vanderBeek2003] D. van der Beek and H.N.W. Lekkerkerker, *Nematic ordering vs. gelation in suspensions of charged platelets*, Europhys. Lett. **61**, 702 (2003).

[vanderBeek2004] D. van der Beek and H.N.W. Lekkerkerker, *Liquid Crystal Phases of Charged Colloidal Platelets*, Langmuir **20**, 8582 (2004).

[vanderHeyden2006] F.H.J. van der Heyden, D. Stein, K. Besteman, S.G. Lemay, and C. Dekker, *Charge Inversion at High Ionic Strength Studied by Streaming Currents*, Phys. Rev. Lett. **96**, 224502 (2006).

[vanderKooij1998] F.M. van der Kooij and H.N.W. Lekkerkerker, *Formation of Nematic Liquid Crystals in Suspensions of Hard Colloidal Platelets*, J. Phys. Chem. B **102**, 7829 (1998).

[vanderKooij2000/1] F.M. van der Kooij, A.P. Philipse, and J.K.G. Dhont, *Sedimentation and Diffusion in Suspensions of Sterically Stabilized Colloidal Platelets*, Langmuir **16**, 5317 (2000).

[vanderKooij2000/2] F.M. van der Kooij and H.N.W. Lekkerkerker, *Liquid-Crystal Phases Formed in Mixed Suspensions of Rod- and Platelike Colloids*, Langmuir **16**, 10144 (2000).

[vanderKooij2001] F.M. van der Kooij, D. van der Beek, and H.N.W. Lekkerkerker, *Isotropic-Nematic Phase Separation in Suspensions of Polydisperse Colloidal Platelets*, J. Phys. Chem. B **105**, 1696 (2001).

[vanderWaals1894] J.D. van der Waals, *Thermodynamische Theorie der Kapillarität unter Voraussetzung stetiger Dichteänderung*, Z. phys. Chem. **13**, 656 (1894).

[vanRiemsdijk1986] W.H. van Riemsdijk, G.H. Bolt, L.K. Koopal, and J. Blaakmeer, *Electrolyte Adsorption on Heterogeneous Surfaces: Adsorption Models*, J. Colloid Interface Sci. *109*, 219 (1986).

[vanRoij1999] R. van Roij and R. Evans, *Phase equilibria in a model of low-salt suspensions of charged colloids*, J. Phys.: Condens. Matter **11**, 10047 (1999).

[vanRoij2000] R. van Roij, *Attraction or repulsion between charged colloids? A connection with Debye-Hückel theory*, J. Phys.: Condens. Matter **12**, A263 (2000).

[vanRoij2005] R. van Roij, *The isotropic and nematic liquid crystal phase of colloidal rods*, Eur. J. Phys. **26**, S57 (2005).

[Varga2005] S. Varga, K. Purdy, A. Galindo, S. Fraden, and G. Jackson, *Nematic-nematic phase separation in binary mixtures of thick and thin hard rods: Results from Onsager-like theories*, Phys. Rev. E **72**, 051704 (2005).

[Veerman1992] J.A.C. Veerman and D. Frenkel, *Phase behavior of disklike hard-core mesogens*, Phys. Rev. A **45**, 5632 (1992).

[Verwey1948] E.J.W. Verwey and J.Th.G. Overbeek, *Theory of the stability of lyophobic colloids* (Elsevier Publishing Company, New York, 1948) [unabridged republication (Dover Publications, Mineola, 1999)].

[Vidal2005] F. Vidal and A. Tadjeddine, *Sum-frequency generation spectroscopy of interfaces*, Rep. Prog. Phys. **68**, 1095 (2005).

[Vink2005/1] R.L.C. Vink and T. Schilling, *Interfacial tension of the isotropic-nematic interface in suspensions of soft spherocylinders*, Phys. Rev. E **71**, 051716 (2005).

[Vink2005/2] R.L.C. Vink, S. Wolfsheimer, and T. Schilling, *Isotropic-nematic interfacial tension of hard and soft rods: Application of advanced grand canonical biased-sampling techniques*, J. Chem. Phys. **123**, 074901 (2005).

[vonGrunberg2001] H.H. von Grünberg, R. van Roij, and G. Klein, *Gas-liquid phase coexistence in colloidal suspensions?*, Europhys. Lett. **55**, 580 (2001).

[Wagner1924] C. Wagner, *Die Oberflächenspannung verdünnter Elektrolytlösungen*, Phys. Z. **25**, 474 (1924).

[Waisman1970] E. Waisman and J.L. Lebowitz, *Exact Solution of an Integral Equation for the Structure of a Primitive Model of Electrolytes*, J. Chem. Phys. **52**, 4307 (1970).

[Waisman1972/1] E. Waisman and J.L. Lebowitz, *Mean Spherical Model Integral Equation for Charged Hard Spheres. I. Method of Solution*, J. Chem. Phys. **56**, 3086 (1972).

[Waisman1972/2] E. Waisman and J.L. Lebowitz, *Mean Spherical Model Integral Equation for Charged Hard Spheres. II. Results*, J. Chem. Phys. **56**, 3093 (1972).

[Wang2005] N. Wang, S. Liu, J. Zhang, Z. Wu, J. Chen, and D. Sun, *Lamellar phase in colloidal suspensions of positively charged LDHs platelets*, Soft Matter **1**, 428 (2005).

[Warren2000] P.B. Warren, *A theory of void formation in charge-stabilized colloidal suspensions at low ionic strength*, J. Chem. Phys. **112**, 4683 (2000).

[Weeks1971] J.D. Weeks, D. Chandler, and H.C. Andersen, *Role of Repulsive Forces in Determining the Equilibrium Structure of Simple Liquids*, J. Chem. Phys. **54**, 5237 (1971).

[Weeks1977] J.D. Weeks, *Structure and thermodynamics of the liquid-vapor interface*, J. Chem. Phys. **67**, 3106 (1977).

[Wensink2001] H.H. Wensink, G.J. Vroege, and H.N.W. Lekkerkerker, *Isotropic-Nematic Density Inversion in a Binary Mixture of Thin and Thick Hard Platelets*, J. Phys. Chem. B **105**, 10610 (2001).

[Wertheim1963] M.S. Wertheim, *Exact solution of the Percus-Yevick integral equation for hard spheres*, Phys. Rev. Lett. **10**, 321 (1963).

[Wertheim1964] M.S. Wertheim, *Analytic Solution of the Percus-Yevick Equation*, J. Math. Phys. **5**, 643 (1964).

[Wertheim1994] M.S. Wertheim, *Fluids of hard convex molecules. I. Basic theory*, Mol. Phys. **83**, 519 (1994).

[Westall1980] J. Westall and H. Hohl, *A comparison of electrostatic models for the oxide / solution interface*, Adv. Colloid Inteface Sci. **12**, 265 (1980).

[Wijnhoven2005] J.E.G.J. Wijnhoven, D.D. van't Zand, D. van der Beek, and H.N.W. Lekkerkerker, *Sedimentation and Phase Transitions of Colloidal Gibbsite Platelets*, Langmuir **21**, 10422 (2005).

[Wu2006] J. Wu, *Density Functional Theory for Chemical Engineering: From Capillarity to Soft Materials*, AIChE **52**, 1168 (2006).

[Zoetekouw2006] B. Zoetekouw and R. van Roij, *Volume terms for charged colloids: A grand-canonical treatment*, Phys. Rev. E **73**, 021403 (2006).

[Zwanzig1954] R. Zwanzig, *High-Temperature Equation of State by a Perturbation Method. I. Nonpolar Gases*, J. Chem. Phys. **22**, 1420 (1954) [Erratum: J. Chem. Phys. **22**, 2099 (1954)].

[Zwanzig1963] R. Zwanzig, *First-Order Phase Transition in a Gas of Long Thin Rods*, J. Chem. Phys. **39**, 1744 (1963).

Index

CV of Markus Bier

1976	Born in Lauda
1983-1996	Primary and secondary school in Boxberg and Bad Mergentheim
1996-1997	Zivildienst (alternative service in lieu of military service)
1997-2003	University education at Stuttgart University Simultaneous study of two separate subjects to degree level: **Physics** Degree: Dipl.-Phys. Thesis: ”Coexisting phases in binary platelet mixtures” (August 2003) Advisers: Prof. Dr. S. Dietrich and Dr. L. Harnau **Mathematics** Degree: Dipl.-Math. Thesis: ”Globale Existenz kleiner Lösungen nichtlinearer Wellengleichungen in Wellenleitern” (November 2002) Adviser: PD Dr. P. Lesky
2003-2006	Doctoral studies at Max-Planck-Institut für Metallforschung in Stuttgart Thesis: ”Interfaces in fluids of charged platelike colloids” (submission October 2006, examination December 2006) Advisers: Prof. Dr. S. Dietrich and Dr. L. Harnau